UPDATE 2017-07-17

L. Di Stasio[1,2], Z. Ayadi[1], J. Varna[2]

[1] EEIGM, Université de Lorraine, Nancy, France

[2] Division of Materials Science, Luleå University of Technology, Luleå, Sweden

July 17, 2017

Outline

- Symbols, Models, Equations & Reference Data
- Results
- Summary & Conclusion

SYMBOLS, MODELS, EQUATIONS & REFERENCE DATA

Symbols

Symbol	Unit	Description
θ	$[^\circ]$	Debond angular position with respect to the center of the arc defined by the debond itself
$\Delta\theta$	$[^\circ]$	Debond semi-angular aperture
δ	$[^\circ]$	Angle subtended by a single element at the fiber/matrix interface
VF_f	$[-]$	Fiber volume fraction
l	$[\mu m]$	Ply's half-length, equal to RVE's half-length (square element)
u	$[\mu m]$	Displacement along x
w	$[\mu m]$	Displacement along z

Symbols

Symbol	Unit	Description
Γ_1	$[-]$	Bonded part of fiber surface
Γ_2	$[-]$	Free (debonded) part of fiber surface
Γ_3	$[-]$	Bonded part of matrix surface
Γ_4	$[-]$	Free (debonded) part of matrix surface

Reference Models

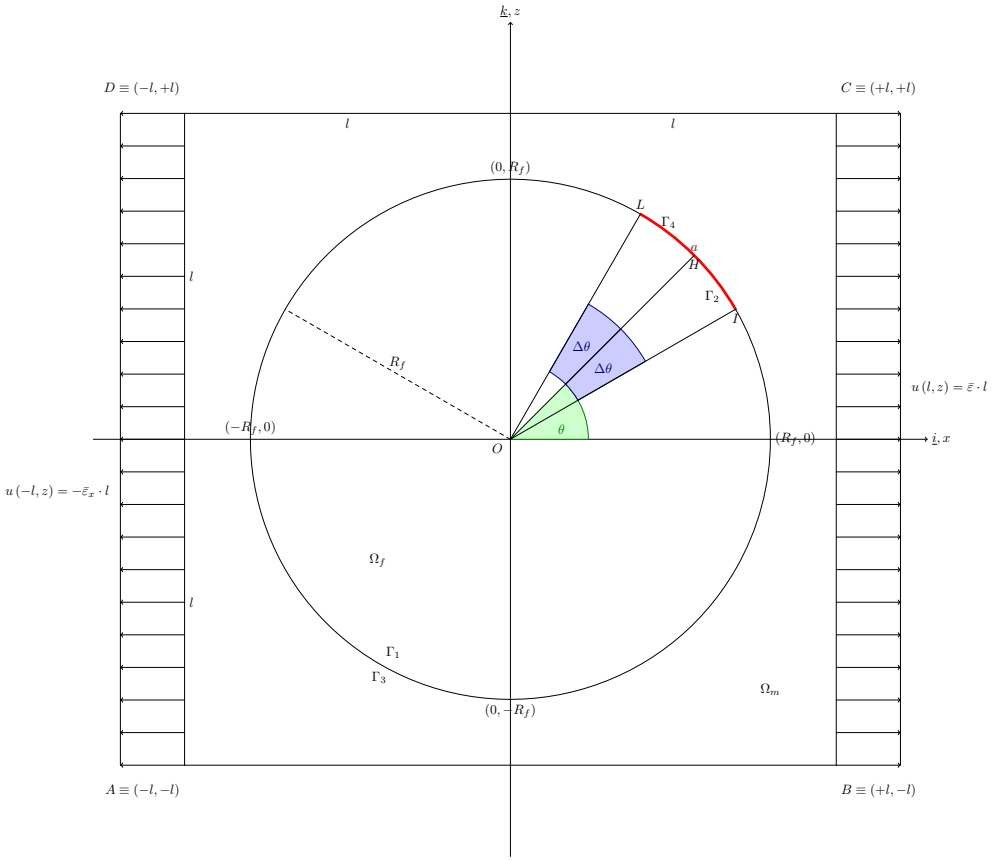

Simple RVE, BC: free.

Reference Models

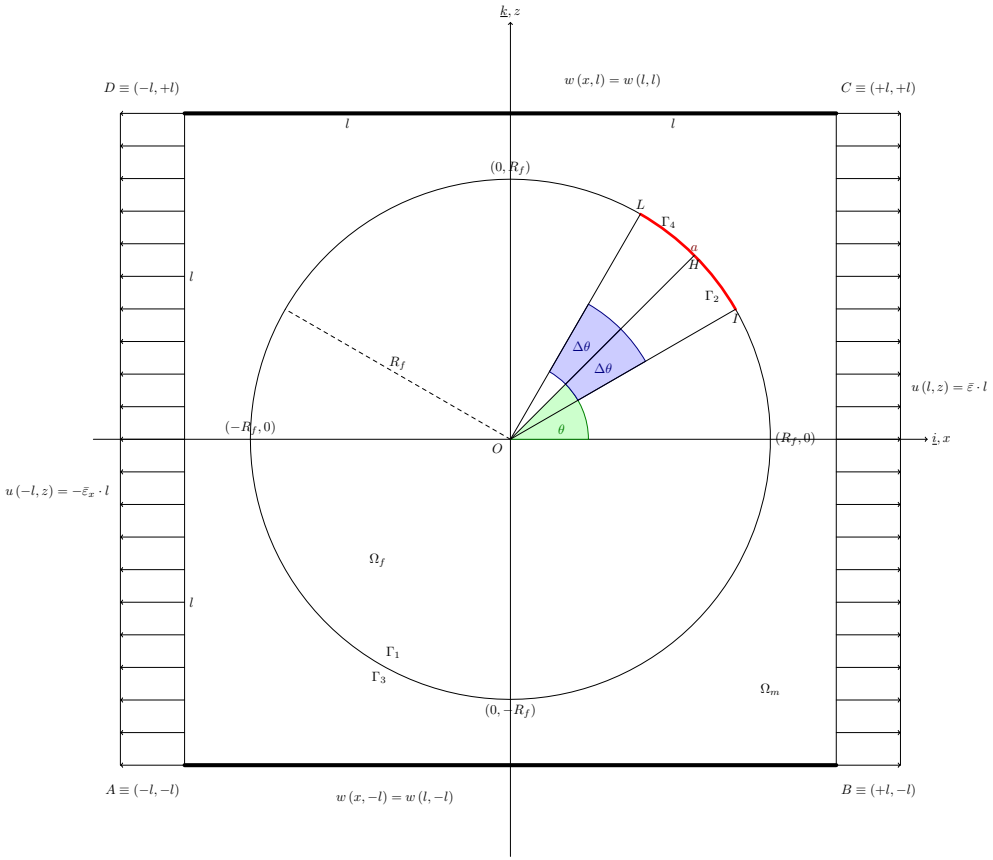

Simple RVE, BC: fixed vertical displacement.

Reference Models

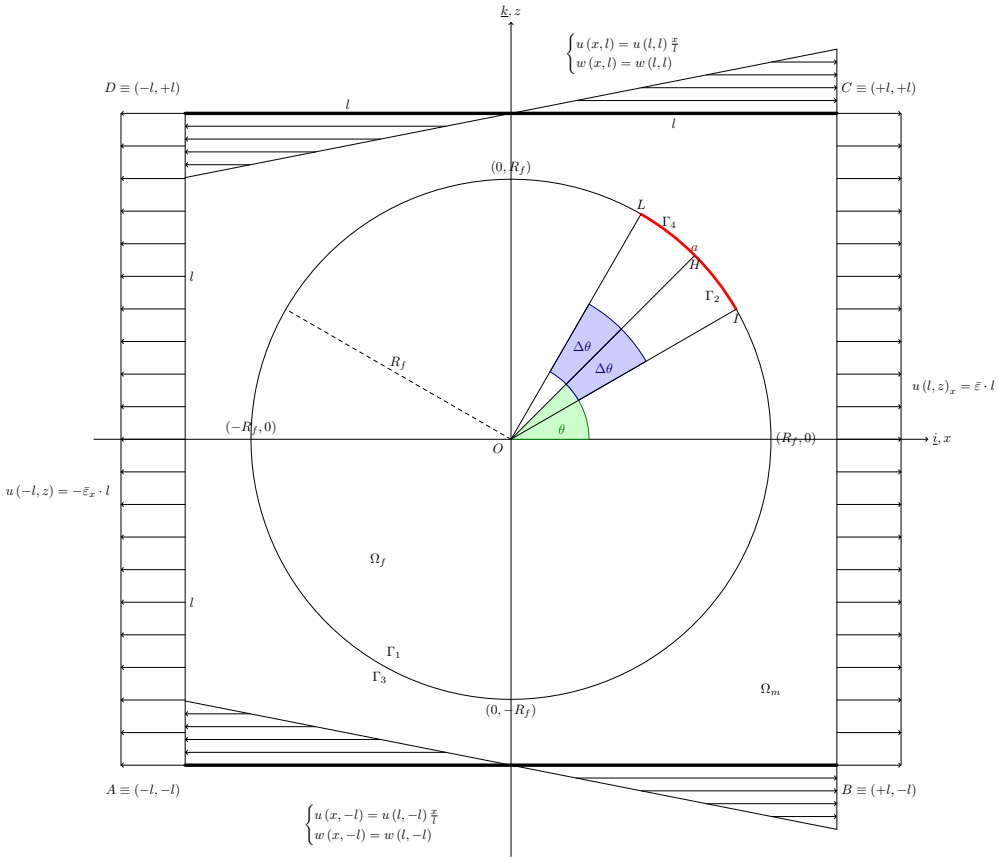

Simple RVE, BC: fixed vertical and homogeneous horizontal displacement.

Angular discretization

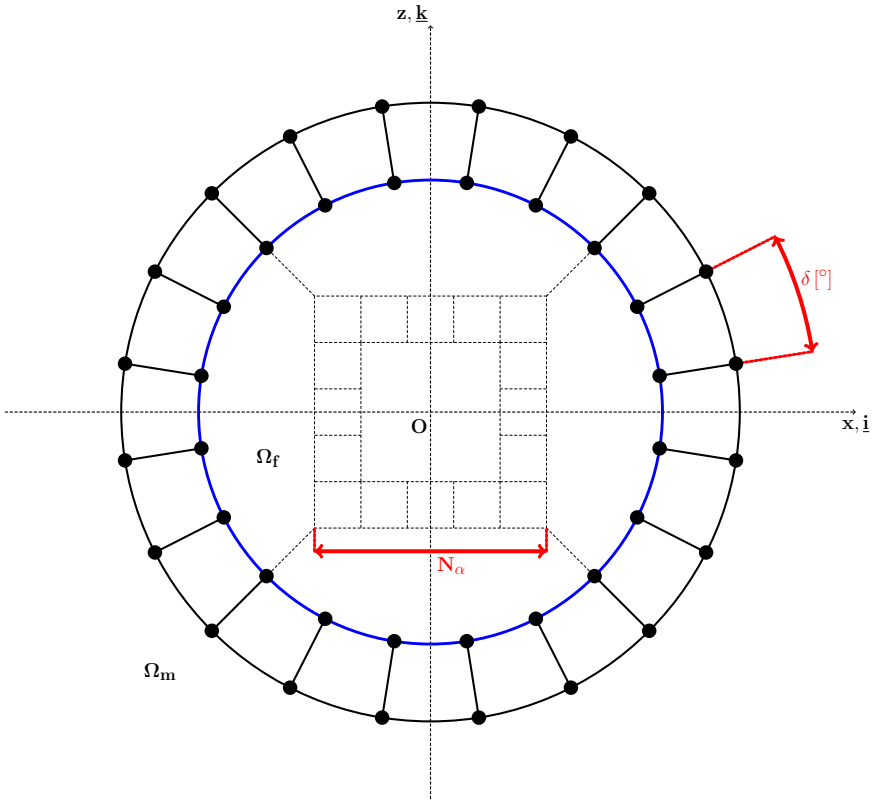

Angular discretization at fiber/matrix interface: $\delta = \frac{360°}{4N_\alpha}$.

Material properties

Material	$E\,[GPa]$	$G\,[GPa]$	$\nu\,[-]$
Glass fiber	70,0	29,2	0,2
Epoxy	3,5	1,25	0,4

Evaluation of G_0

$$G_0 = \pi R_f \sigma_0^2 \frac{1 + k_m}{8 G_m} \tag{1}$$

$$k_m = 3 - 4\nu_m \tag{2}$$

$$\sigma_0^{undamaged} = \frac{E_m}{1 - \nu_m^2} \varepsilon_{xx} \tag{3}$$

Virtual Crack Closure Technique (Nodal Forces at Crack Tip)

$$\Delta u = \left| \Delta u^{matrix}_{\text{1 element before crack tip}} - \Delta u^{fiber}_{\text{1 element before crack tip}} \right| \tag{4}$$

$$\Delta w = \left| \Delta w^{matrix}_{\text{1 element before crack tip}} - \Delta w^{fiber}_{\text{1 element before crack tip}} \right| \tag{5}$$

$$\beta = \arctan\left(\frac{z^{matrix,undef}_{\text{crack tip}}}{x^{matrix,undef}_{\text{crack tip}}} \right) \tag{6}$$

$$\Delta_r = \cos(\beta)\Delta u + \sin(\beta)\Delta w \qquad \Delta_\theta = -\sin(\beta)\Delta u + \cos(\beta)\Delta w \tag{7}$$

$$F_r = \cos(\beta)F_x^{reaction} + \sin(\beta)F_z^{reaction} \qquad F_\theta = -\sin(\beta)F_x^{reaction} + \cos(\beta)F_z^{reaction} \tag{8}$$

$$G_I = \frac{1}{2}\frac{F_r \Delta_r}{R_f \delta} \qquad G_{II} = \frac{1}{2}\frac{F_\theta \Delta_\theta}{R_f \delta} \qquad b = 1.0 \leftrightarrow \Delta A = b R_f \delta \tag{9}$$

Virtual Crack Closure Integral (Stress at Surface Nodes)

$$G_I = \frac{1}{2\Delta A}\int_0^{\Delta c}\sigma_n(s)\,\delta u_n(s-\Delta c)\,ds \quad G_{II} = \frac{1}{2\Delta A}\int_0^{\Delta c}\tau_{sn}(s)\,\delta u_s(s-\Delta c)\,ds \tag{10}$$

with the reference frame centered on the crack tip and rotated according to the orientation of the crack tip.

$$\beta = \arctan\left(\frac{z^{matrix,undef}_{\text{crack tip}}}{x^{matrix,undef}_{\text{crack tip}}}\right) \tag{11}$$

$$\Delta u^i = \left|\Delta u^{matrix}_{\text{i elements before crack tip}} - \Delta u^{fiber}_{\text{i elements before crack tip}}\right| \tag{12}$$

$$\Delta w^i = \left|\Delta w^{matrix}_{\text{i elements before crack tip}} - \Delta w^{fiber}_{\text{i elements before crack tip}}\right| \tag{13}$$

$$\Delta^i_r = \cos(\beta)\Delta u^i + \sin(\beta)\Delta w^i \qquad \Delta^i_\theta = -\sin(\beta)\Delta u^i + \cos(\beta)\Delta w^i \tag{14}$$

Virtual Crack Closure Integral (Stress at Surface Nodes)

$$\sigma_{rr}^{m,i} = \sigma_{xx}^{m,\text{i elements after c.t.}} \cos^2\beta + \sigma_{zz}^{m,\text{i elements after c.t.}} \sin^2\beta + 2\tau_{xz}^{m,\text{i elements after c.t.}} \sin\beta\cos\beta \tag{15}$$

$$\tau_{r\theta}^{m,i} = \left(\sigma_{zz}^{m,\text{i elements after crack tip}} - \sigma_{xx}^{m,\text{i elements after c.t.}}\right) \sin\beta\cos\beta + \tau_{xz}^{m,\text{i elements after c.t.}} \left(\cos^2\beta - \sin^2\beta\right) \tag{16}$$

where m stands for material, i.e. stresses can be extracted either on the fiber or the matrix surface.

$$G_I^m = \frac{1}{2R_f\delta b} \sum_{i=1}^{N\ Int\ El} \frac{1}{2} R_f\delta \left(\sigma_{rr}^{m,i}\Delta_r^i + \sigma_{rr}^{m,i-1}\Delta_r^{i-1}\right) \qquad G_{II}^m = \frac{1}{2R_f\delta b} \sum_{i=1}^{N\ Int\ El} \frac{1}{2} R_f\delta \left(\tau_{r\theta}^{m,i}\Delta_\theta^i + \tau_{r\theta}^{m,i-1}\Delta_\theta^{i-1}\right) \tag{17}$$

remembering $b = 1$, i.e. unit depth in the out-of-plane direction, they simplify to

$$G_I^m = \frac{1}{4}\left(\sigma_{rr}^{m,0}\Delta_r^0 + \sum_{i=1}^{N\ Int\ El-1}\left(2\sigma_{rr}^{m,i}\Delta_r^i\right) + \sigma_{rr}^{m,N\ Int\ El}\Delta_r^{N\ Int\ El}\right) \tag{18}$$

$$G_{II}^m = \frac{1}{4}\left(\tau_{r\theta}^{m,0}\Delta_\theta^0 + \sum_{i=1}^{N\ Int\ El-1}\left(2\tau_{r\theta}^{m,i}\Delta_\theta^i\right) + \tau_{r\theta}^{m,N\ Int\ El}\Delta_\theta^{N\ Int\ El}\right) \tag{19}$$

↘ RESULTS

Model Data

Quantity	Value
$\theta\,[°]$	0
$\Delta\theta\,[°]$	$\in [10, 150]$
$\delta\,[°]$	$\in [1, 0.2]$
$VF_f\,[-]$	$7.9 \cdot 10^{-5}$
$\frac{L}{R_f}\,[-]$	~ 100
$R_f\,[\mu m]$	1

σ_0, $\delta = 1.0°$

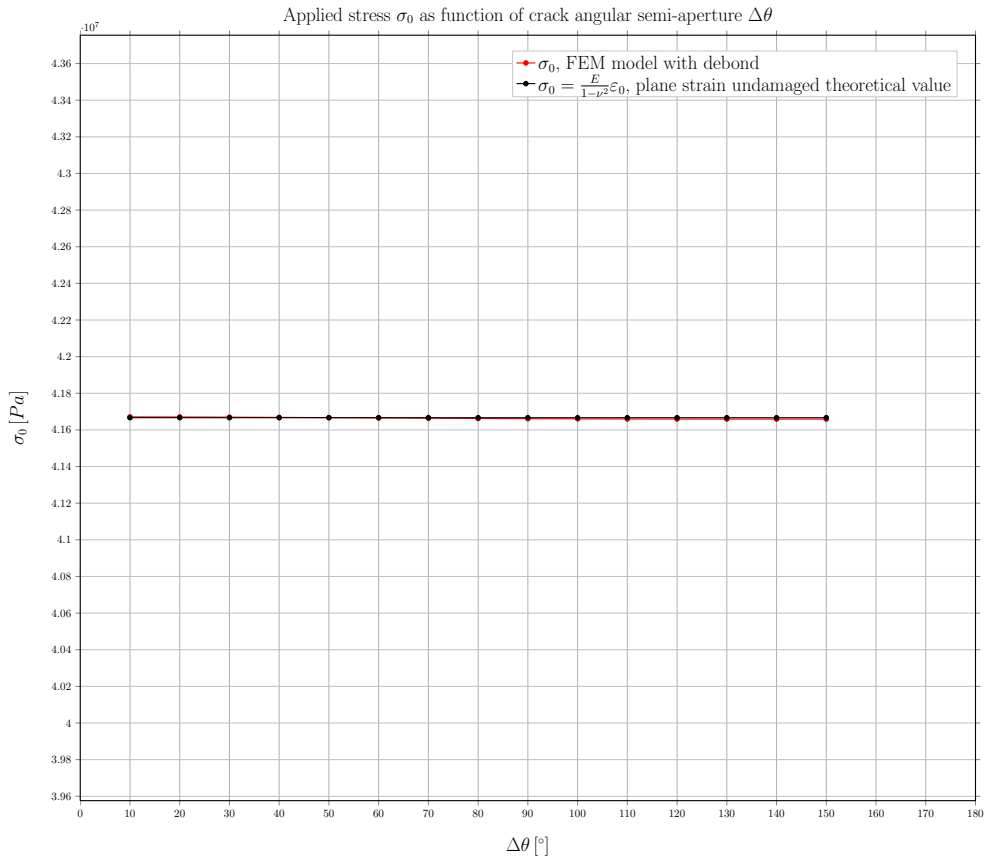

In red small strain FEM, in black analytical plain strain value.

G_0, $\delta = 1.0°$

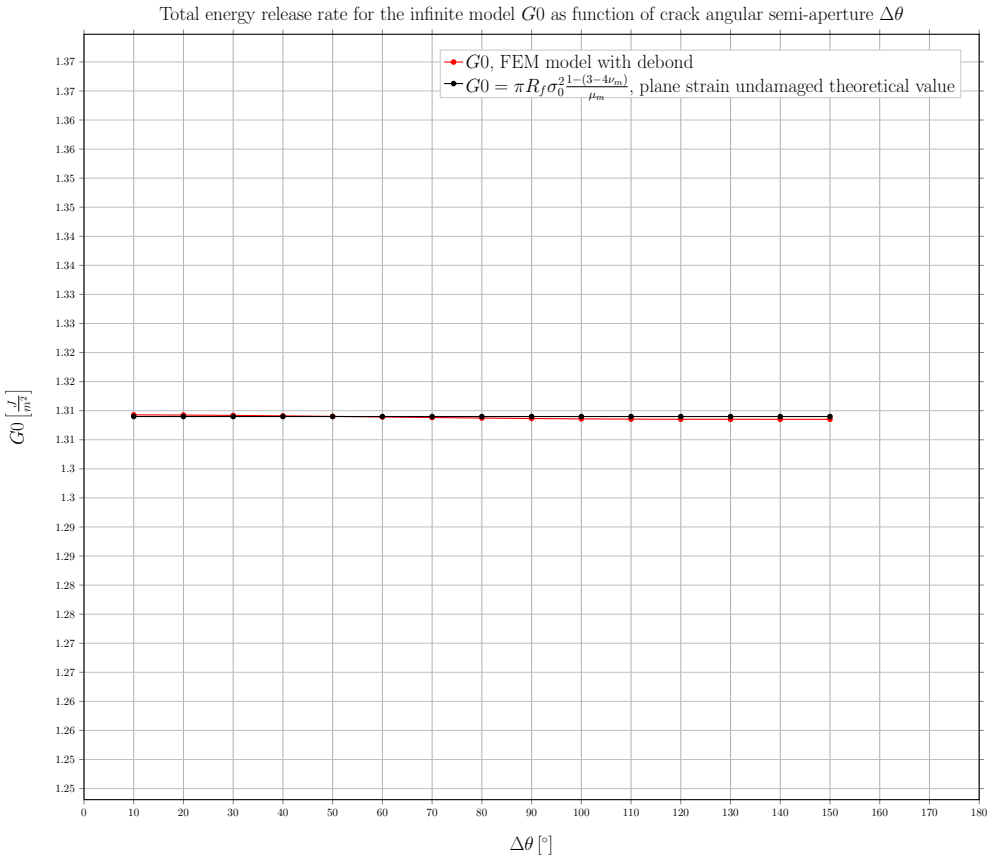

In red small strain FEM, in black analytical plain strain value.

J-Integral (Abaqus built-in routine), $\delta = 1.0°$

Normalized total energy release rate $\frac{G_{TOT}}{G_0}$ as function of crack angular semi-aperture $\Delta\theta$, calculated with Abaqus built-in J-Integral post-processing routine (*CONTOUR INTEGRAL)

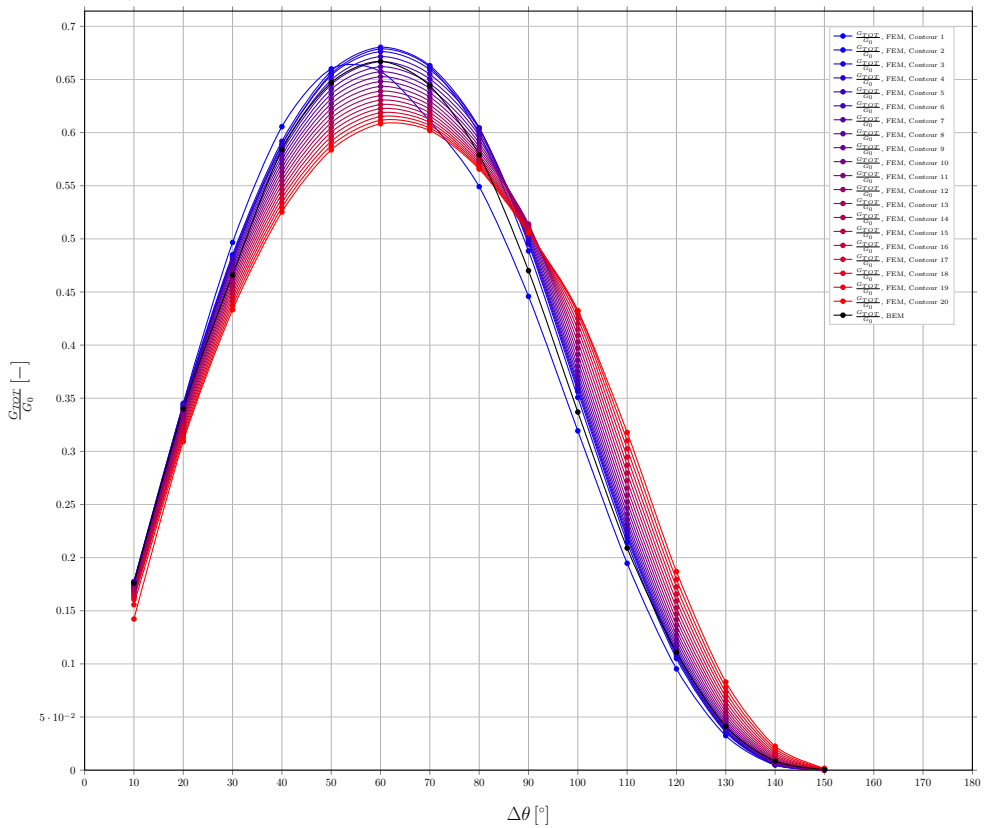

Fading from blue to red for contours further from the crack tip, FEM results; in black BEM results.

VCCT in forces (in-house Python routine), $\delta = 1.0°$

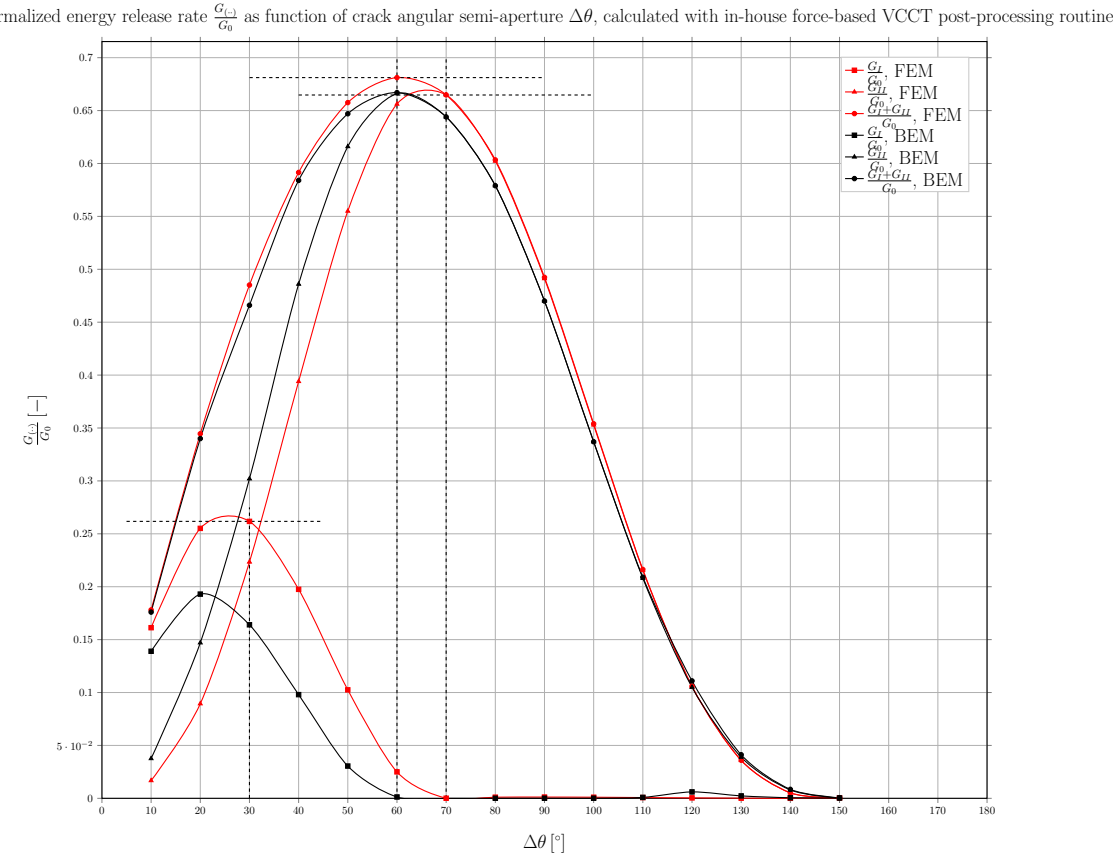

In green VCCT from FEM results, in black BEM results; positions of maxima highlighted by dashed lines.

J-Integral and VCCT in forces, $\delta = 1.0°$

Normalized energy release rate $\frac{G_{(-)}}{G_0}$ as function of crack angular semi-aperture $\Delta\theta$, calculated with in-house force-based VCCT and Abaqus built-in J-Integral (*CONTOUR INTEGRAL) post-processing routines

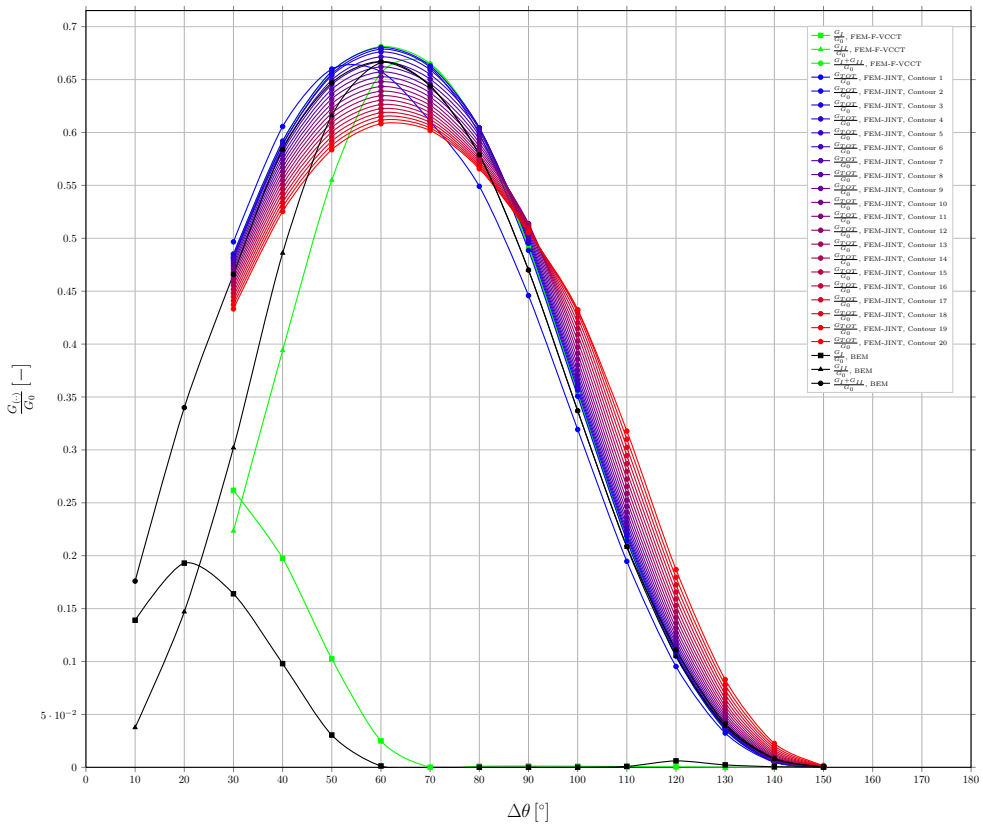

Fading from blue to red for contours further from the crack tip, J-Integral from FEM results; in green VCCT from FEM results; in black BEM results.

G_I from VCCI, stresses extracted on fiber surface, $\delta = 1.0°$

Normalized energy release rate $\frac{G_{(\cdot)}}{G_0}$ as function of crack angular semi-aperture $\Delta\theta$, calculated with in-house force-based and stress-based VCCT post-processing routines with stresses extracted on the fiber side of the interface

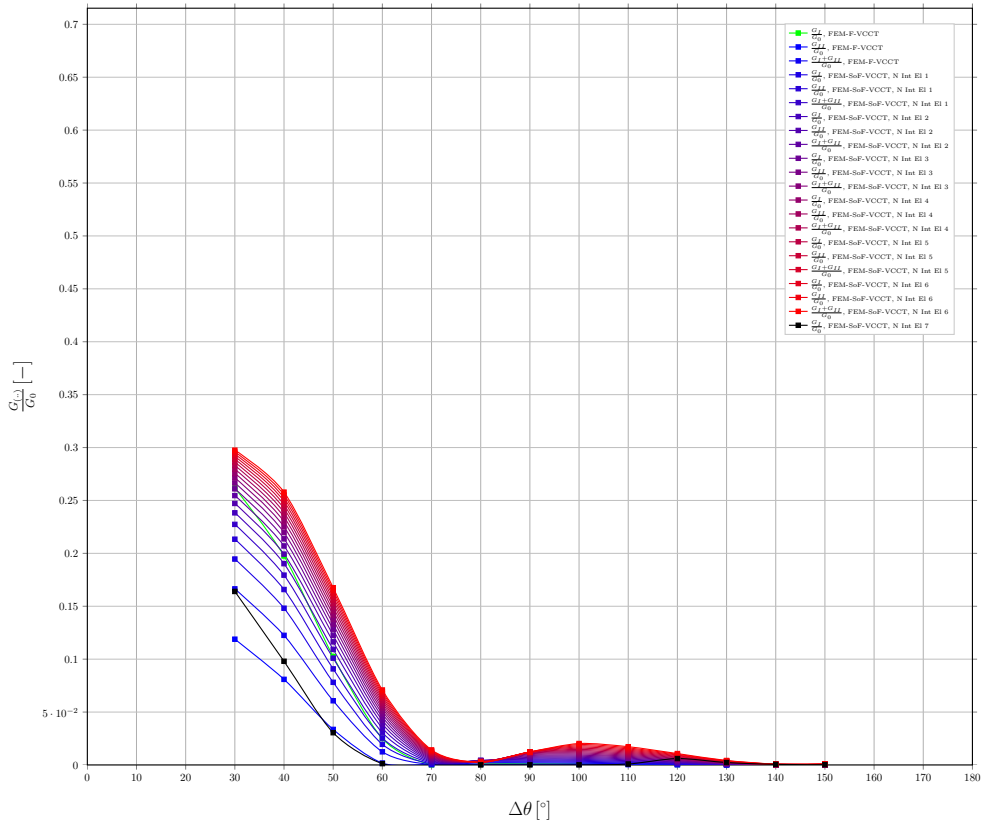

Fading from blue to red for increasing number of integration elements, Virtual Crack Closure Integral (VCCI) from FEM results; in green VCCT from FEM results; in black BEM results

$G_{//}$ from VCCI, stresses extracted on fiber surface, $\delta = 1.0°$

Normalized energy release rate $\frac{G_{(-)}}{G_0}$ as function of crack angular semi-aperture $\Delta\theta$, calculated with in-house force-based and stress-based VCCT post-processing routines with stresses extracted on the fiber side of the interface

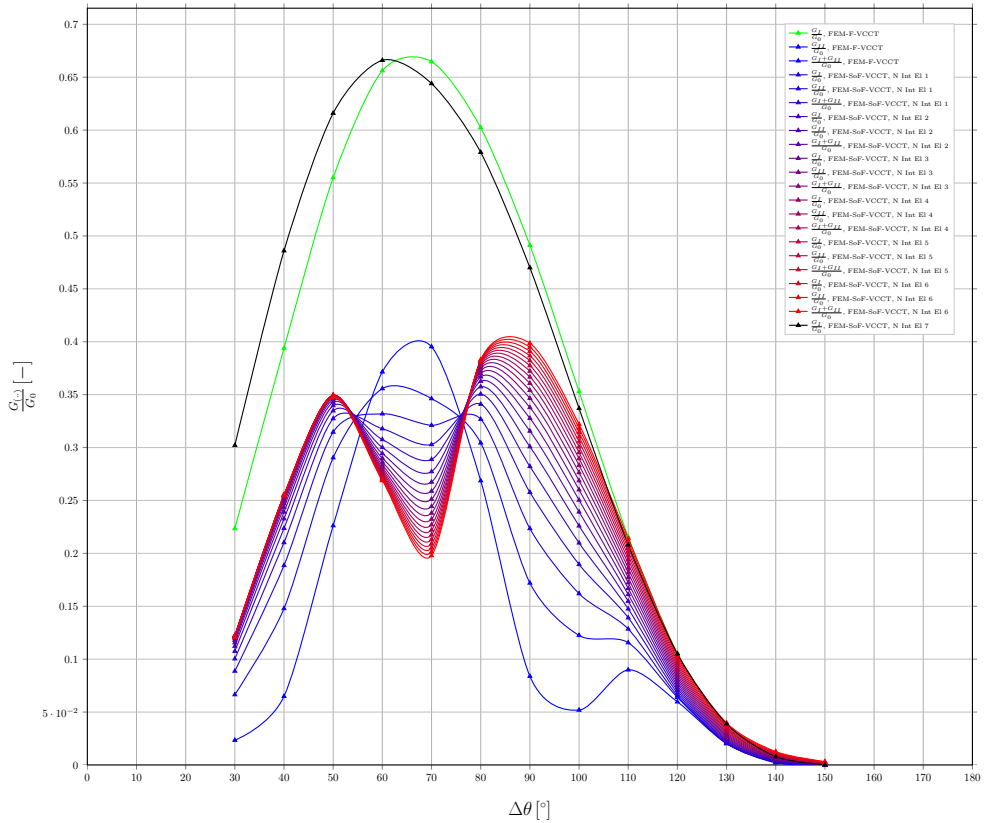

Fading from blue to red for increasing number of integration elements, Virtual Crack Closure Integral (VCCI) from FEM results; in green VCCT from FEM results; in black BEM results

G_{TOT} from VCCI, stresses extracted on fiber surface, $\delta = 1.0°$

Normalized energy release rate $\frac{G_{(\cdot)}}{G_0}$ as function of crack angular semi-aperture $\Delta\theta$, calculated with in-house force-based and stress-based VCCT post-processing routines with stresses extracted on the fiber side of the interface

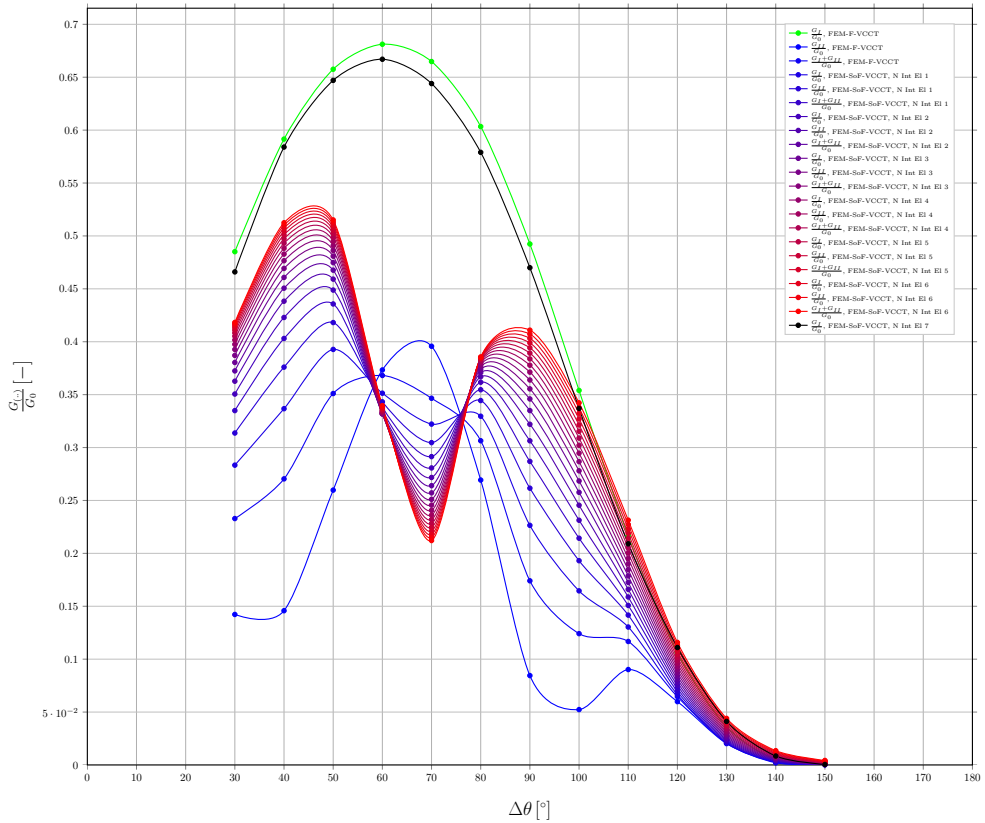

Fading from blue to red for increasing number of integration elements, Virtual Crack Closure Integral (VCCI) from FEM results; in green VCCT from FEM results; in black BEM results

Summary of $G_{(..)}$ from VCCI, stresses extracted on fiber surface,

$\delta = 1.0°$ Normalized energy release rate $\frac{G_{(..)}}{G_0}$ as function of crack angular semi-aperture $\Delta\theta$, calculated with in-house force-based and stress-based VCCT post-processing routines with stresses extracted on the fiber side of the interface

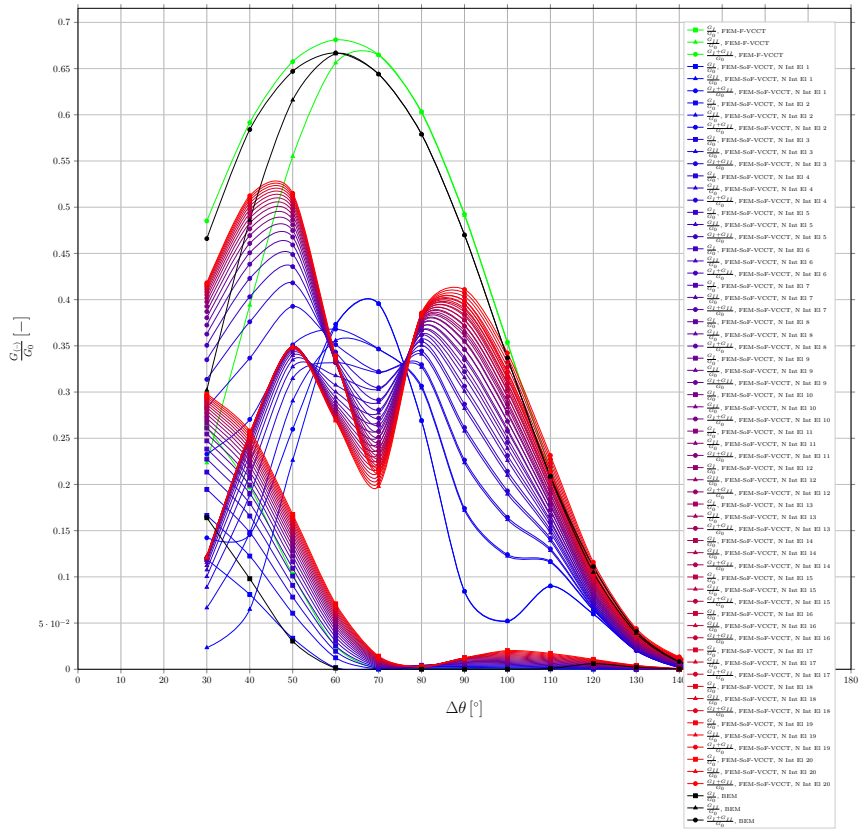

Fading from blue to red for increasing number of integration elements, Virtual Crack Closure Integral (VCCI) from FEM results; in green VCCT from FEM results; in black BEM results.

G_I from VCCI, stresses extracted on matrix surface, $\delta = 1.0°$

Normalized energy release rate $\frac{G_{(\cdot)}}{G_0}$ as function of crack angular semi-aperture $\Delta\theta$, calculated with in-house force-based and stress-based VCCT post-processing routines with stresses extracted on the matrix side of the interface

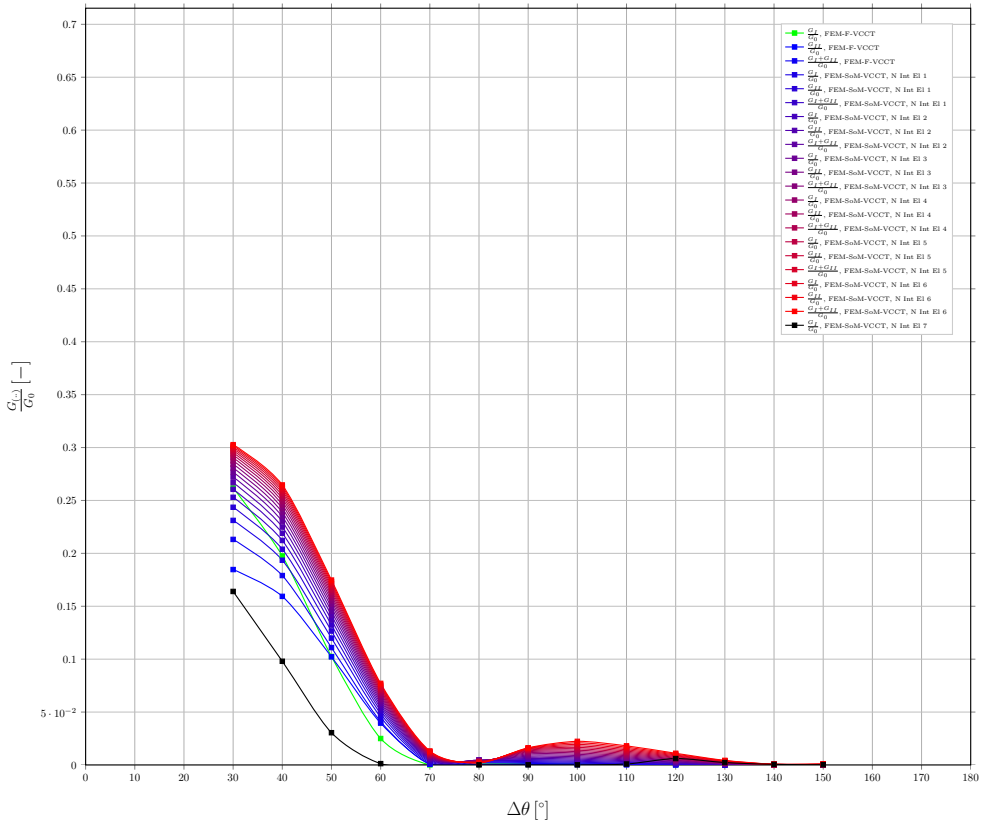

Fading from blue to red for increasing number of integration elements, Virtual Crack Closure Integral (VCCI) from FEM results; in green VCCT from FEM results; in black BEM results

$G_{//}$ from VCCI, stresses extracted on matrix surface, $\delta = 1.0°$

Normalized energy release rate $\frac{G_{(-)}}{G_0}$ as function of crack angular semi-aperture $\Delta\theta$, calculated with in-house force-based and stress-based VCCT post-processing routines with stresses extracted on the matrix side of the interface

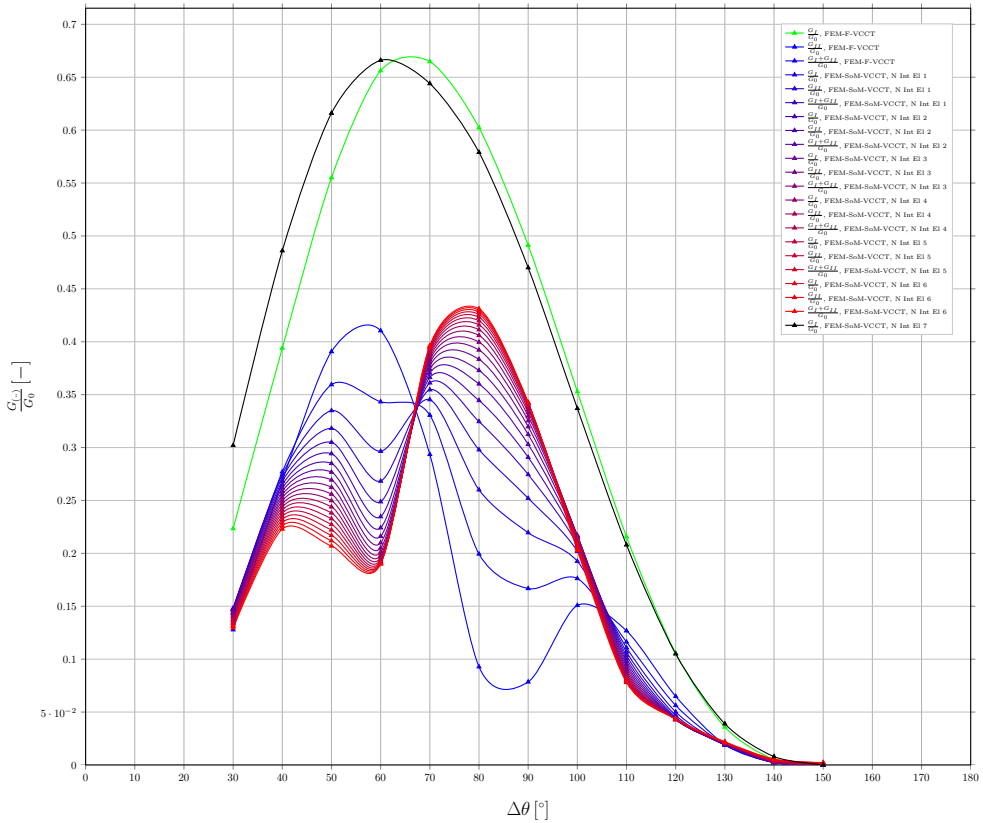

Fading from blue to red for increasing number of integration elements, Virtual Crack Closure Integral (VCCI) from FEM results; in green VCCT from FEM results; in black BEM results

G_{TOT} from VCCI, stresses extracted on matrix surface, $\delta = 1.0°$

Normalized energy release rate $\frac{G_{(-)}}{G_0}$ as function of crack angular semi-aperture $\Delta\theta$, calculated with in-house force-based and stress-based VCCT post-processing routines with stresses extracted on the matrix side of the interface

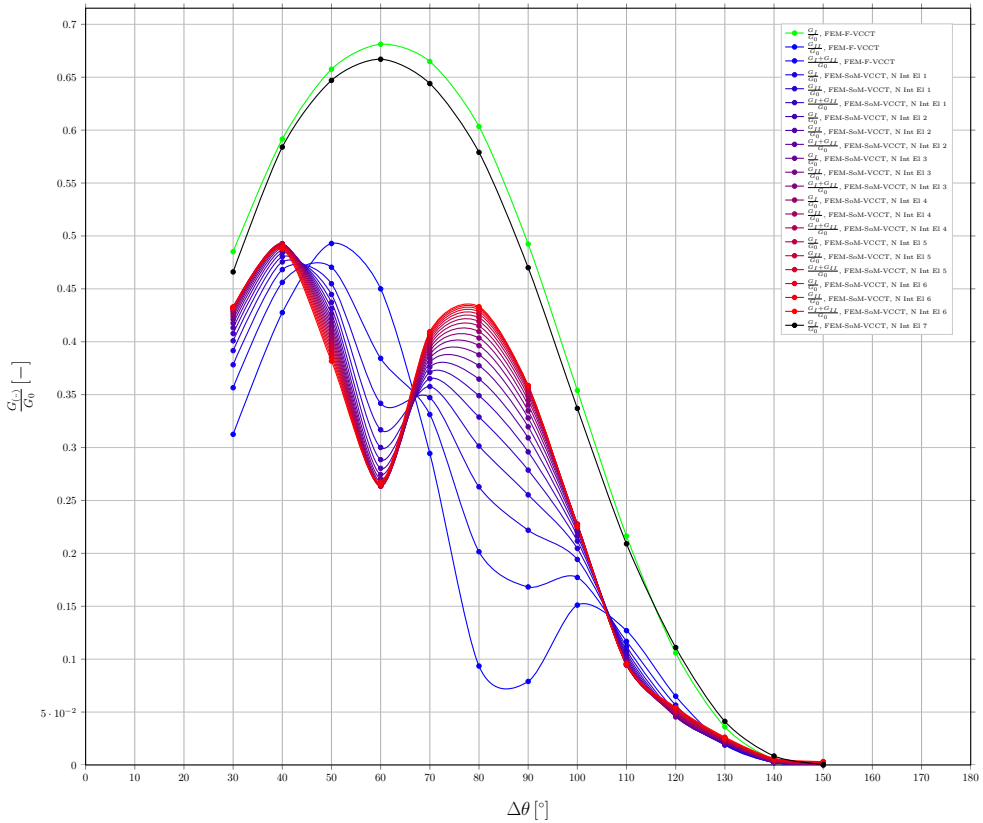

Fading from blue to red for increasing number of integration elements, Virtual Crack Closure Integral (VCCI) from FEM results; in green VCCT from FEM results; in black BEM results

Summary of $G_{(..)}$ from VCCI, stresses extracted on matrix surface,

$\delta = 1.0°$ Normalized energy release rate $\frac{G_{(..)}}{G_0}$ as function of crack angular semi-aperture $\Delta\theta$, calculated with in-house force-based and stress-based VCCT post-processing routines with stresses extracted on the matrix side of the interface

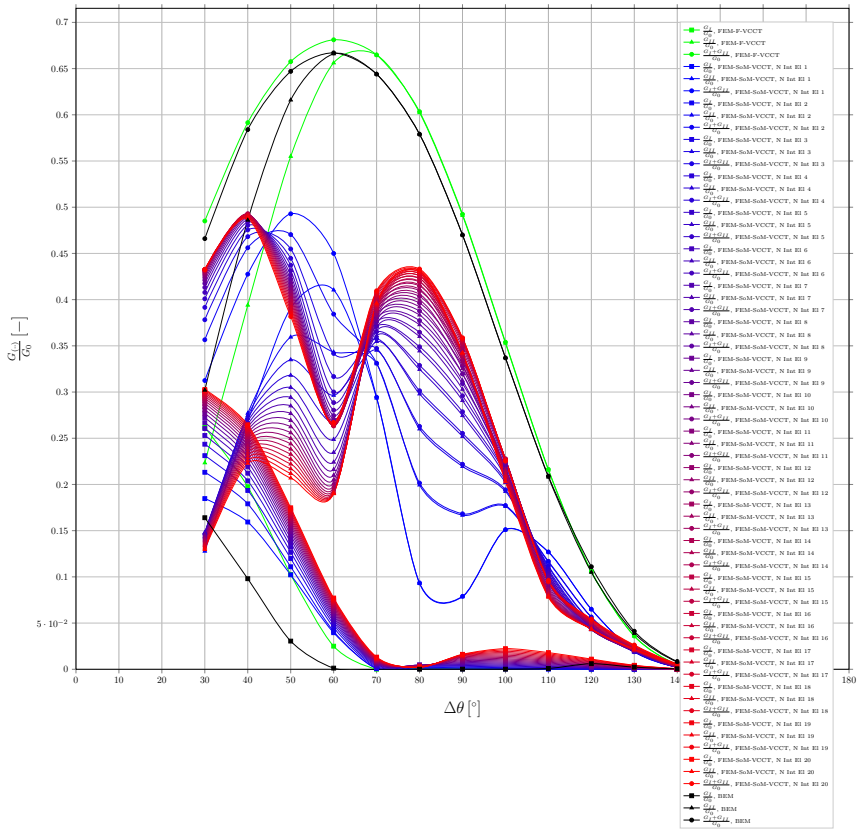

Fading from blue to red for increasing number of integration elements, Virtual Crack Closure Integral (VCCI) from FEM results; in green VCCT from FEM results; in black BEM results.

σ_0, $\delta = 0.9°$

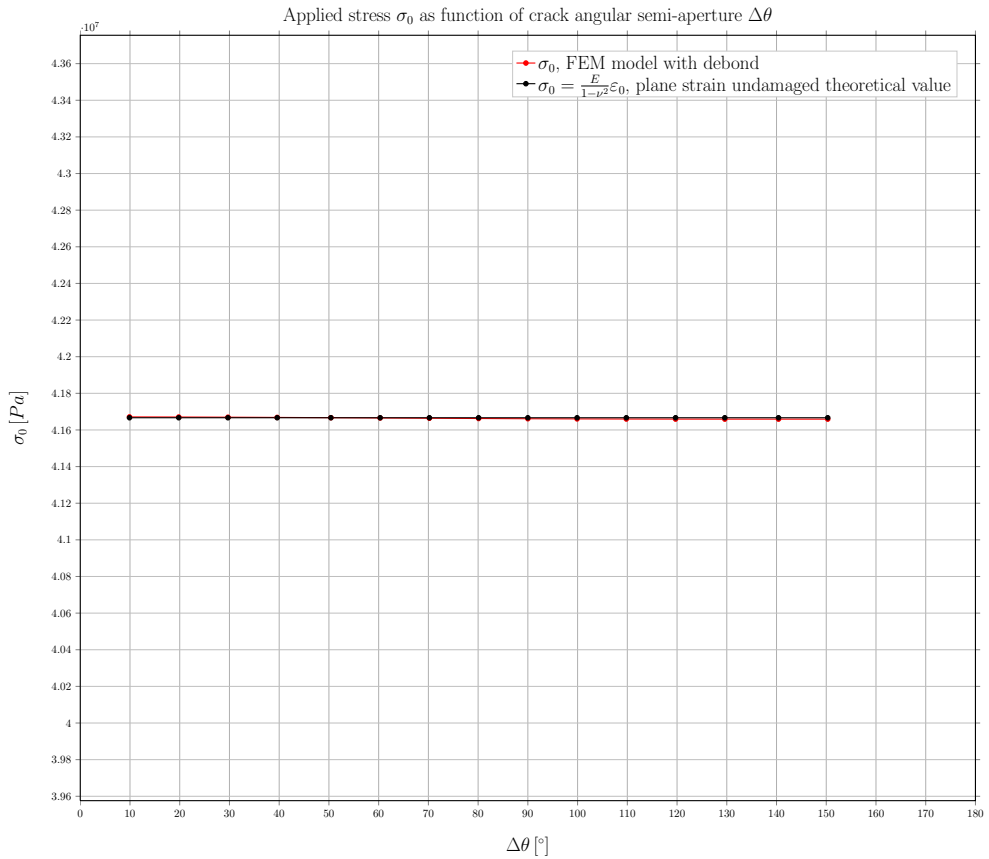

In red small strain FEM, in black analytical plain strain value.

G_0, $\delta = 0.9°$

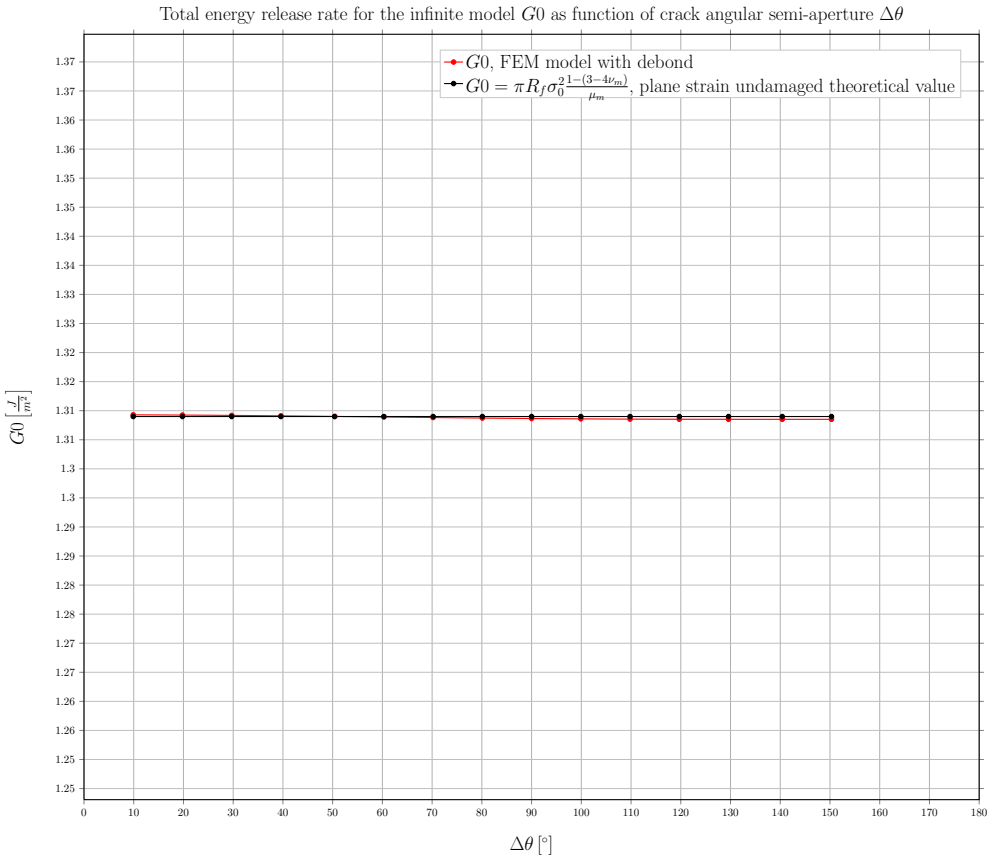

In red small strain FEM, in black analytical plain strain value.

J-Integral (Abaqus built-in routine), $\delta = 0.9°$

Normalized total energy release rate $\frac{G_{TOT}}{G_0}$ as function of crack angular semi-aperture $\Delta\theta$, calculated with Abaqus built-in J-Integral post-processing routine (*CONTOUR INTEGRAL)

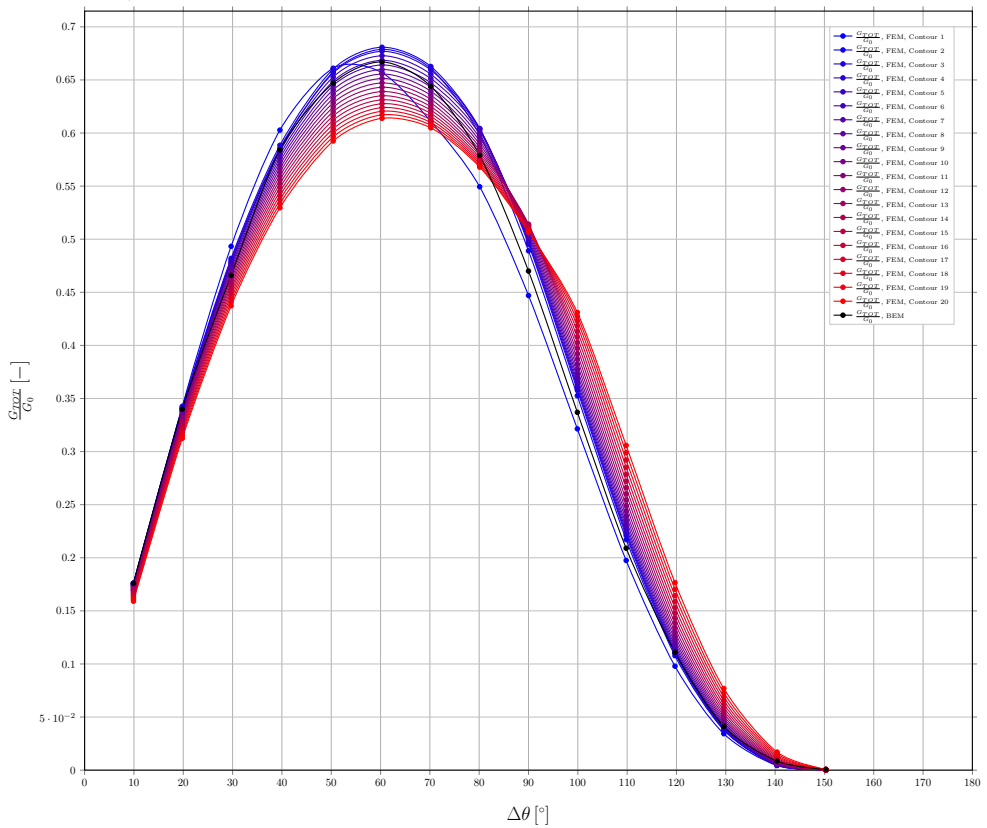

Fading from blue to red for contours further from the crack tip, FEM results; in black BEM results.

VCCT in forces (in-house Python routine), $\delta = 0.9°$

Normalized energy release rate $\frac{G_{(\cdot)}}{G_0}$ as function of crack angular semi-aperture $\Delta\theta$, calculated with in-house force-based VCCT post-processing routine

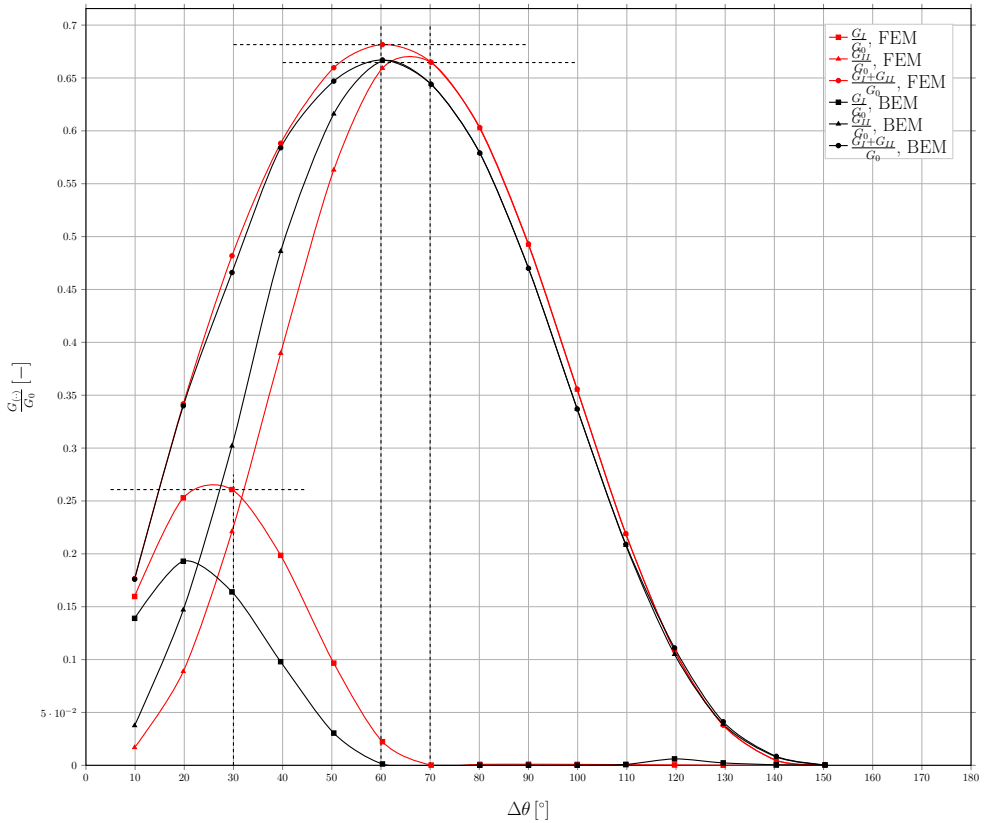

In green VCCT from FEM results, in black BEM results; positions of maxima highlighted by dashed lines.

J-Integral and VCCT in forces, $\delta = 0.9°$

Normalized energy release rate $\frac{G_{(\cdot)}}{G_0}$ as function of crack angular semi-aperture $\Delta\theta$, calculated with in-house force-based VCCT and Abaqus built-in J-Integral (*CONTOUR INTEGRAL) post-processing routines

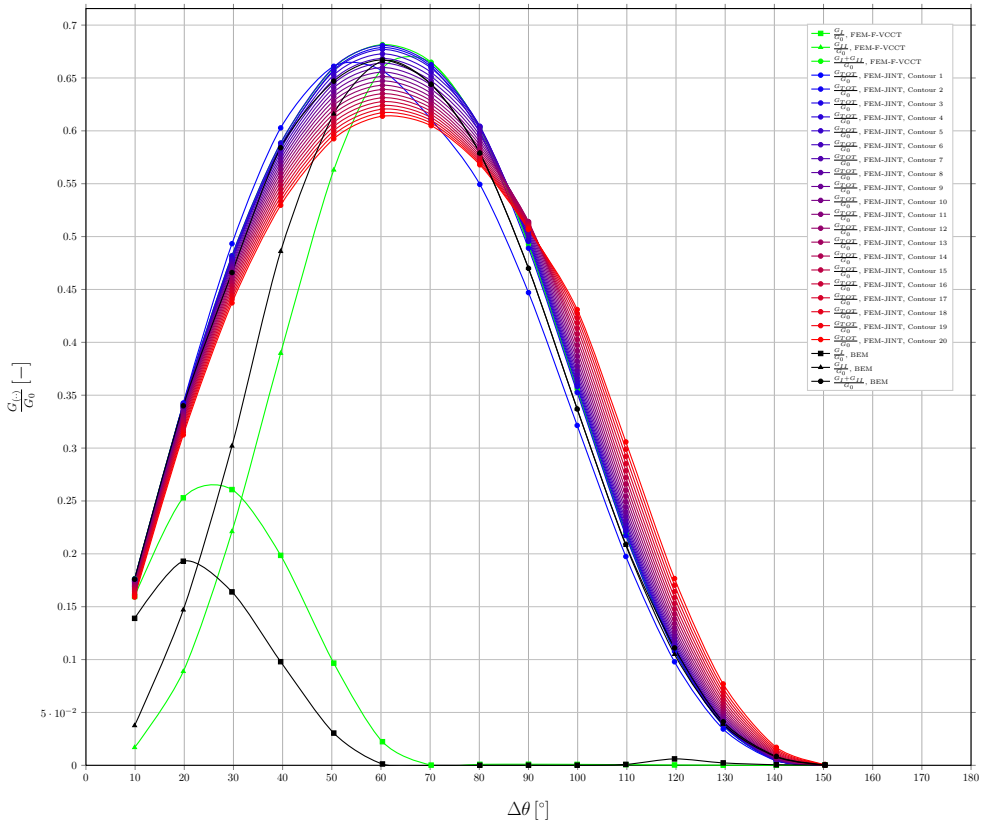

Fading from blue to red for contours further from the crack tip, J-Integral from FEM results; in green VCCT from FEM results; in black BEM results.

G_I from VCCI, stresses extracted on fiber surface, $\delta = 9.0°$

Normalized energy release rate $\frac{G_{(-)}}{G_0}$ as function of crack angular semi-aperture $\Delta\theta$, calculated with in-house force-based and stress-based VCCT post-processing routines with stresses extracted on the fiber side of the interface

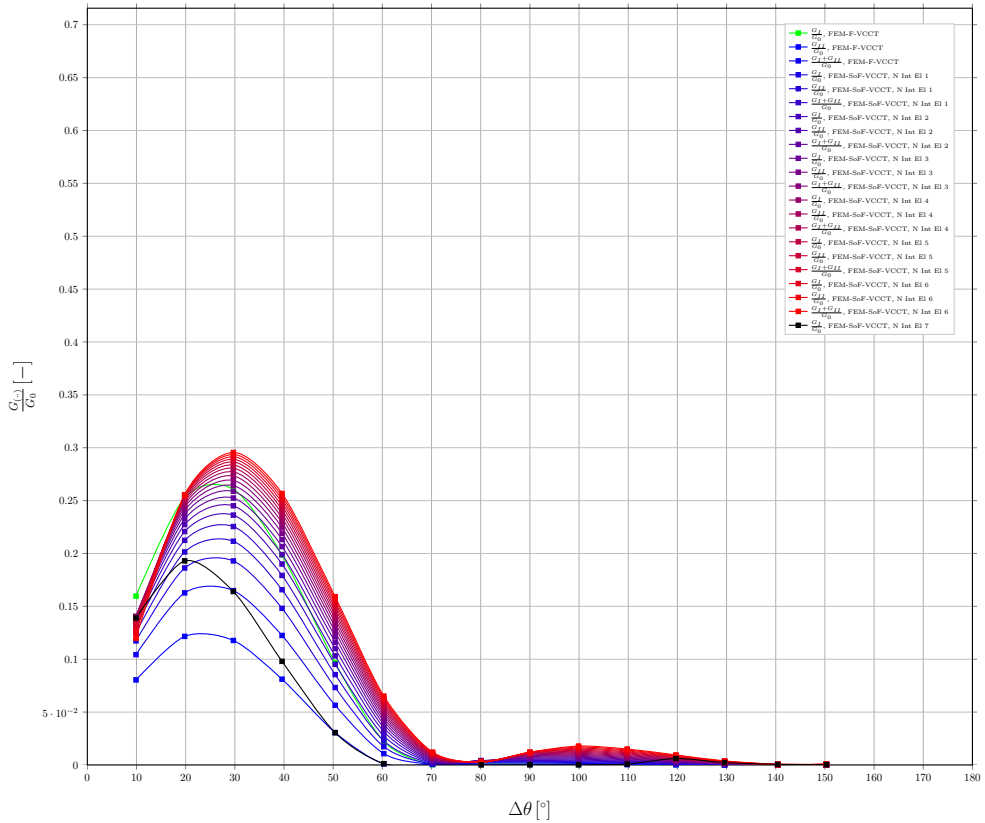

Fading from blue to red for increasing number of integration elements, Virtual Crack Closure Integral (VCCI) from FEM results; in green VCCT from FEM results; in black BEM results

$G_{//}$ from VCCI, stresses extracted on fiber surface, $\delta = 9.0°$

Normalized energy release rate $\frac{G_{(-)}}{G_0}$ as function of crack angular semi-aperture $\Delta\theta$, calculated with in-house force-based and stress-based VCCT post-processing routines with stresses extracted on the fiber side of the interface

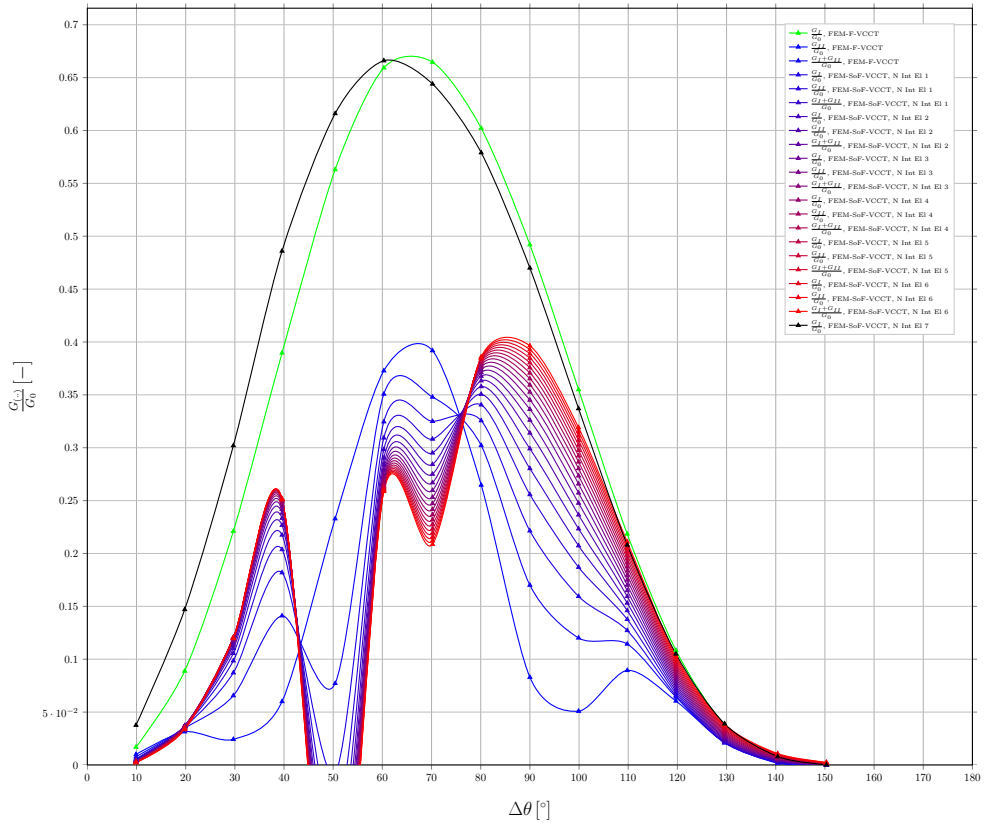

Fading from blue to red for increasing number of integration elements, Virtual Crack Closure Integral (VCCI) from FEM results; in green VCCT from FEM results; in black BEM results

G_{TOT} from VCCI, stresses extracted on fiber surface, $\delta = 9.0°$

Normalized energy release rate $\frac{G_{(\cdot)}}{G_0}$ as function of crack angular semi-aperture $\Delta\theta$, calculated with in-house force-based and stress-based VCCT post-processing routines with stresses extracted on the fiber side of the interface

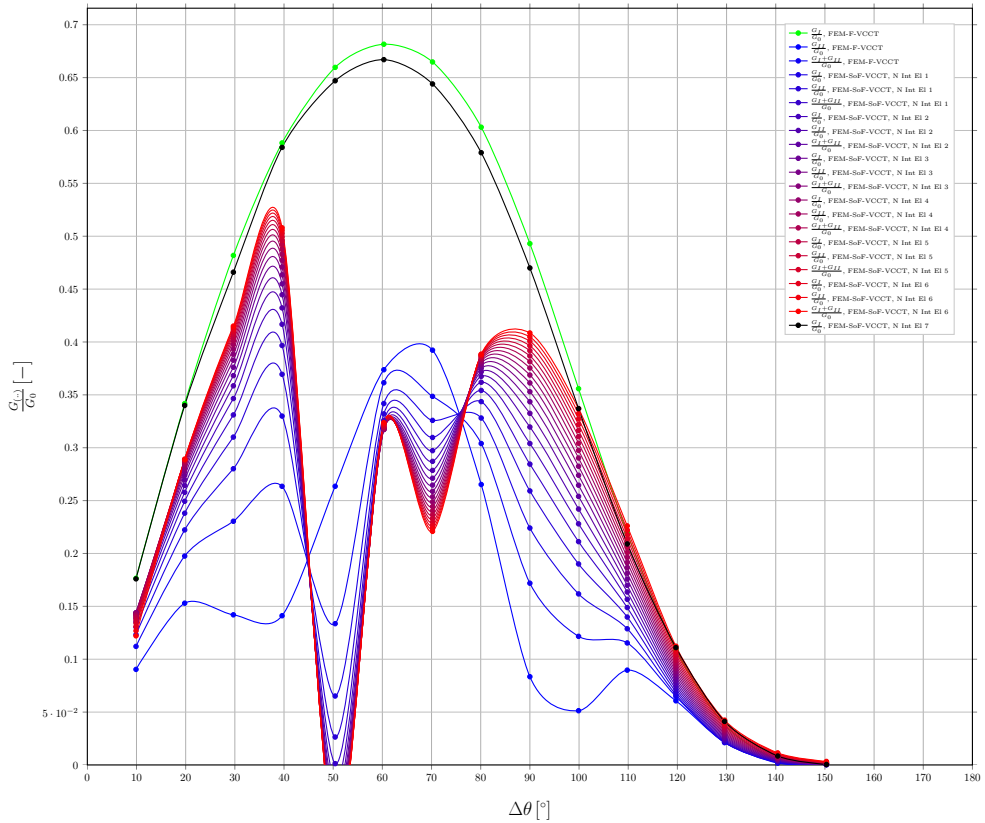

Fading from blue to red for increasing number of integration elements, Virtual Crack Closure Integral (VCCI) from FEM results; in green VCCT from FEM results; in black BEM results

Summary of $G_{(..)}$ from VCCI, stresses extracted on fiber surface,

$\delta = 9.0°$ Normalized energy release rate $\frac{G_{(..)}}{G_0}$ as function of crack angular semi-aperture $\Delta\theta$, calculated with in-house force-based and stress-based VCCT post-processing routines with stresses extracted on the fiber side of the interface

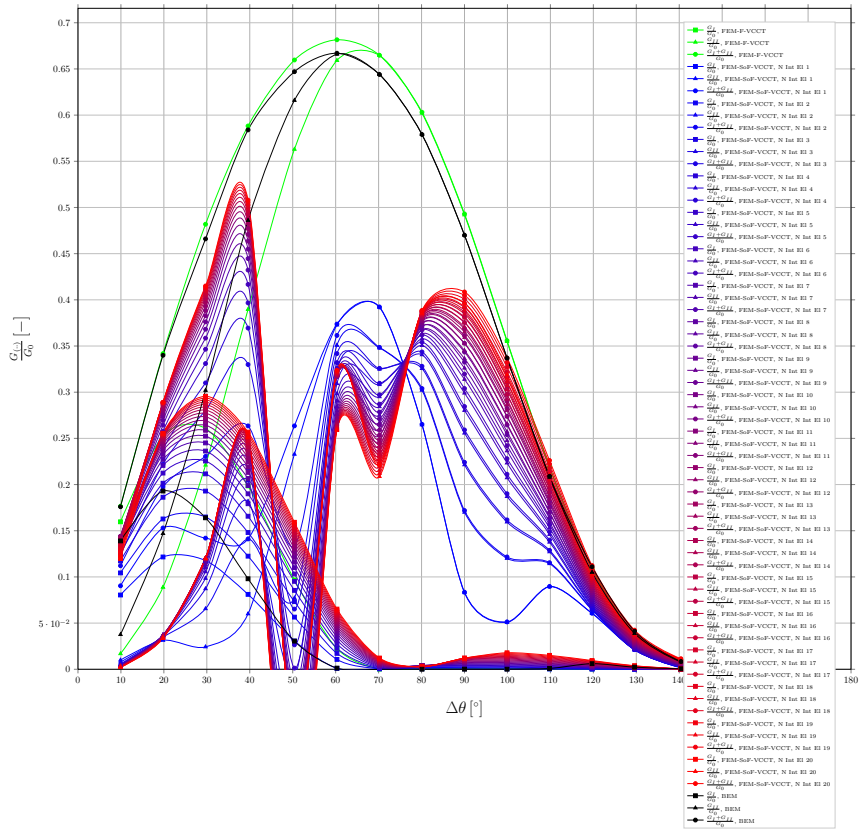

Fading from blue to red for increasing number of integration elements, Virtual Crack Closure Integral (VCCI) from FEM results; in green VCCT from FEM results; in black BEM results.

G_I from VCCI, stresses extracted on matrix surface, $\delta = 9.0°$

Normalized energy release rate $\frac{G_{(\cdot)}}{G_0}$ as function of crack angular semi-aperture $\Delta\theta$, calculated with in-house force-based and stress-based VCCT post-processing routines with stresses extracted on the matrix side of the interface

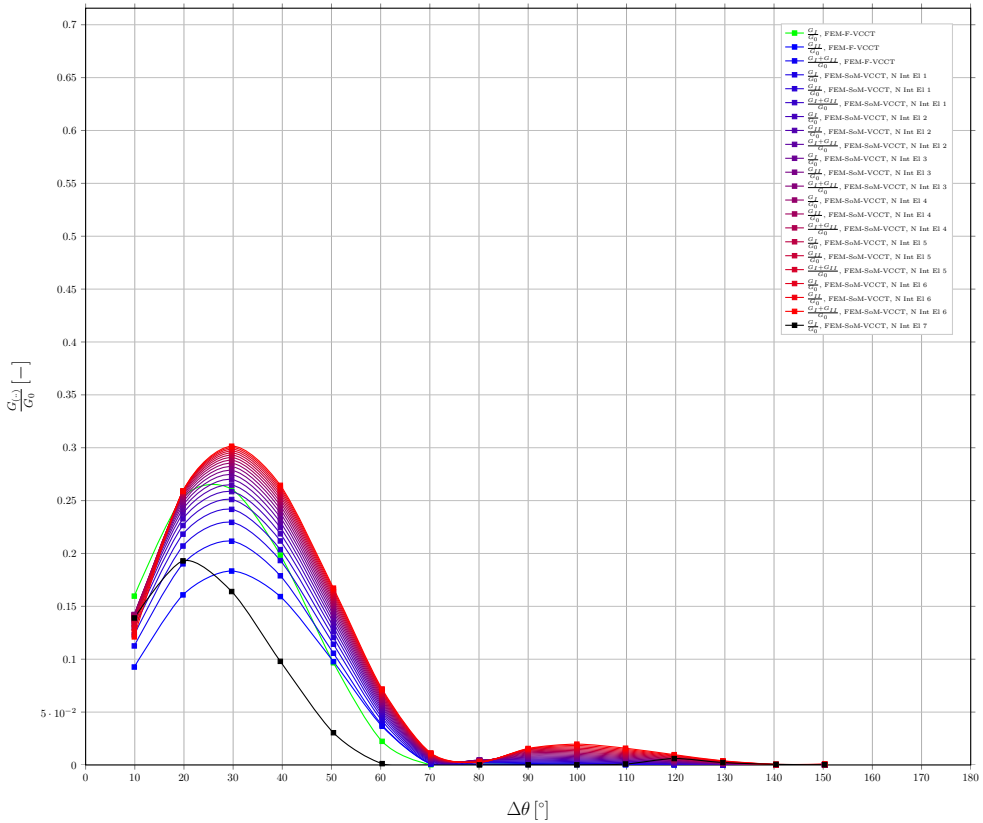

Fading from blue to red for increasing number of integration elements, Virtual Crack Closure Integral (VCCI) from FEM results; in green VCCT from FEM results; in black BEM results

G_{II} from VCCI, stresses extracted on matrix surface, $\delta = 9.0°$

Normalized energy release rate $\frac{G_{(\cdot)}}{G_0}$ as function of crack angular semi-aperture $\Delta\theta$, calculated with in-house force-based and stress-based VCCT post-processing routines with stresses extracted on the matrix side of the interface

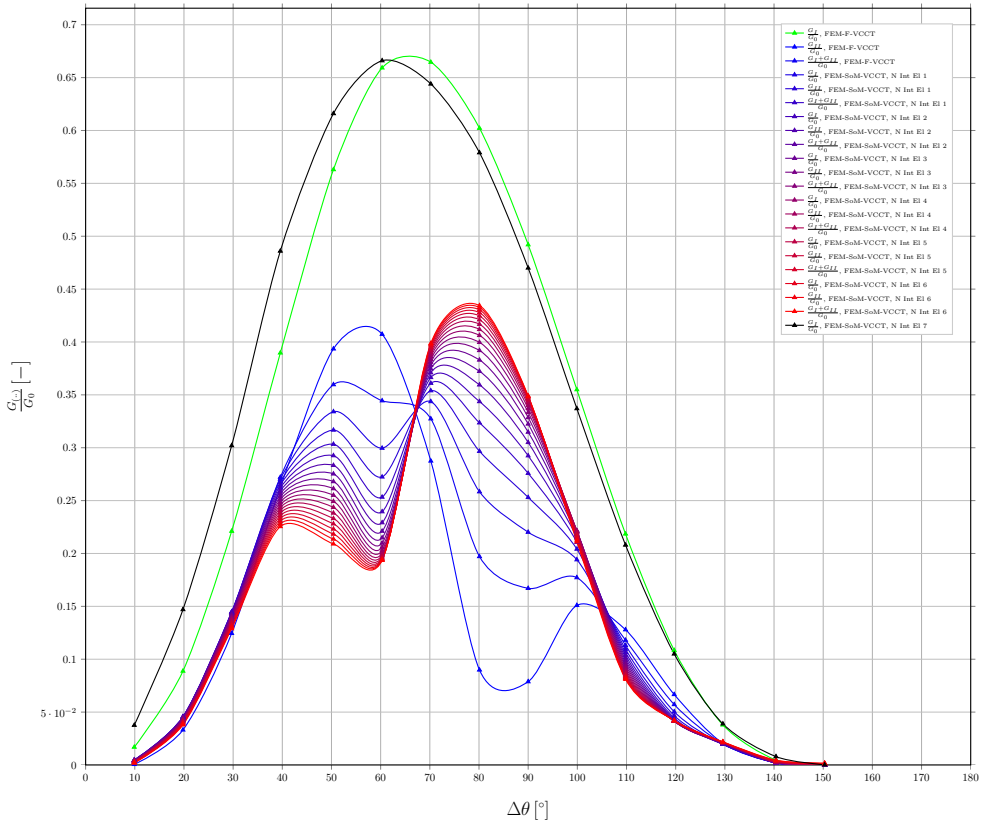

Fading from blue to red for increasing number of integration elements, Virtual Crack Closure Integral (VCCI) from FEM results; in green VCCT from FEM results; in black BEM results.

G_{TOT} from VCCI, stresses extracted on matrix surface, $\delta = 9.0°$

Normalized energy release rate $\frac{G_{(-)}}{G_0}$ as function of crack angular semi-aperture $\Delta\theta$, calculated with in-house force-based and stress-based VCCT post-processing routines with stresses extracted on the matrix side of the interface

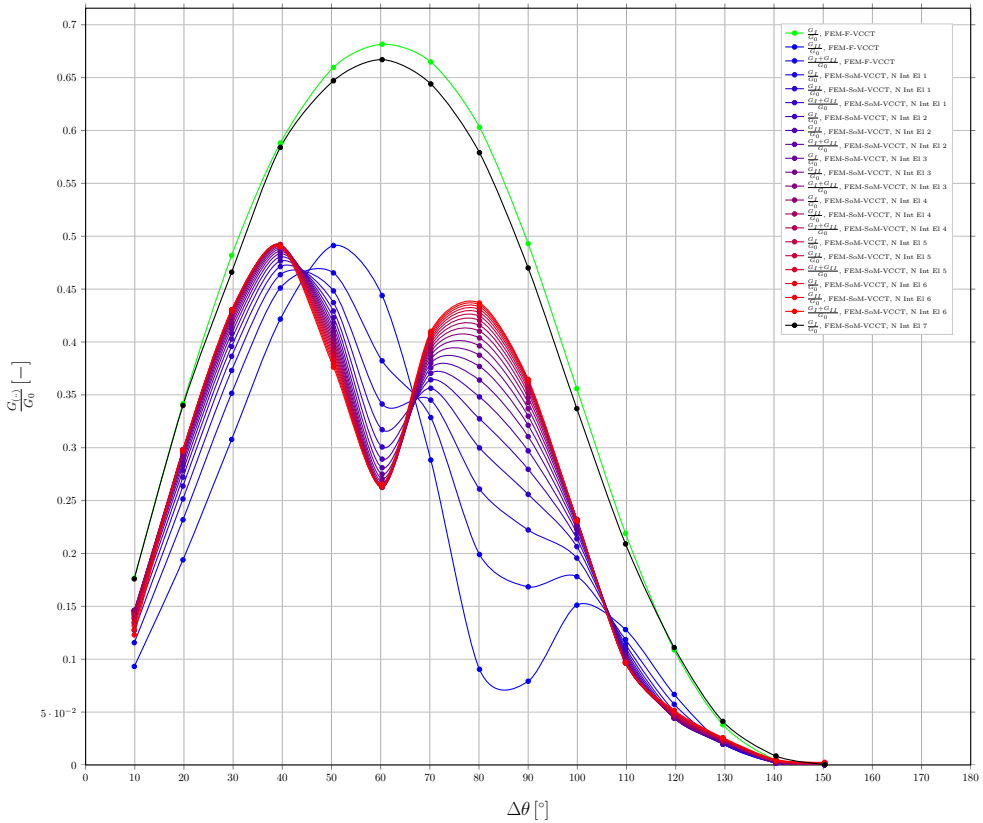

Fading from blue to red for increasing number of integration elements, Virtual Crack Closure Integral (VCCI) from FEM results; in green VCCT from FEM results; in black BEM results.

Summary of $G_{(..)}$ from VCCI, stresses extracted on matrix surface,

$\delta = 9.0°$

Normalized energy release rate $\frac{G_{(..)}}{G_0}$ as function of crack angular semi-aperture $\Delta\theta$, calculated with in-house force-based and stress-based VCCT post-processing routines with stresses extracted on the matrix side of the interface

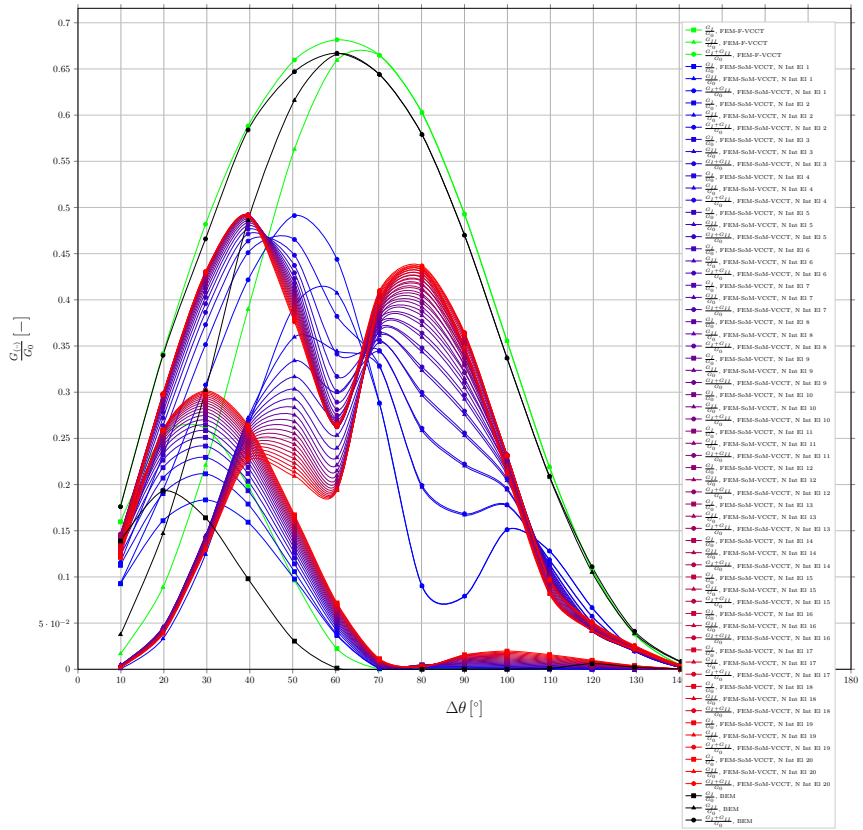

Fading from blue to red for increasing number of integration elements, Virtual Crack Closure Integral (VCCI) from FEM results; in green VCCT from FEM results; in black BEM results.

σ_0, $\delta = 0.8°$

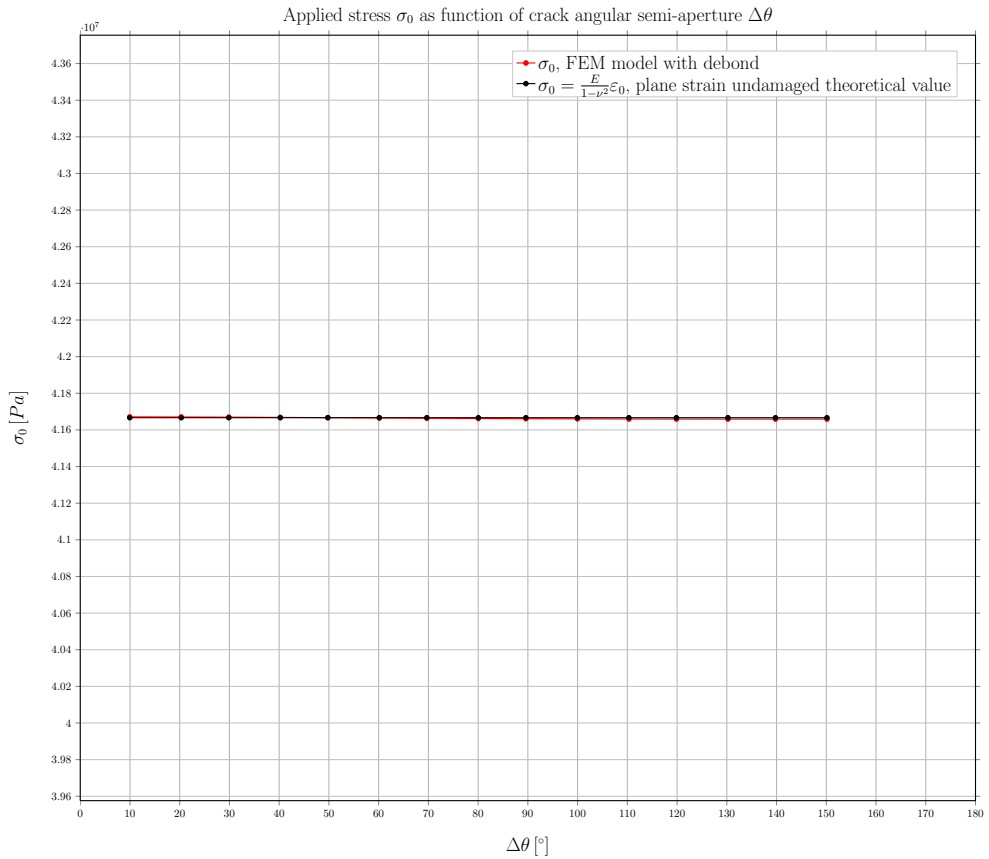

In red small strain FEM, in black analytical plain strain value.

G_0, $\delta = 0.8°$

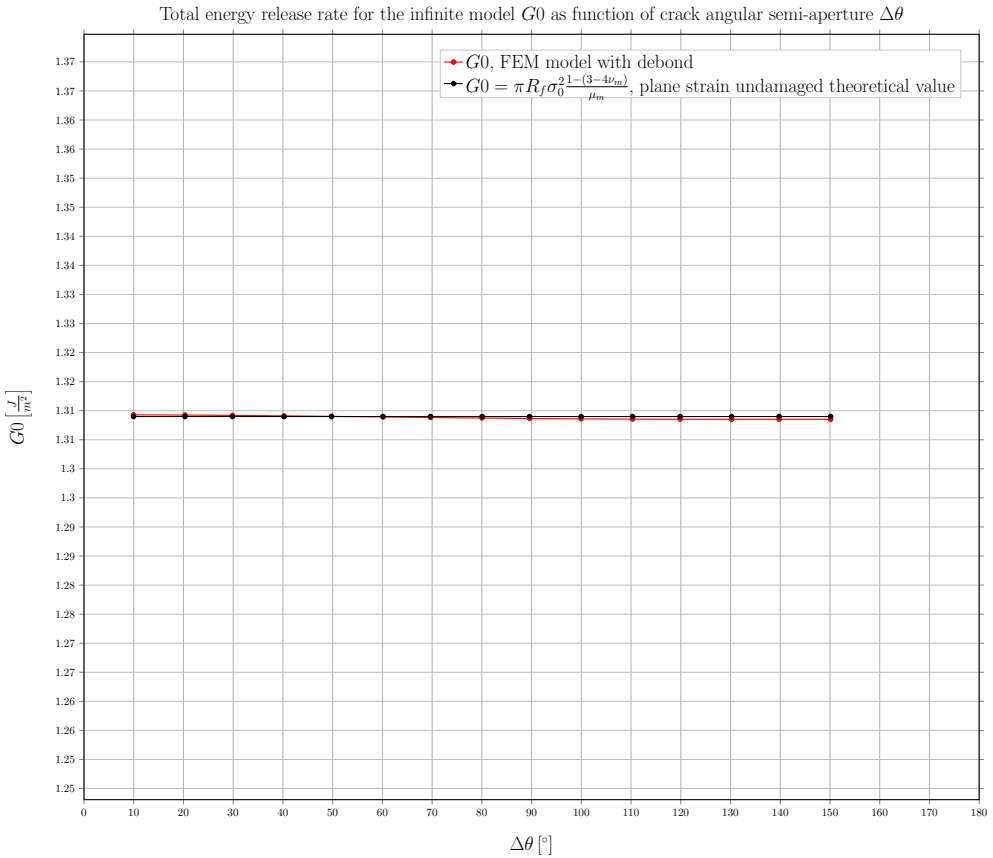

In red small strain FEM, in black analytical plain strain value.

J-Integral (Abaqus built-in routine), $\delta = 0.8°$

Normalized total energy release rate $\frac{G_{TOT}}{G_0}$ as function of crack angular semi-aperture $\Delta\theta$, calculated with Abaqus built-in J-Integral post-processing routine (*CONTOUR INTEGRAL)

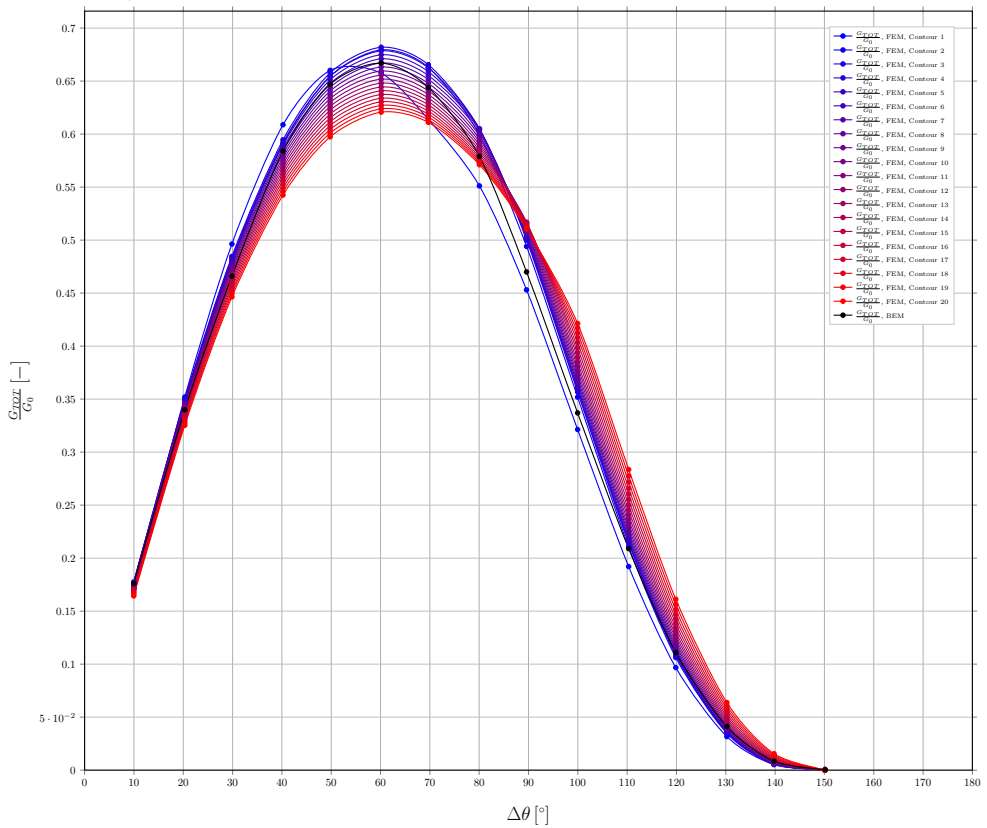

Fading from blue to red for contours further from the crack tip, FEM results; in black BEM results.

VCCT in forces (in-house Python routine), $\delta = 0.8°$

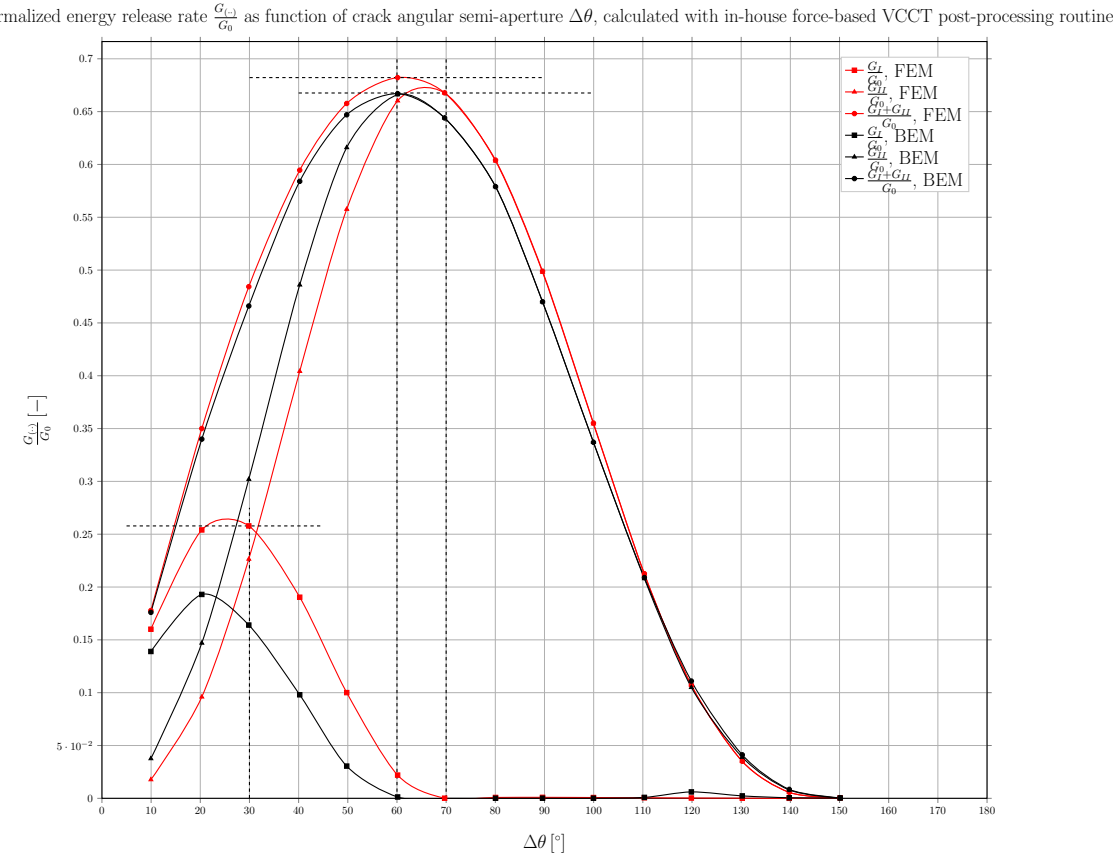

In green VCCT from FEM results, in black BEM results; positions of maxima highlighted by dashed lines.

J-Integral and VCCT in forces, $\delta = 0.8°$

Normalized energy release rate $\frac{G_{(\cdot)}}{G_0}$ as function of crack angular semi-aperture $\Delta\theta$, calculated with in-house force-based VCCT and Abaqus built-in J-Integral (*CONTOUR INTEGRAL) post-processing routines

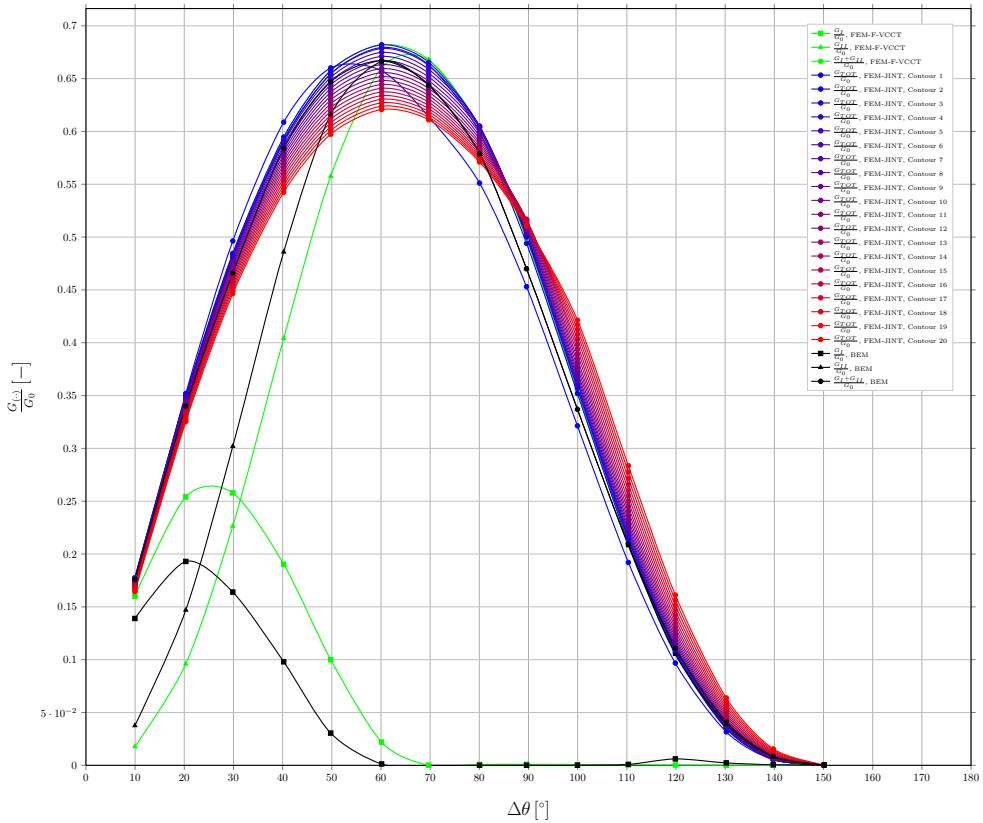

Fading from blue to red for contours further from the crack tip, J-Integral from FEM results; in green VCCT from FEM results; in black BEM results.

G_I from VCCI, stresses extracted on fiber surface, $\delta = 8.0°$

Normalized energy release rate $\frac{G_{(\cdot)}}{G_0}$ as function of crack angular semi-aperture $\Delta\theta$, calculated with in-house force-based and stress-based VCCT post-processing routines with stresses extracted on the fiber side of the interface

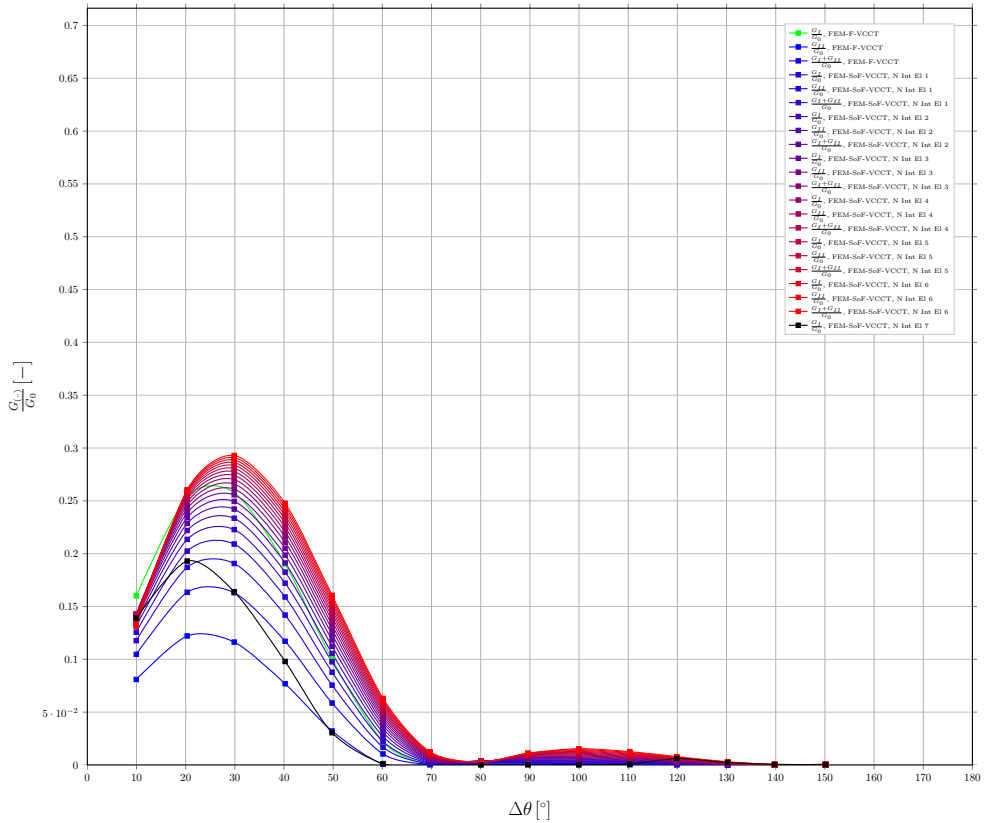

Fading from blue to red for increasing number of integration elements, Virtual Crack Closure Integral (VCCI) from FEM results; in green VCCT from FEM results; in black BEM results

$G_{//}$ from VCCI, stresses extracted on fiber surface, $\delta = 8.0°$

Normalized energy release rate $\frac{G_{(-)}}{G_0}$ as function of crack angular semi-aperture $\Delta\theta$, calculated with in-house force-based and stress-based VCCT post-processing routines with stresses extracted on the fiber side of the interface

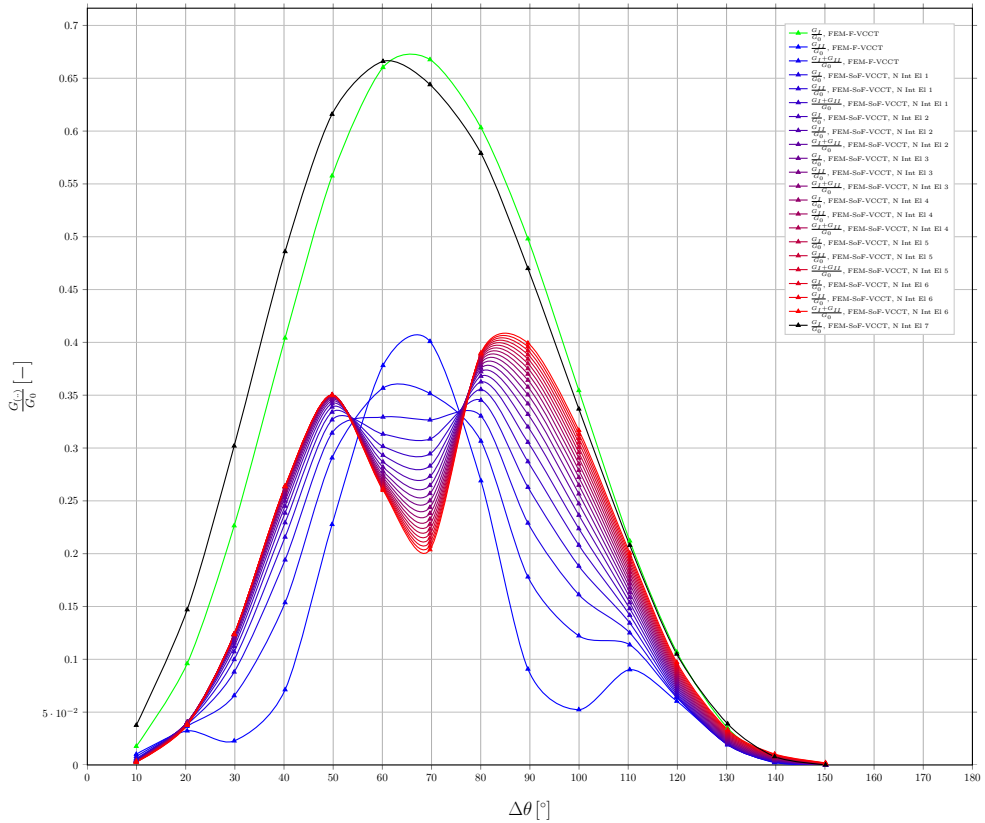

Fading from blue to red for increasing number of integration elements, Virtual Crack Closure Integral (VCCI) from FEM results; in green VCCT from FEM results; in black BEM results

G_{TOT} from VCCI, stresses extracted on fiber surface, $\delta = 8.0°$

Normalized energy release rate $\frac{G_{(-)}}{G_0}$ as function of crack angular semi-aperture $\Delta\theta$, calculated with in-house force-based and stress-based VCCT post-processing routines with stresses extracted on the fiber side of the interface

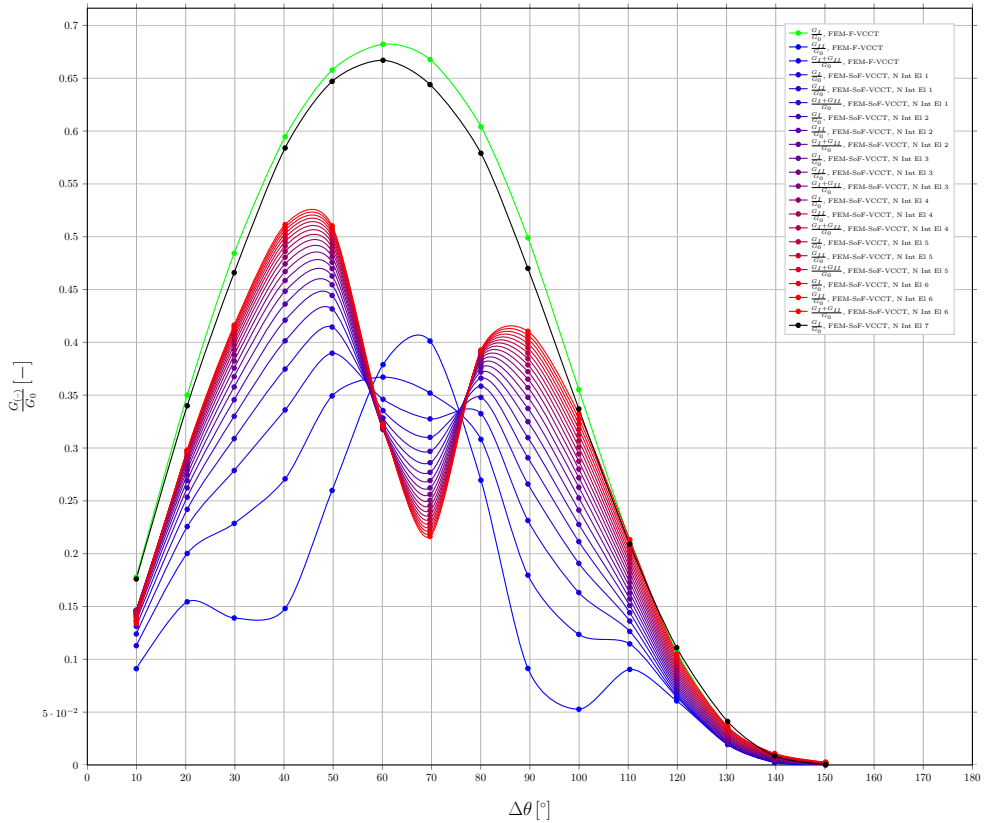

Fading from blue to red for increasing number of integration elements, Virtual Crack Closure Integral (VCCI) from FEM results; in green VCCT from FEM results; in black BEM results

Summary of $G_{(..)}$ from VCCI, stresses extracted on fiber surface,

$\delta = 8.0°$ Normalized energy release rate $\frac{G_{(..)}}{G_0}$ as function of crack angular semi-aperture $\Delta\theta$, calculated with in-house force-based and stress-based VCCT post-processing routines with stresses extracted on the fiber side of the interface

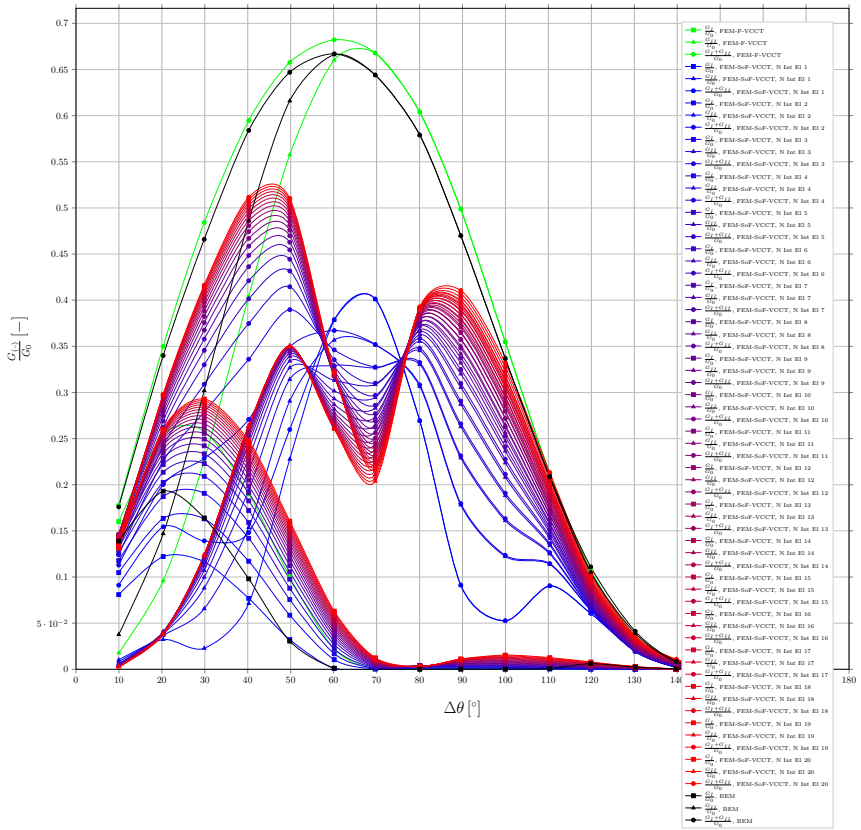

Fading from blue to red for increasing number of integration elements, Virtual Crack Closure Integral (VCCI) from FEM results; in green VCCT from FEM results; in black BEM results.

G_I from VCCI, stresses extracted on matrix surface, $\delta = 8.0°$

Normalized energy release rate $\frac{G_{(-)}}{G_0}$ as function of crack angular semi-aperture $\Delta\theta$, calculated with in-house force-based and stress-based VCCT post-processing routines with stresses extracted on the matrix side of the interface

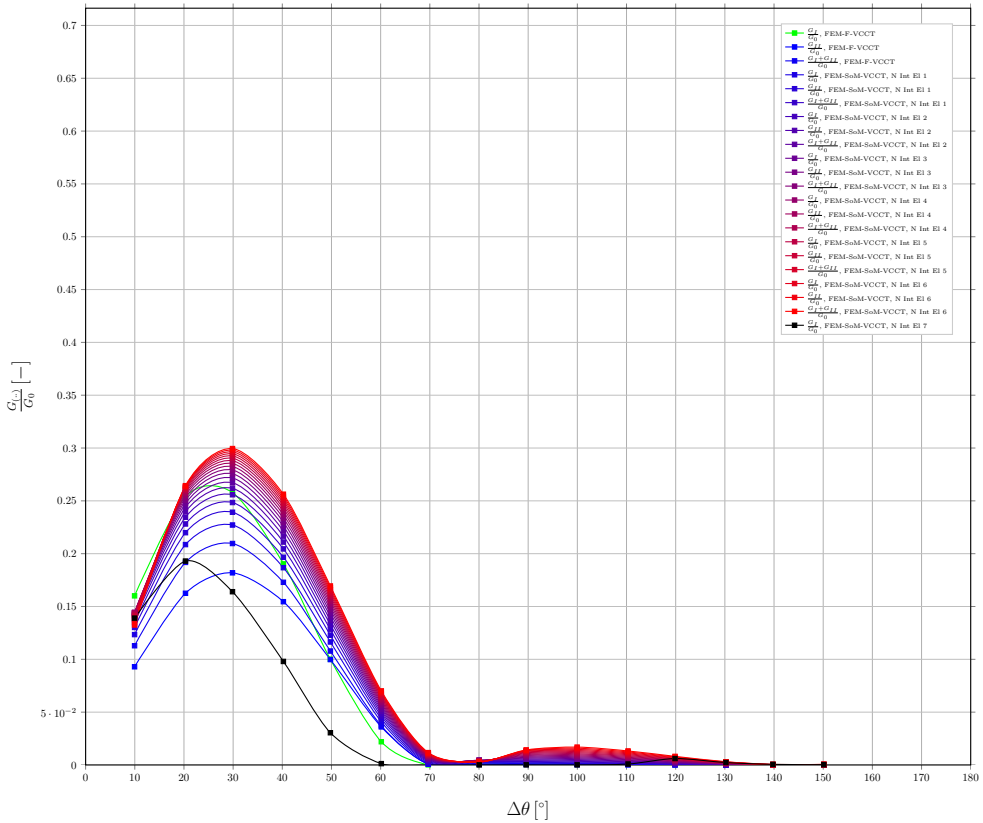

Fading from blue to red for increasing number of integration elements, Virtual Crack Closure Integral (VCCI) from FEM results; in green VCCT from FEM results; in black BEM results

$G_{//}$ from VCCI, stresses extracted on matrix surface, $\delta = 8.0°$

Normalized energy release rate $\frac{G_{(-)}}{G_0}$ as function of crack angular semi-aperture $\Delta\theta$, calculated with in-house force-based and stress-based VCCT post-processing routines with stresses extracted on the matrix side of the interface

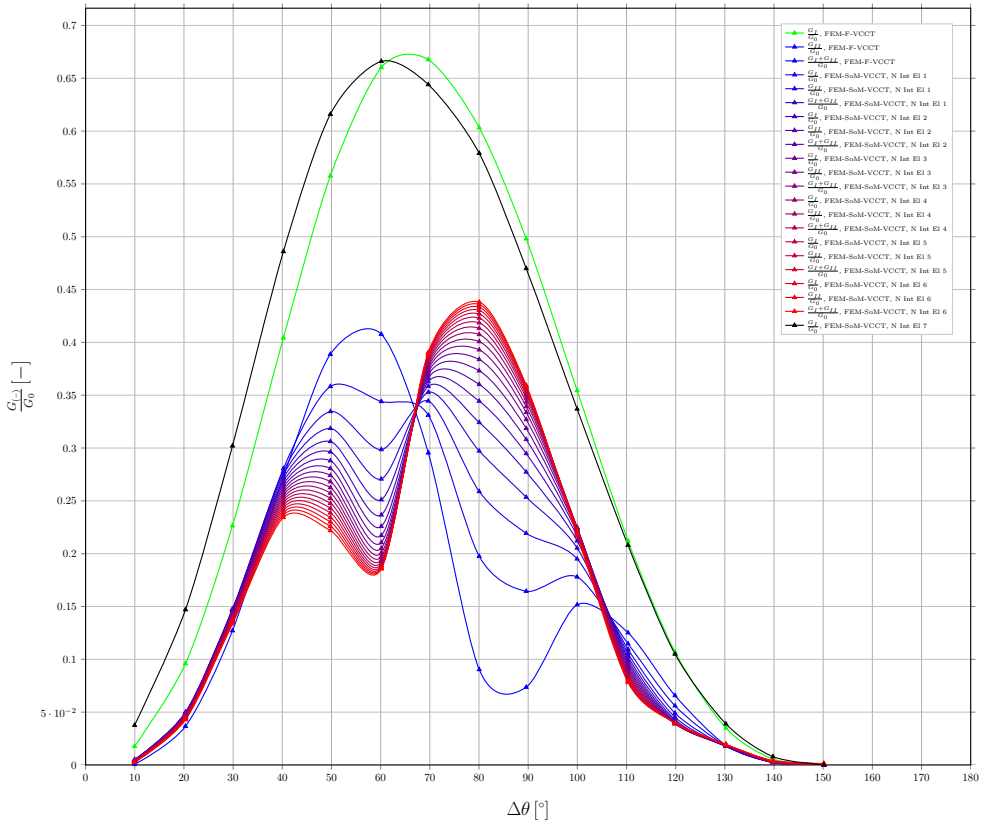

Fading from blue to red for increasing number of integration elements, Virtual Crack Closure Integral (VCCI) from FEM results; in green VCCT from FEM results; in black BEM results

G_{TOT} from VCCI, stresses extracted on matrix surface, $\delta = 8.0°$

Normalized energy release rate $\frac{G_{(-)}}{G_0}$ as function of crack angular semi-aperture $\Delta\theta$, calculated with in-house force-based and stress-based VCCT post-processing routines with stresses extracted on the matrix side of the interface

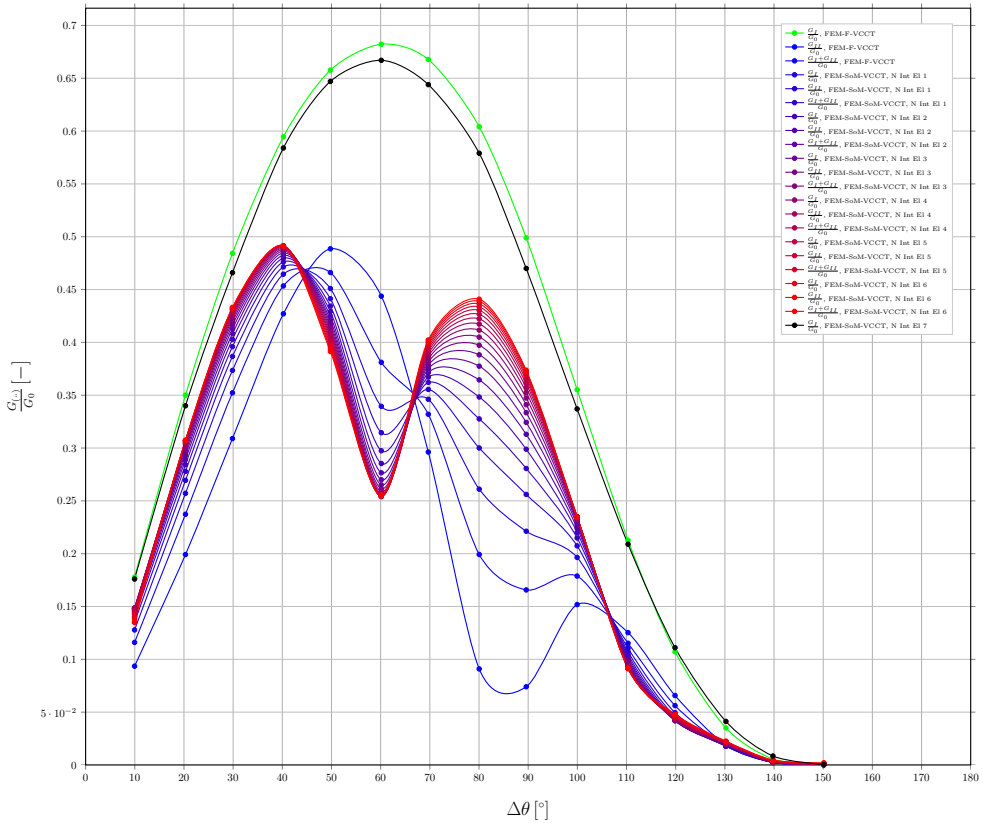

Fading from blue to red for increasing number of integration elements, Virtual Crack Closure Integral (VCCI) from FEM results; in green VCCT from FEM results; in black BEM results.

Summary of $G_{(..)}$ from VCCI, stresses extracted on matrix surface,

$\delta = 8.0°$ Normalized energy release rate $\frac{G_{(..)}}{G_0}$ as function of crack angular semi-aperture $\Delta\theta$, calculated with in-house force-based and stress-based VCCT post-processing routines with stresses extracted on the matrix side of the interface

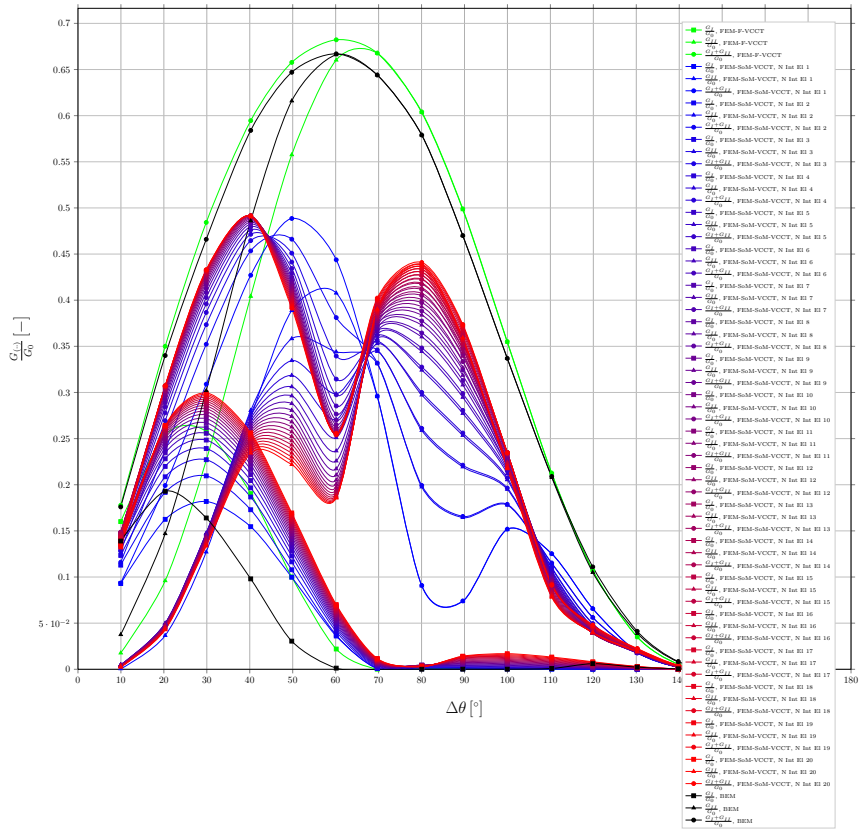

Fading from blue to red for increasing number of integration elements, Virtual Crack Closure Integral (VCCI) from FEM results; in green VCCT from FEM results; in black BEM results.

σ_0, $\delta = 0.7°$

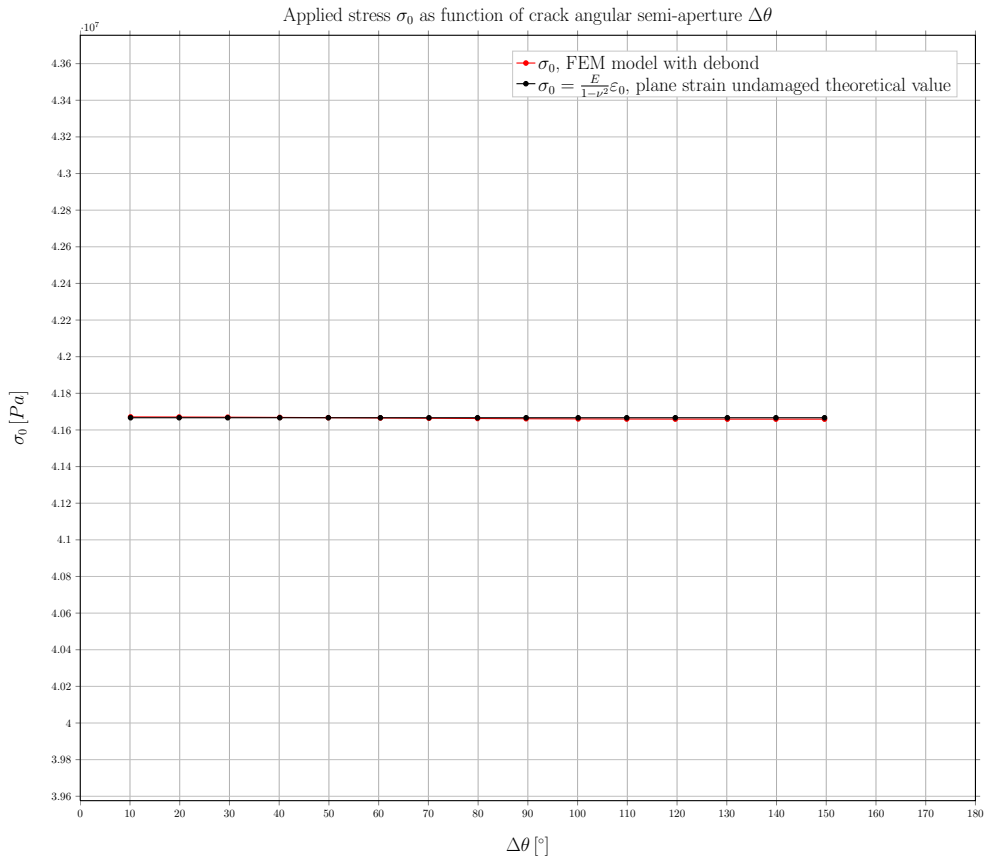

In red small strain FEM, in black analytical plain strain value.

G_0, $\delta = 0.7°$

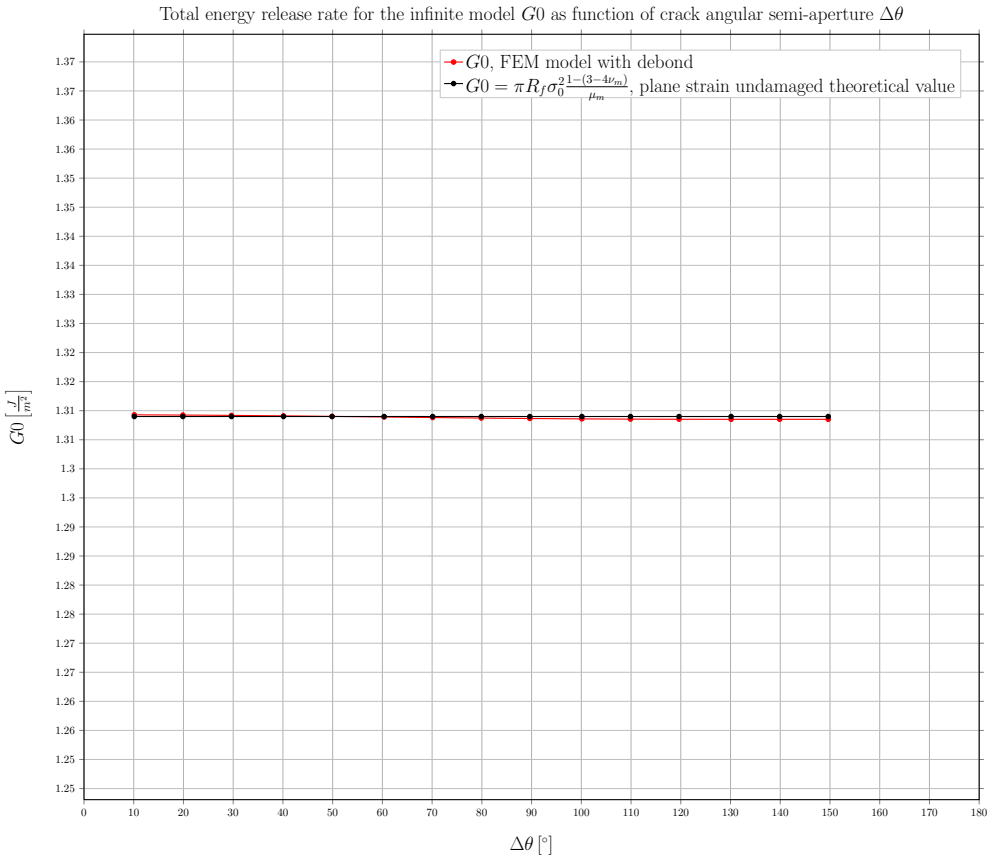

In red small strain FEM, in black analytical plain strain value.

J-Integral (Abaqus built-in routine), $\delta = 0.7°$

Normalized total energy release rate $\frac{G_{TOT}}{G_0}$ as function of crack angular semi-aperture $\Delta\theta$, calculated with Abaqus built-in J-Integral post-processing routine (*CONTOUR INTEGRAL)

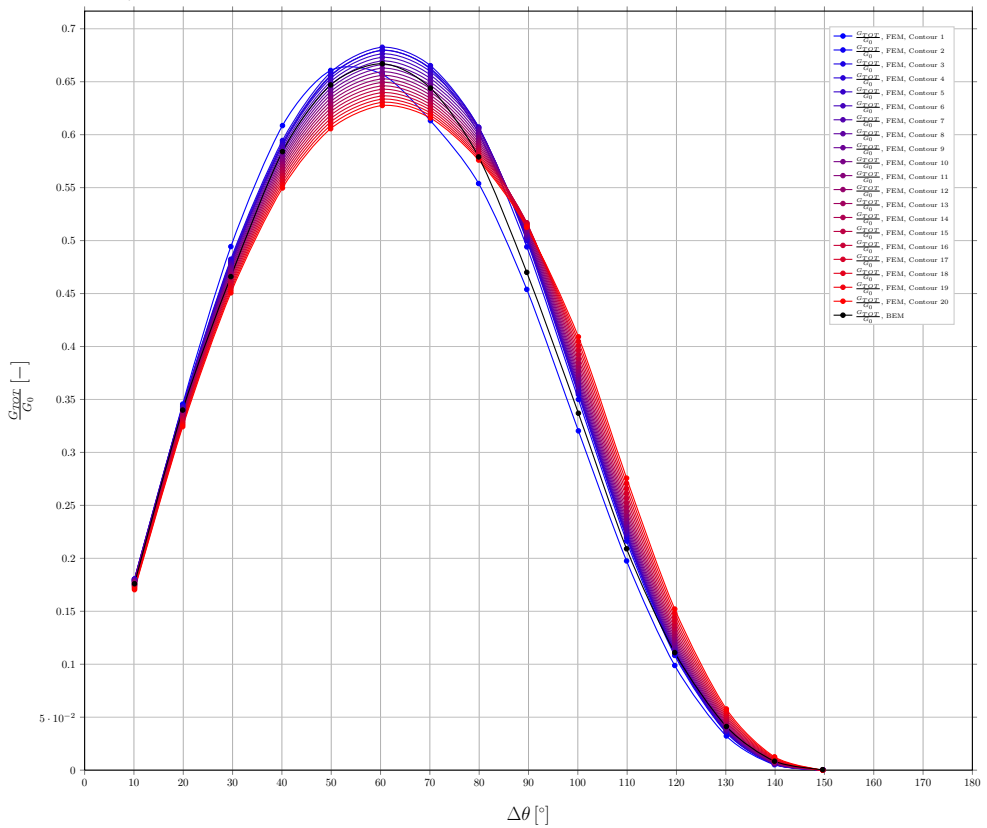

Fading from blue to red for contours further from the crack tip, FEM results; in black BEM results.

VCCT in forces (in-house Python routine), $\delta = 0.7°$

Normalized energy release rate $\frac{G_{(\cdot)}}{G_0}$ as function of crack angular semi-aperture $\Delta\theta$, calculated with in-house force-based VCCT post-processing routine

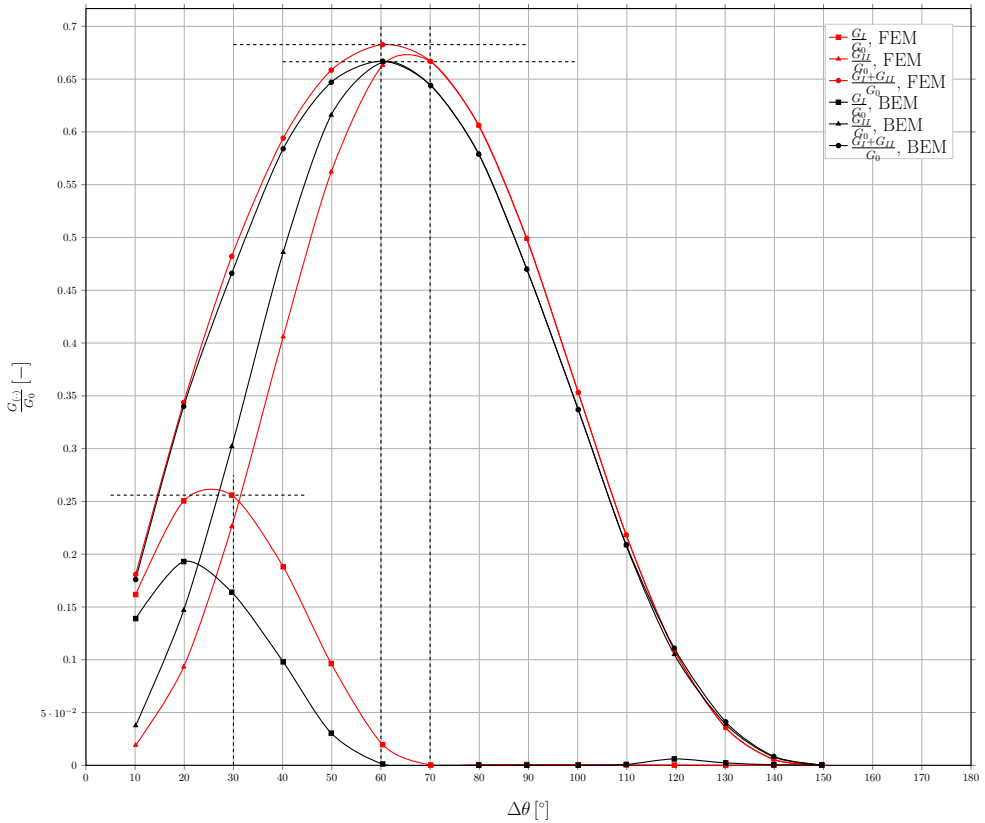

In green VCCT from FEM results, in black BEM results; positions of maxima highlighted by dashed lines.

J-Integral and VCCT in forces, $\delta = 0.7°$

Normalized energy release rate $\frac{G_{(-)}}{G_0}$ as function of crack angular semi-aperture $\Delta\theta$, calculated with in-house force-based VCCT and Abaqus built-in J-Integral (*CONTOUR INTEGRAL) post-processing routines

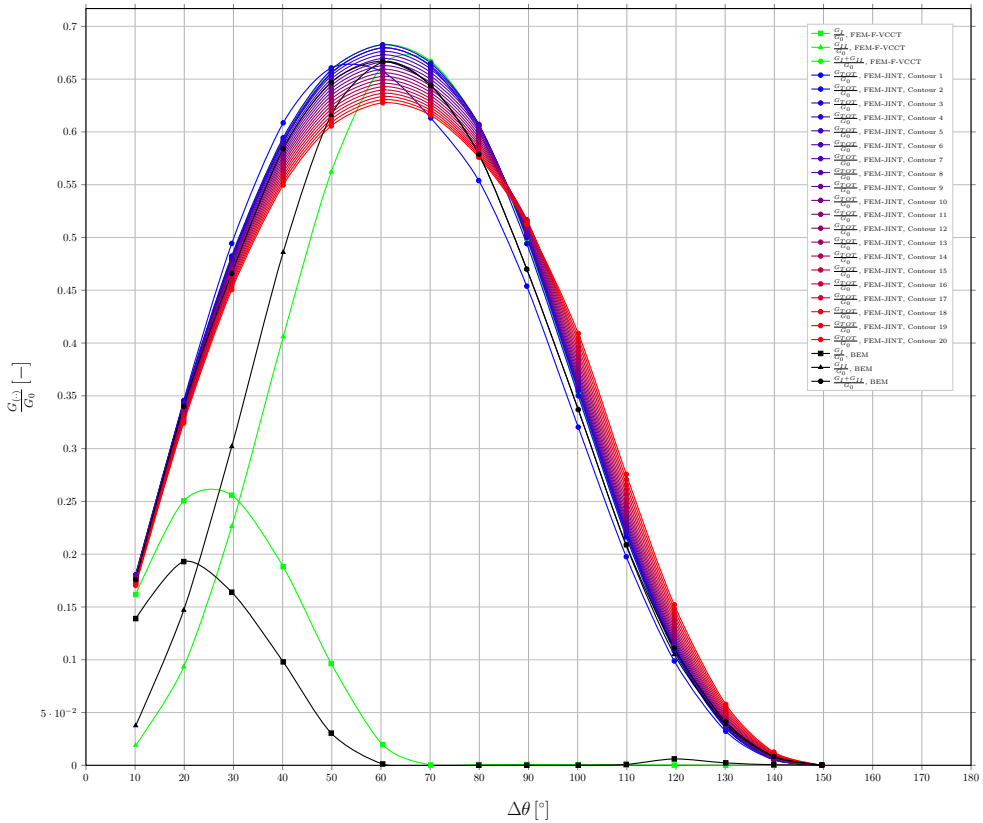

Fading from blue to red for contours further from the crack tip, J-Integral from FEM results; in green VCCT from FEM results; in black BEM results.

G_I from VCCI, stresses extracted on fiber surface, $\delta = 7.0°$

Normalized energy release rate $\frac{G_{(-)}}{G_0}$ as function of crack angular semi-aperture $\Delta\theta$, calculated with in-house force-based and stress-based VCCT post-processing routines with stresses extracted on the fiber side of the interface

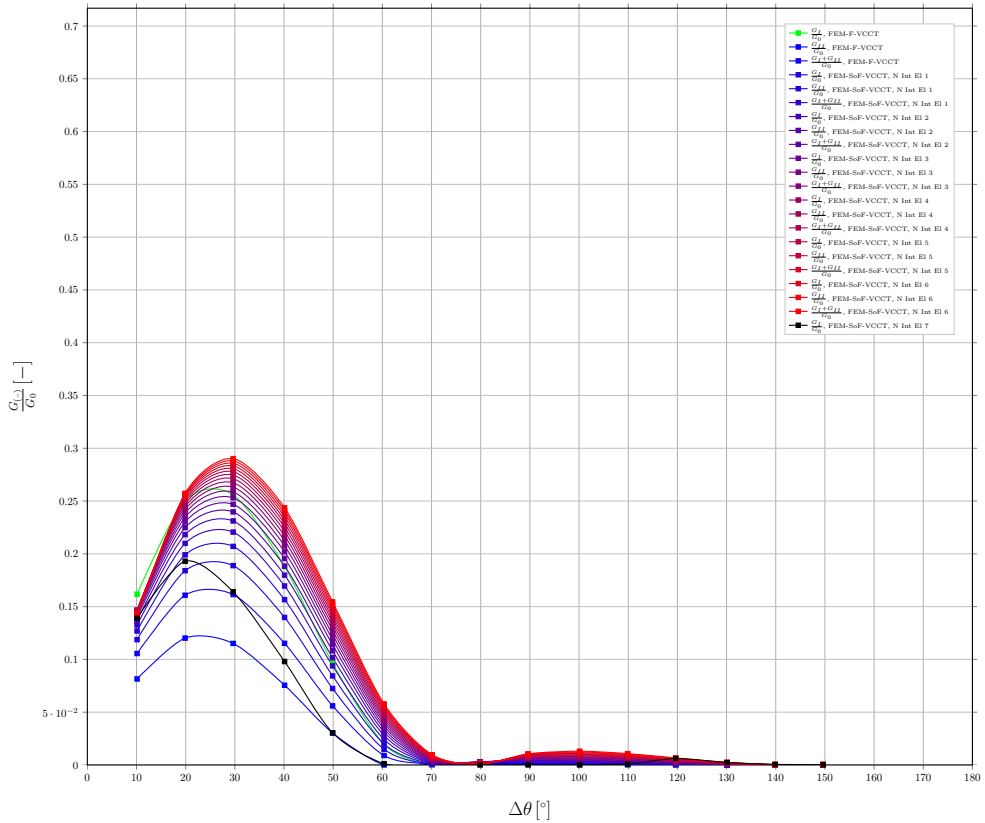

Fading from blue to red for increasing number of integration elements, Virtual Crack Closure Integral (VCCI) from FEM results; in green VCCT from FEM results; in black BEM results

$G_{//}$ from VCCI, stresses extracted on fiber surface, $\delta = 7.0°$

Normalized energy release rate $\frac{G_{(-)}}{G_0}$ as function of crack angular semi-aperture $\Delta\theta$, calculated with in-house force-based and stress-based VCCT post-processing routines with stresses extracted on the fiber side of the interface

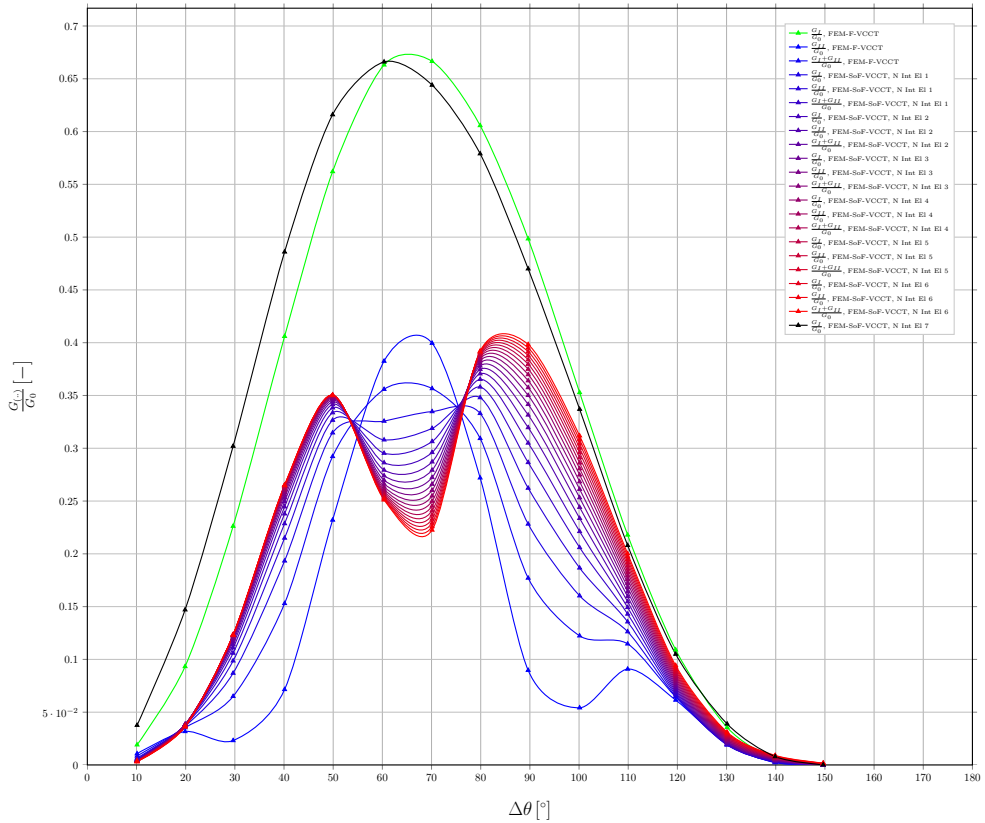

Fading from blue to red for increasing number of integration elements, Virtual Crack Closure Integral (VCCI) from FEM results; in green VCCT from FEM results; in black BEM results

G_{TOT} from VCCI, stresses extracted on fiber surface, $\delta = 7.0°$

Normalized energy release rate $\frac{G_{(-)}}{G_0}$ as function of crack angular semi-aperture $\Delta\theta$, calculated with in-house force-based and stress-based VCCT post-processing routines with stresses extracted on the fiber side of the interface

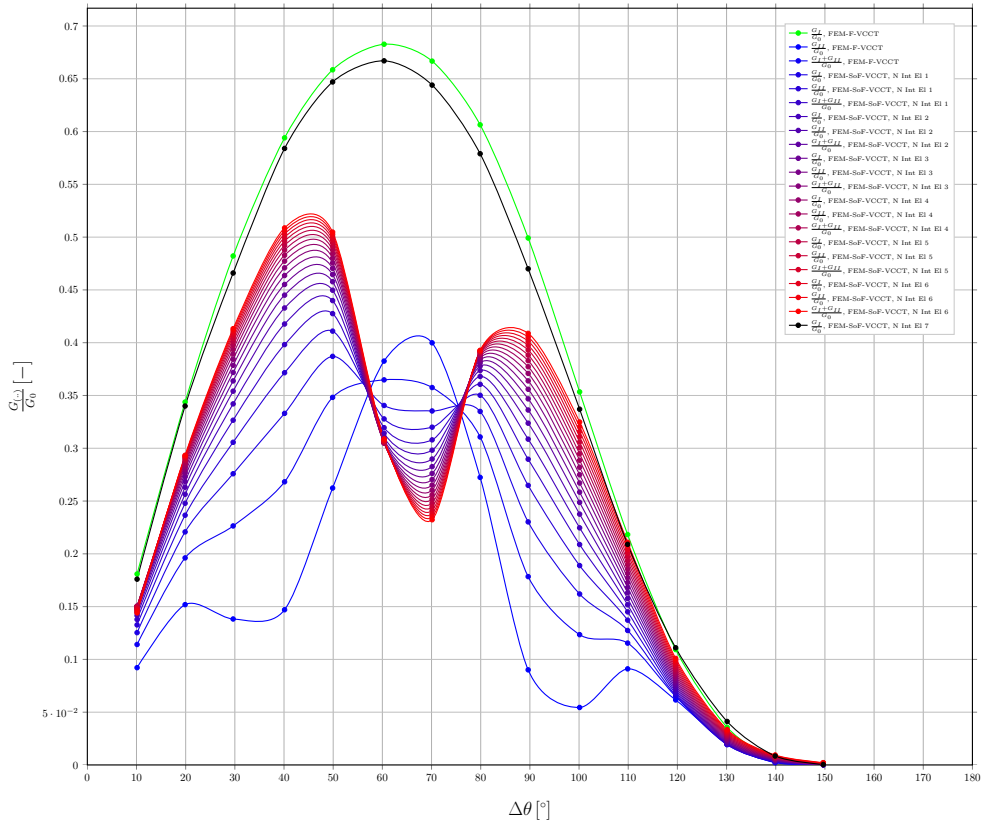

Fading from blue to red for increasing number of integration elements, Virtual Crack Closure Integral (VCCI) from FEM results; in green VCCT from FEM results; in black BEM results

Summary of $G_{(..)}$ from VCCI, stresses extracted on fiber surface,

$\delta = 7.0°$ Normalized energy release rate $\frac{G_{(..)}}{G_0}$ as function of crack angular semi-aperture $\Delta\theta$, calculated with in-house force-based and stress-based VCCT post-processing routines with stresses extracted on the fiber side of the interface

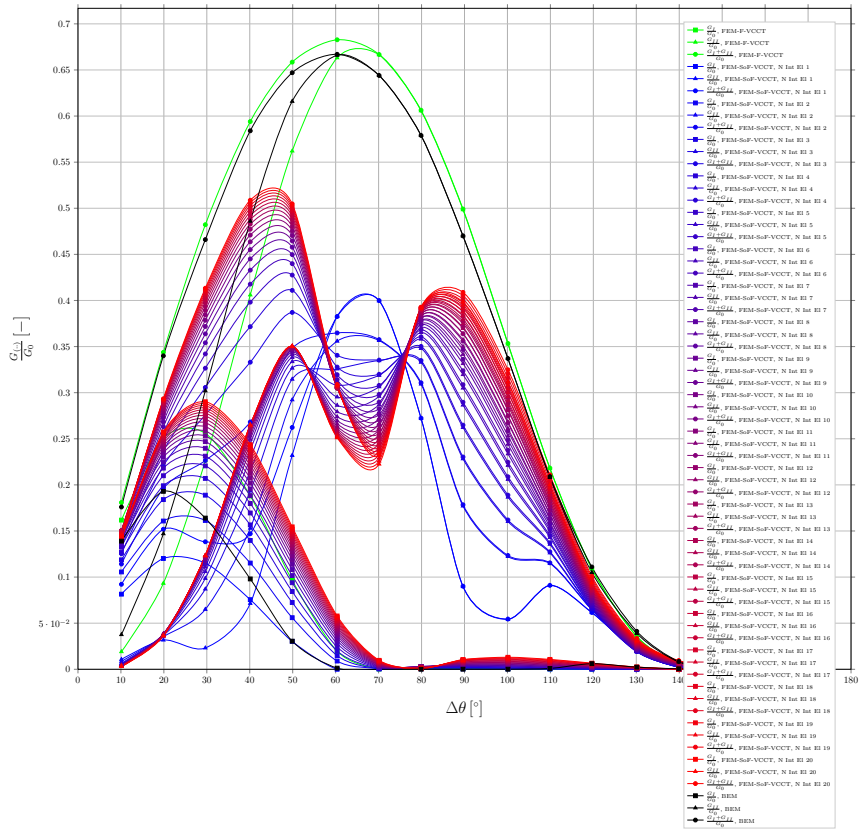

Fading from blue to red for increasing number of integration elements, Virtual Crack Closure Integral (VCCI) from FEM results; in green VCCT from FEM results; in black BEM results.

G_I from VCCI, stresses extracted on matrix surface, $\delta = 7.0°$

Normalized energy release rate $\frac{G_{(-)}}{G_0}$ as function of crack angular semi-aperture $\Delta\theta$, calculated with in-house force-based and stress-based VCCT post-processing routines with stresses extracted on the matrix side of the interface

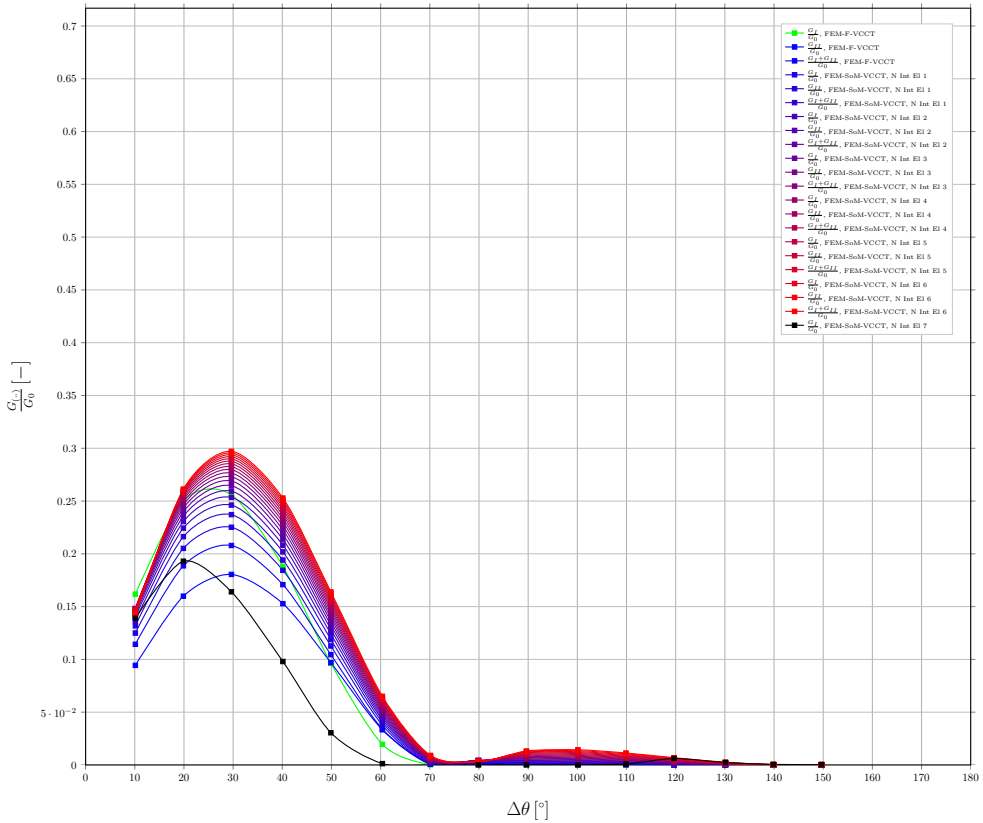

Fading from blue to red for increasing number of integration elements, Virtual Crack Closure Integral (VCCI) from FEM results; in green VCCT from FEM results; in black BEM results

G_{II} from VCCI, stresses extracted on matrix surface, $\delta = 7.0°$

Normalized energy release rate $\frac{G_{(-)}}{G_0}$ as function of crack angular semi-aperture $\Delta\theta$, calculated with in-house force-based and stress-based VCCT post-processing routines with stresses extracted on the matrix side of the interface

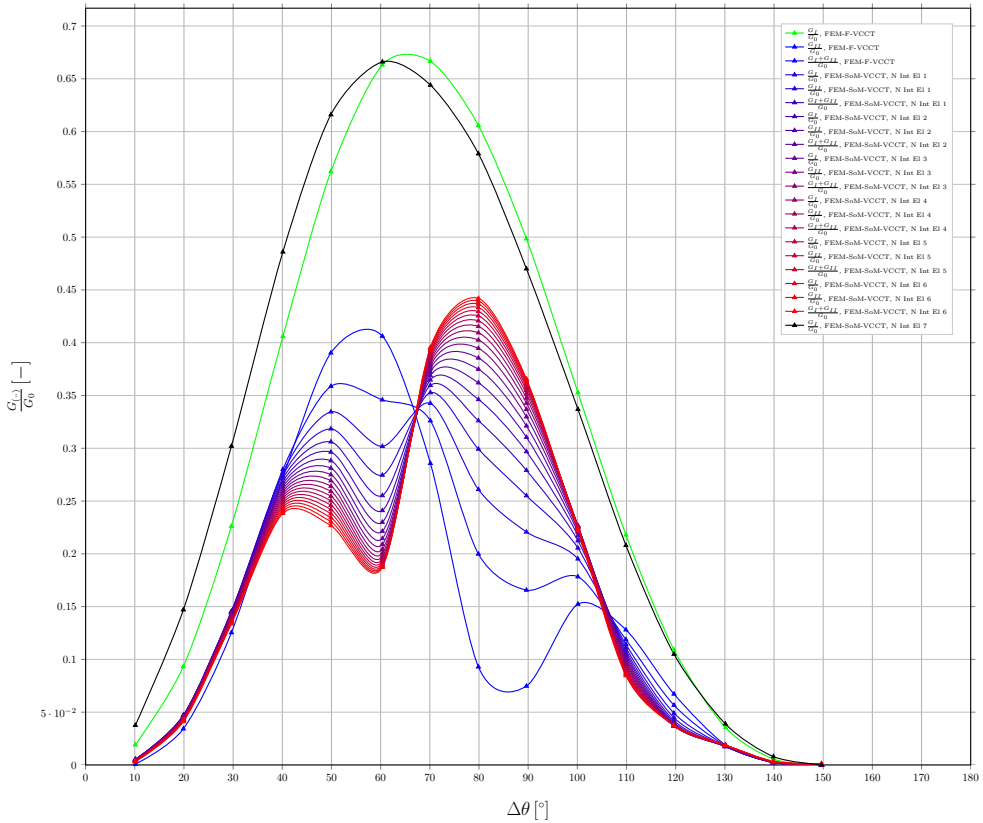

Fading from blue to red for increasing number of integration elements, Virtual Crack Closure Integral (VCCI) from FEM results; in green VCCT from FEM results; in black BEM results

G_{TOT} from VCCI, stresses extracted on matrix surface, $\delta = 7.0°$

Normalized energy release rate $\frac{G_{(-)}}{G_0}$ as function of crack angular semi-aperture $\Delta\theta$, calculated with in-house force-based and stress-based VCCT post-processing routines with stresses extracted on the matrix side of the interface

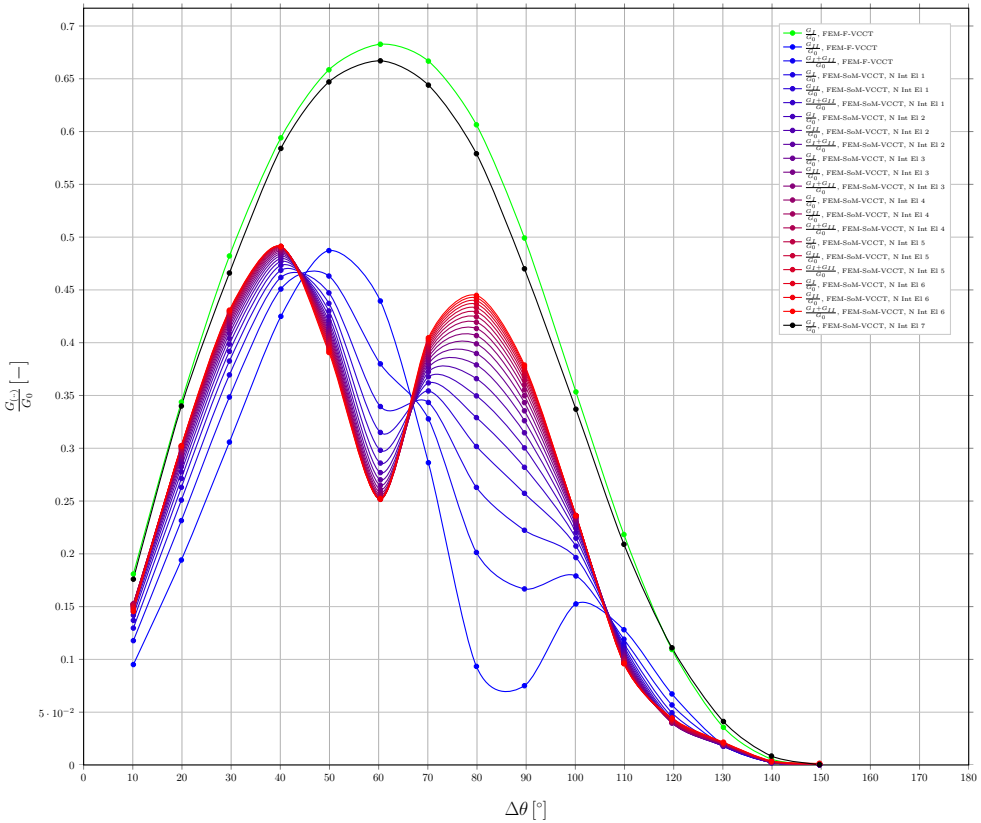

Fading from blue to red for increasing number of integration elements, Virtual Crack Closure Integral (VCCI) from FEM results; in green VCCT from FEM results; in black BEM results.

Summary of $G_{(..)}$ from VCCI, stresses extracted on matrix surface, $\delta = 7.0°$

Normalized energy release rate $\frac{G_{(..)}}{G_0}$ as function of crack angular semi-aperture $\Delta\theta$, calculated with in-house force-based and stress-based VCCT post-processing routines with stresses extracted on the matrix side of the interface

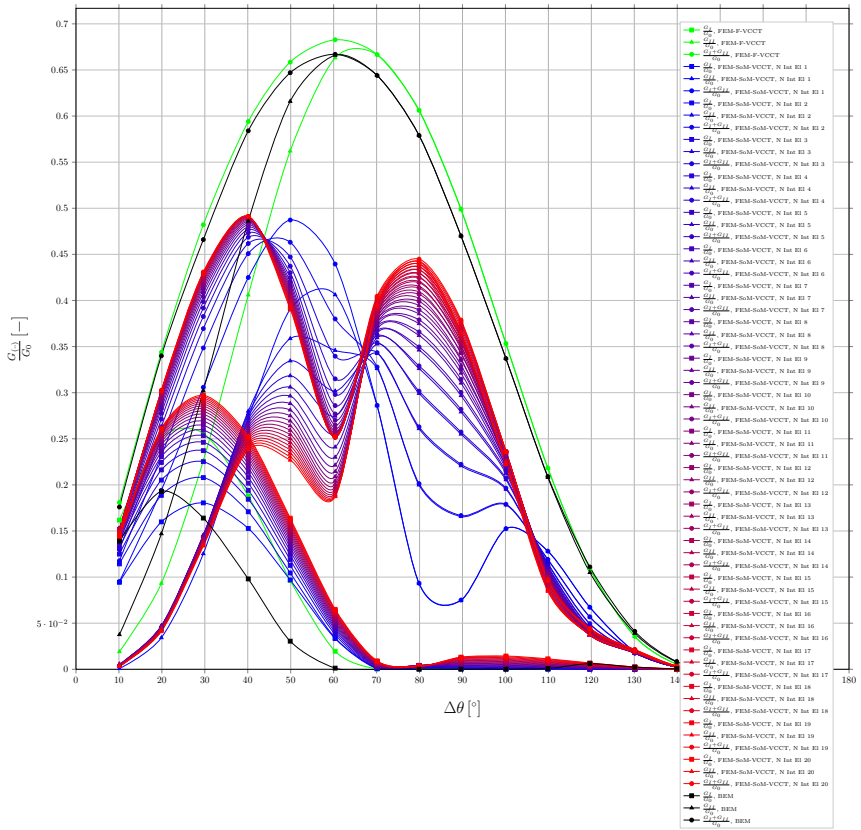

Fading from blue to red for increasing number of integration elements, Virtual Crack Closure Integral (VCCI) from FEM results; in green VCCT from FEM results; in black BEM results.

σ_0, $\delta = 0.6°$

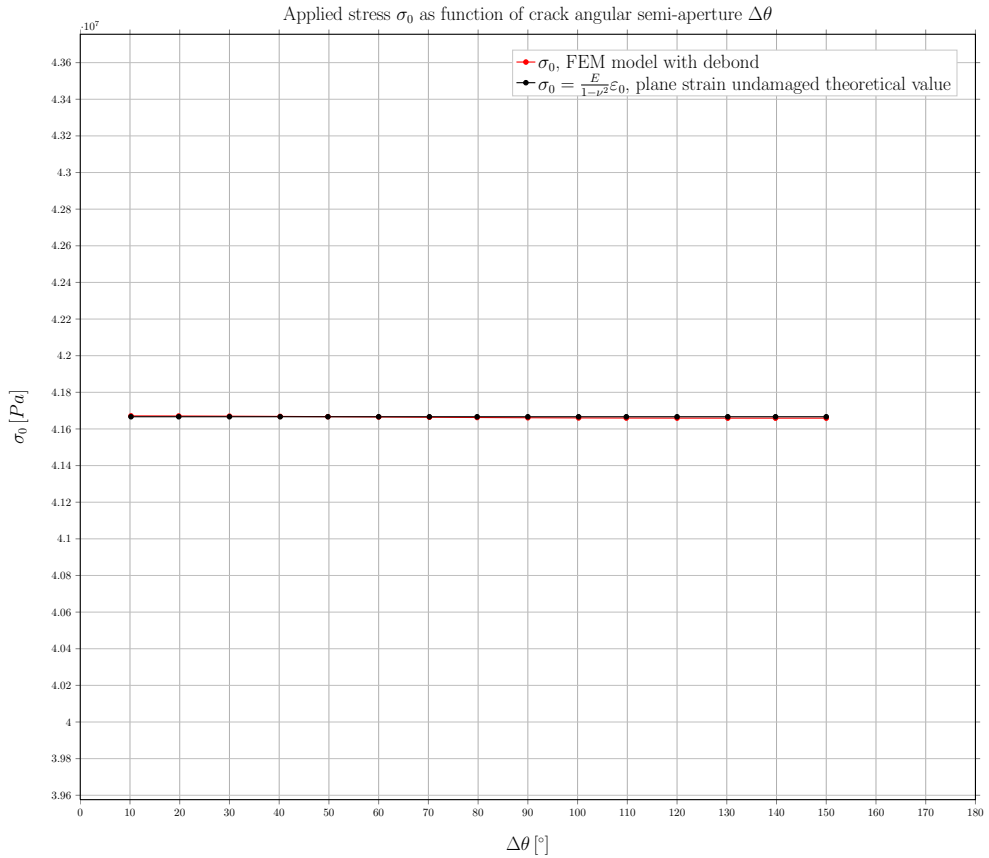

In red small strain FEM, in black analytical plain strain value.

G_0, $\delta = 0.6°$

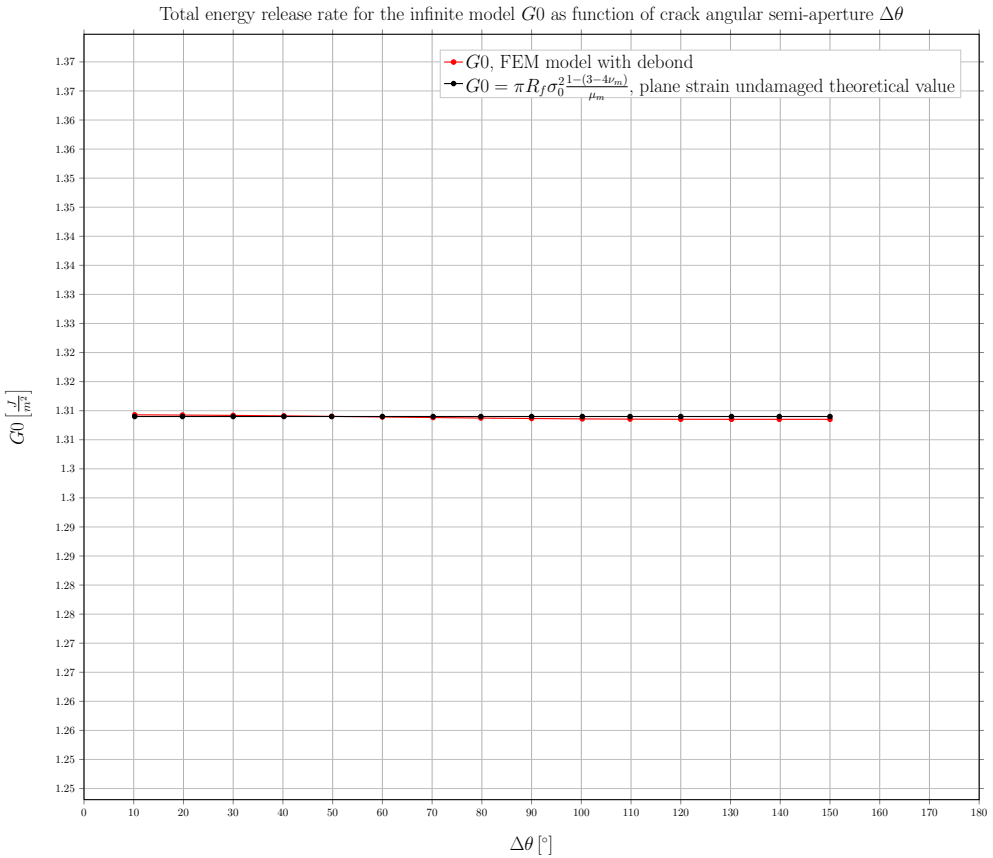

In red small strain FEM, in black analytical plain strain value.

J-Integral (Abaqus built-in routine), $\delta = 0.6°$

Normalized total energy release rate $\frac{G_{TOT}}{G_0}$ as function of crack angular semi-aperture $\Delta\theta$, calculated with Abaqus built-in J-Integral post-processing routine (*CONTOUR INTEGRAL)

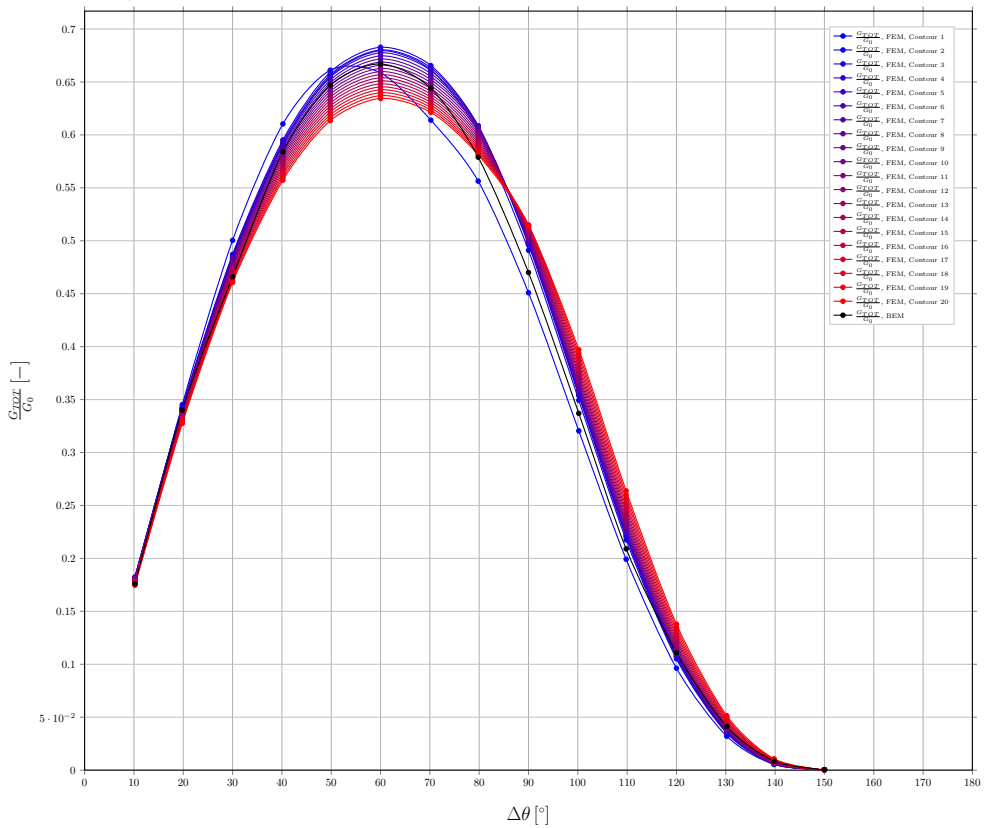

Fading from blue to red for contours further from the crack tip, FEM results; in black BEM results.

VCCT in forces (in-house Python routine), $\delta = 0.6°$

Normalized energy release rate $\frac{G_{(\cdot)}}{G_0}$ as function of crack angular semi-aperture $\Delta\theta$, calculated with in-house force-based VCCT post-processing routine

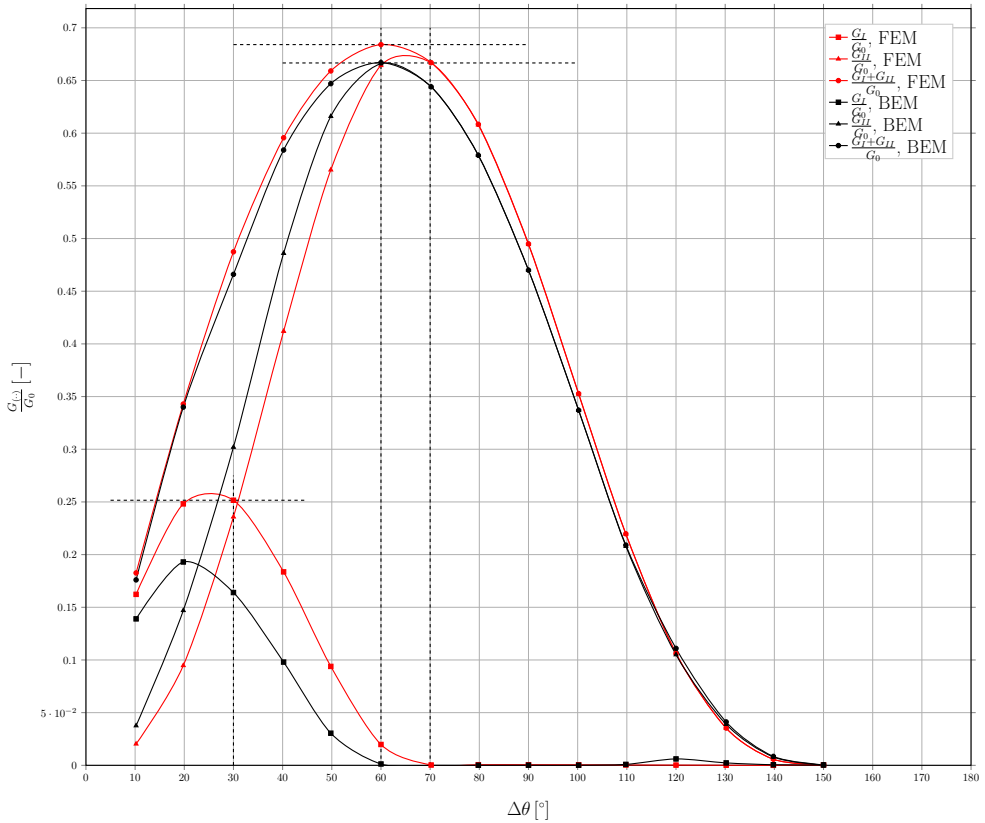

In green VCCT from FEM results, in black BEM results; positions of maxima highlighted by dashed lines.

J-Integral and VCCT in forces, $\delta = 0.6°$

Normalized energy release rate $\frac{G_{(\cdot)}}{G_0}$ as function of crack angular semi-aperture $\Delta\theta$, calculated with in-house force-based VCCT and Abaqus built-in J-Integral (*CONTOUR INTEGRAL) post-processing routines

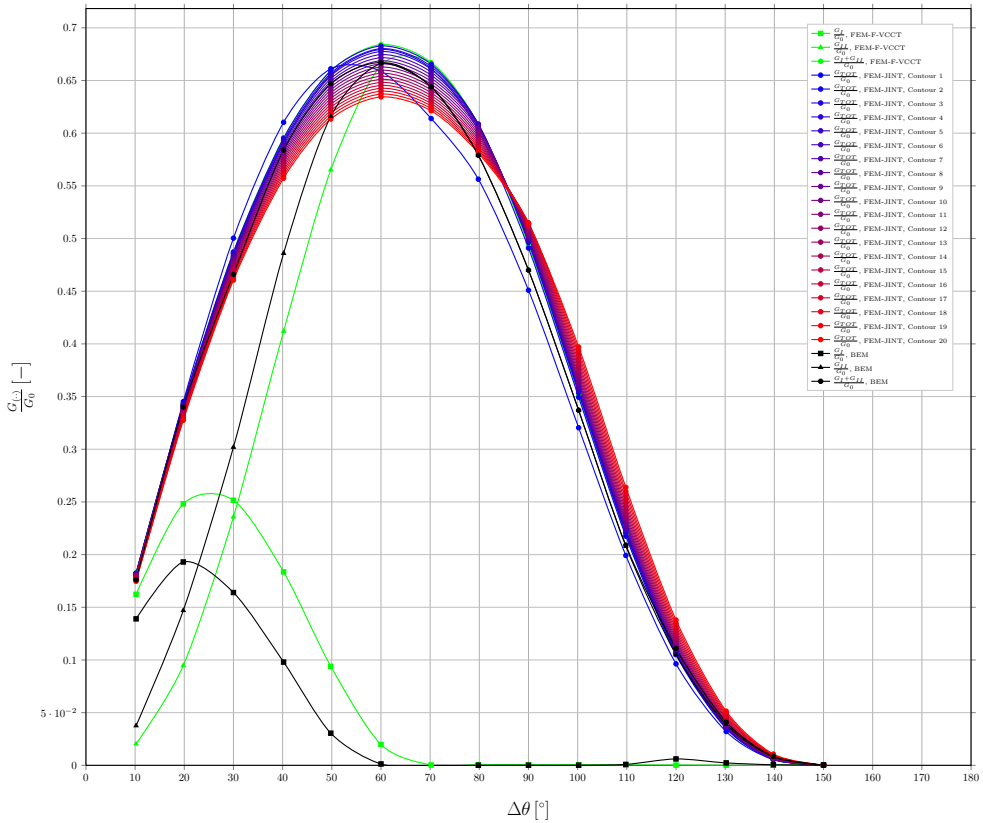

Fading from blue to red for contours further from the crack tip, J-Integral from FEM results; in green VCCT from FEM results; in black BEM results.

G_I from VCCI, stresses extracted on fiber surface, $\delta = 6.0°$

Normalized energy release rate $\frac{G_{(\cdot)}}{G_0}$ as function of crack angular semi-aperture $\Delta\theta$, calculated with in-house force-based and stress-based VCCT post-processing routines with stresses extracted on the fiber side of the interface

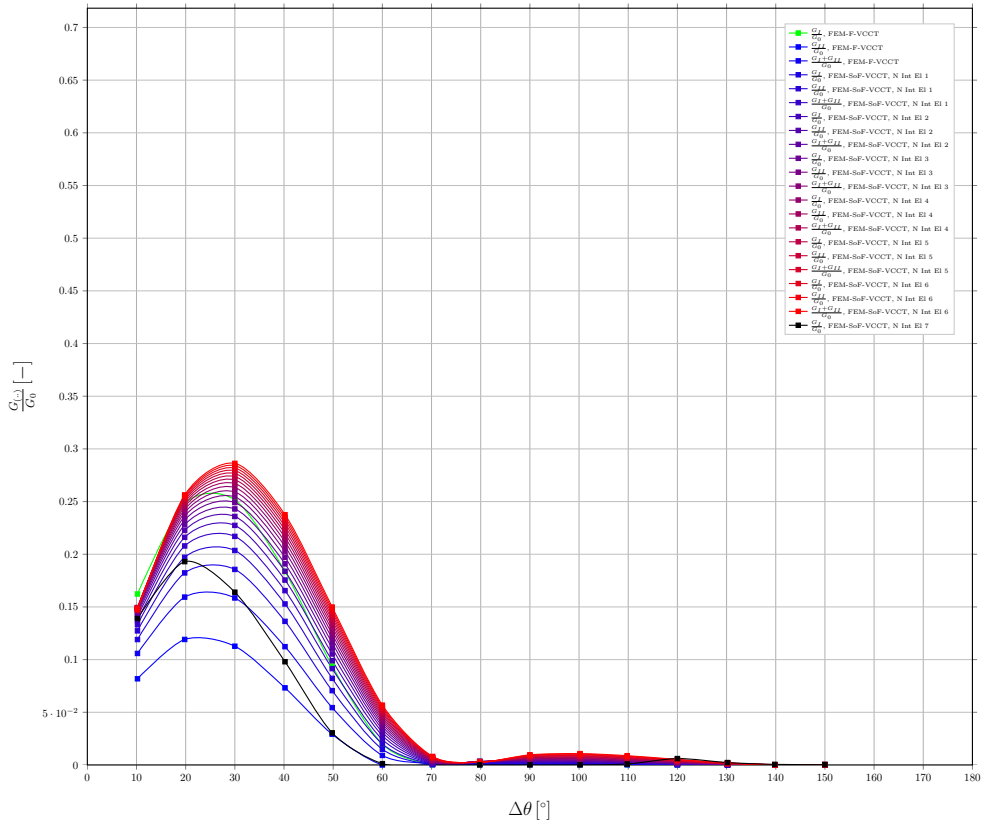

Fading from blue to red for increasing number of integration elements, Virtual Crack Closure Integral (VCCI) from FEM results; in green VCCT from FEM results; in black BEM results

$G_{//}$ from VCCI, stresses extracted on fiber surface, $\delta = 6.0°$

Normalized energy release rate $\frac{G_{(-)}}{G_0}$ as function of crack angular semi-aperture $\Delta\theta$, calculated with in-house force-based and stress-based VCCT post-processing routines with stresses extracted on the fiber side of the interface

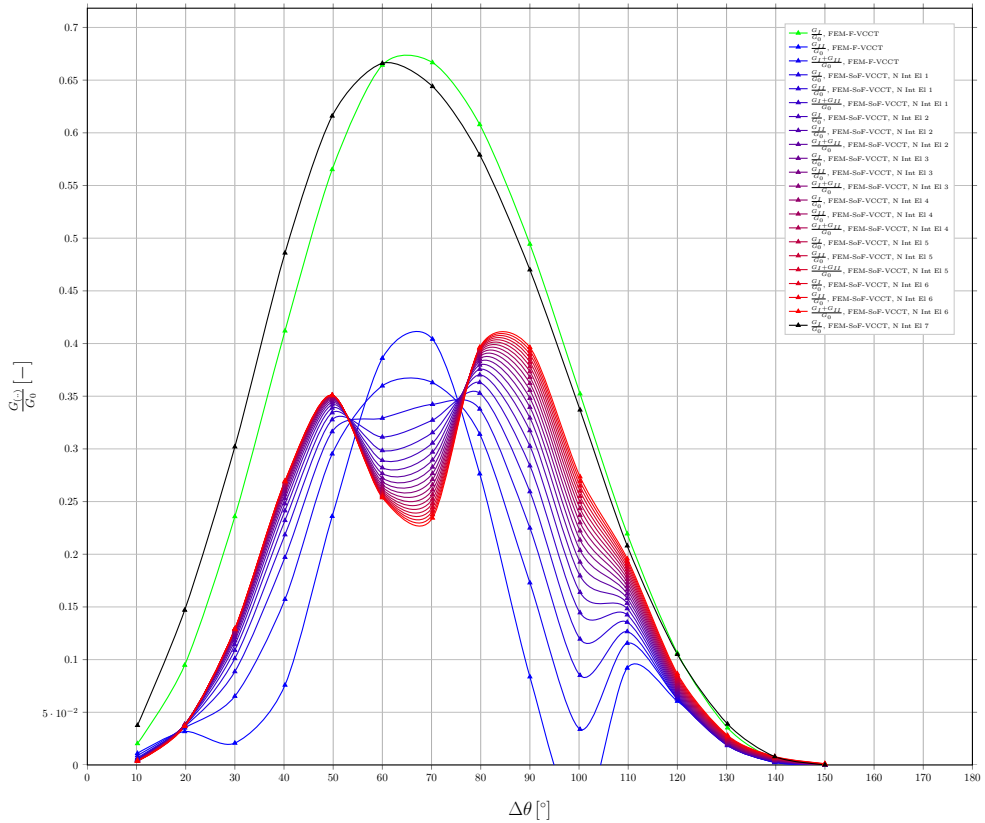

Fading from blue to red for increasing number of integration elements, Virtual Crack Closure Integral (VCCI) from FEM results; in green VCCT from FEM results; in black BEM results.

G_{TOT} from VCCI, stresses extracted on fiber surface, $\delta = 6.0°$

Normalized energy release rate $\frac{G_{(-)}}{G_0}$ as function of crack angular semi-aperture $\Delta\theta$, calculated with in-house force-based and stress-based VCCT post-processing routines with stresses extracted on the fiber side of the interface

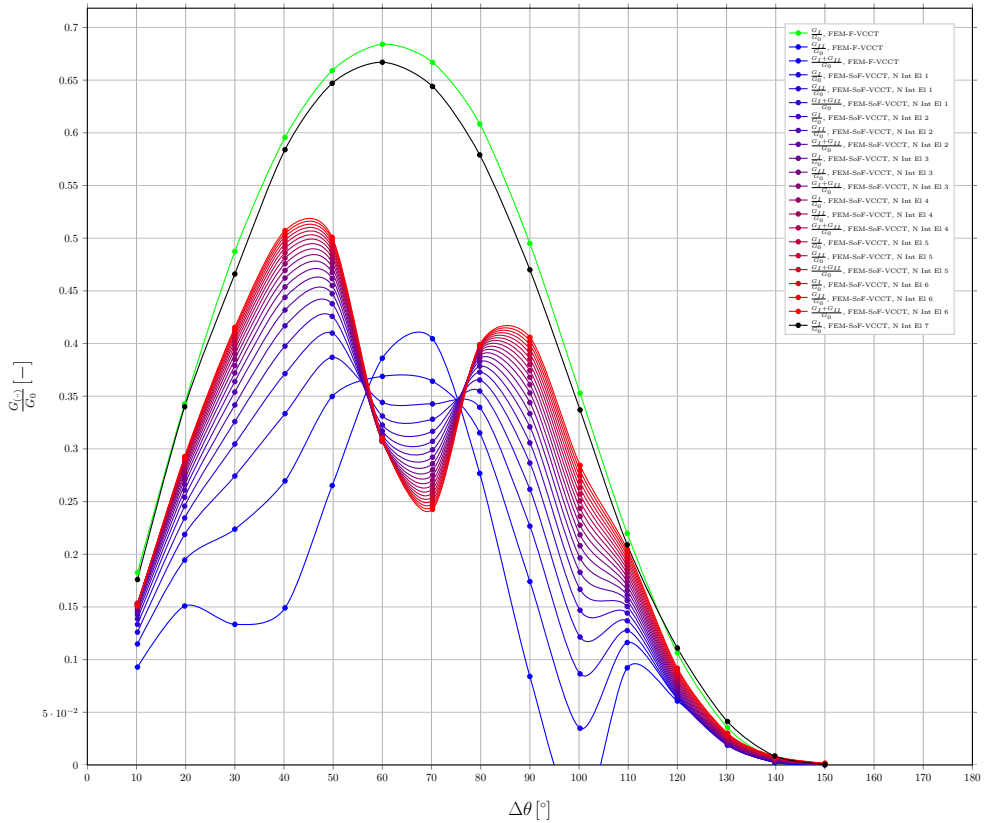

Fading from blue to red for increasing number of integration elements, Virtual Crack Closure Integral (VCCI) from FEM results; in green VCCT from FEM results; in black BEM results

Summary of $G_{(..)}$ from VCCI, stresses extracted on fiber surface,

$\delta = 6.0°$ Normalized energy release rate $\frac{G_{(..)}}{G_0}$ as function of crack angular semi-aperture $\Delta\theta$, calculated with in-house force-based and stress-based VCCT post-processing routines with stresses extracted on the fiber side of the interface

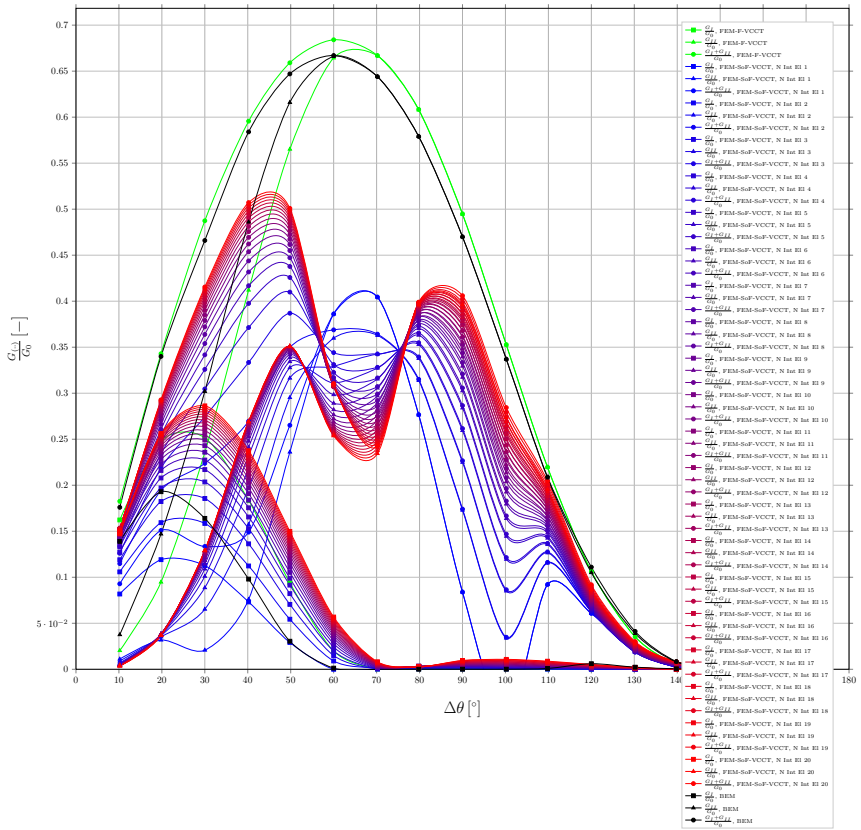

Fading from blue to red for increasing number of integration elements, Virtual Crack Closure Integral (VCCI) from FEM results; in green VCCT from FEM results; in black BEM results.

G_I from VCCI, stresses extracted on matrix surface, $\delta = 6.0°$

Normalized energy release rate $\frac{G_{(\cdot)}}{G_0}$ as function of crack angular semi-aperture $\Delta\theta$, calculated with in-house force-based and stress-based VCCT post-processing routines with stresses extracted on the matrix side of the interface

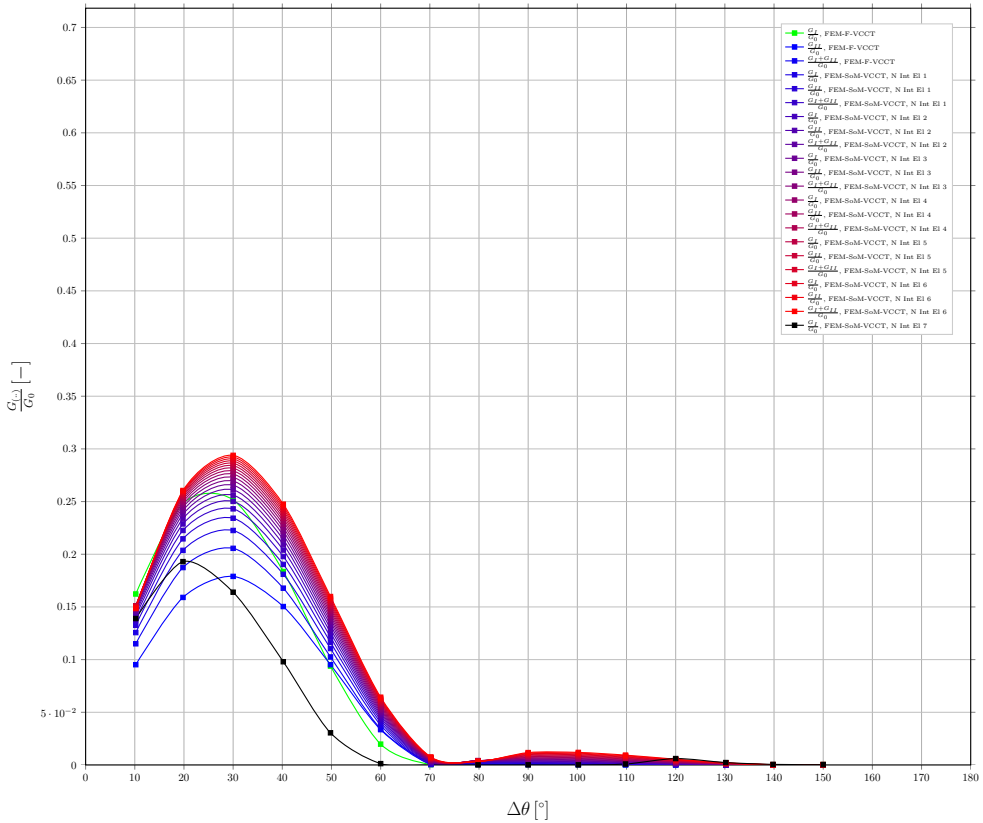

Fading from blue to red for increasing number of integration elements, Virtual Crack Closure Integral (VCCI) from FEM results; in green VCCT from FEM results; in black BEM results

$G_{//}$ from VCCI, stresses extracted on matrix surface, $\delta = 6.0°$

Normalized energy release rate $\frac{G_{(-)}}{G_0}$ as function of crack angular semi-aperture $\Delta\theta$, calculated with in-house force-based and stress-based VCCT post-processing routines with stresses extracted on the matrix side of the interface

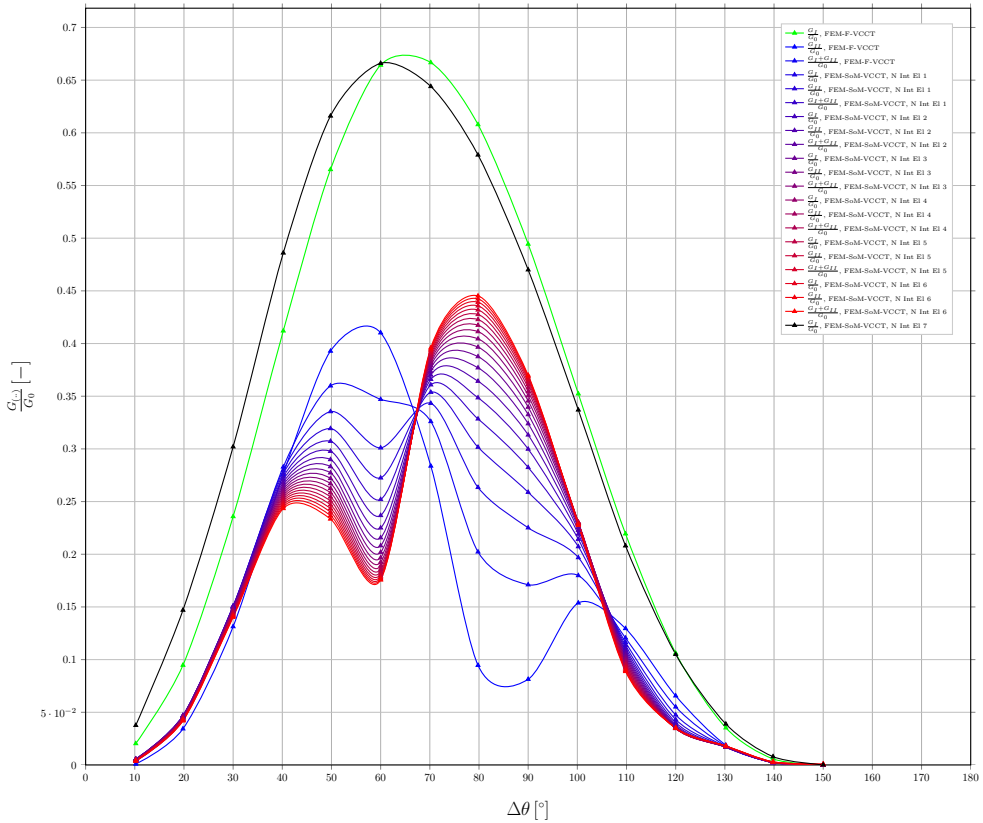

Fading from blue to red for increasing number of integration elements, Virtual Crack Closure Integral (VCCI) from FEM results; in green VCCT from FEM results; in black BEM results.

G_{TOT} from VCCI, stresses extracted on matrix surface, $\delta = 6.0°$

Normalized energy release rate $\frac{G_{(-)}}{G_0}$ as function of crack angular semi-aperture $\Delta\theta$, calculated with in-house force-based and stress-based VCCT post-processing routines with stresses extracted on the matrix side of the interface

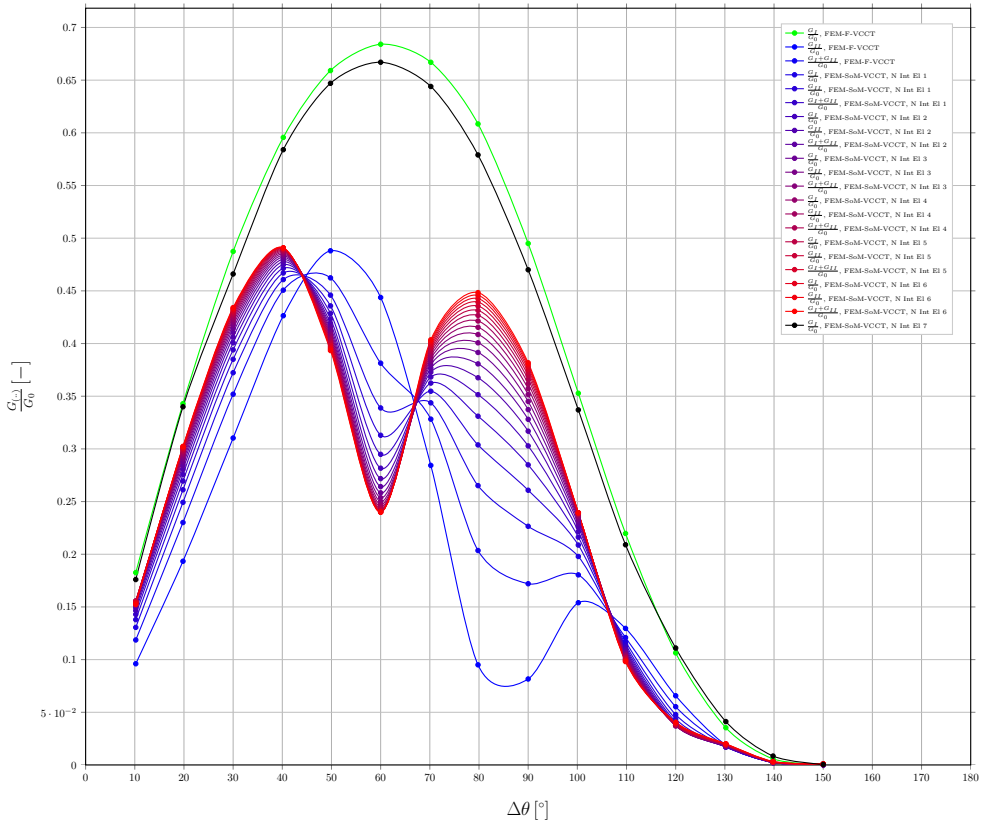

Fading from blue to red for increasing number of integration elements, Virtual Crack Closure Integral (VCCI) from FEM results; in green VCCT from FEM results; in black BEM results.

Summary of $G_{(..)}$ from VCCI, stresses extracted on matrix surface,

$\delta = 6.0°$

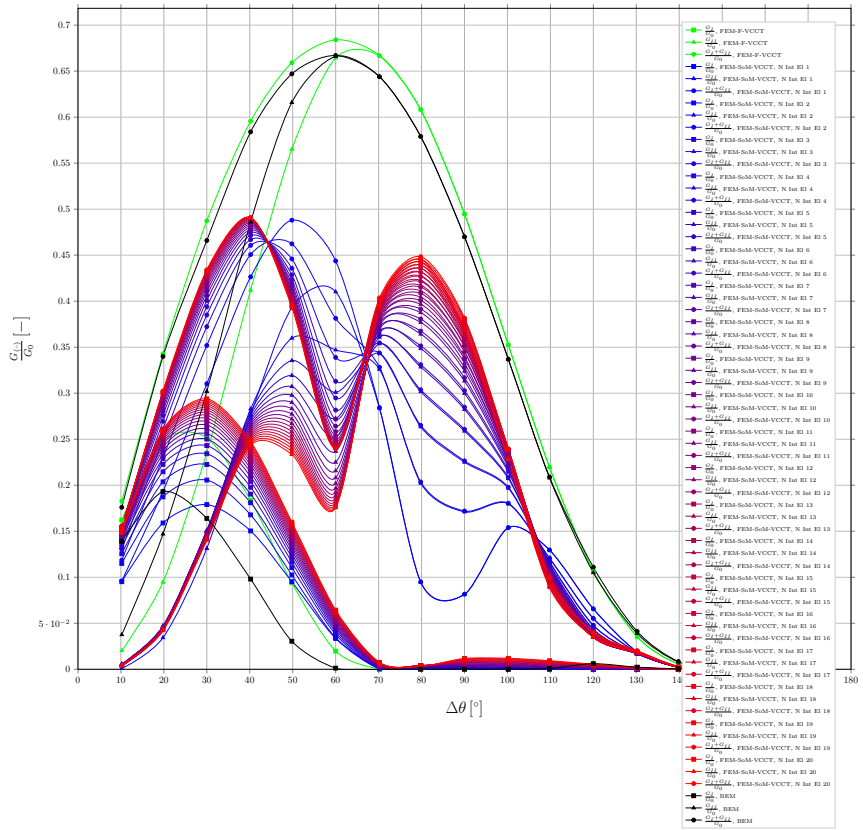

Fading from blue to red for increasing number of integration elements, Virtual Crack Closure Integral (VCCI) from FEM results; in green VCCT from FEM results; in black BEM results.

σ_0, $\delta = 0.5°$

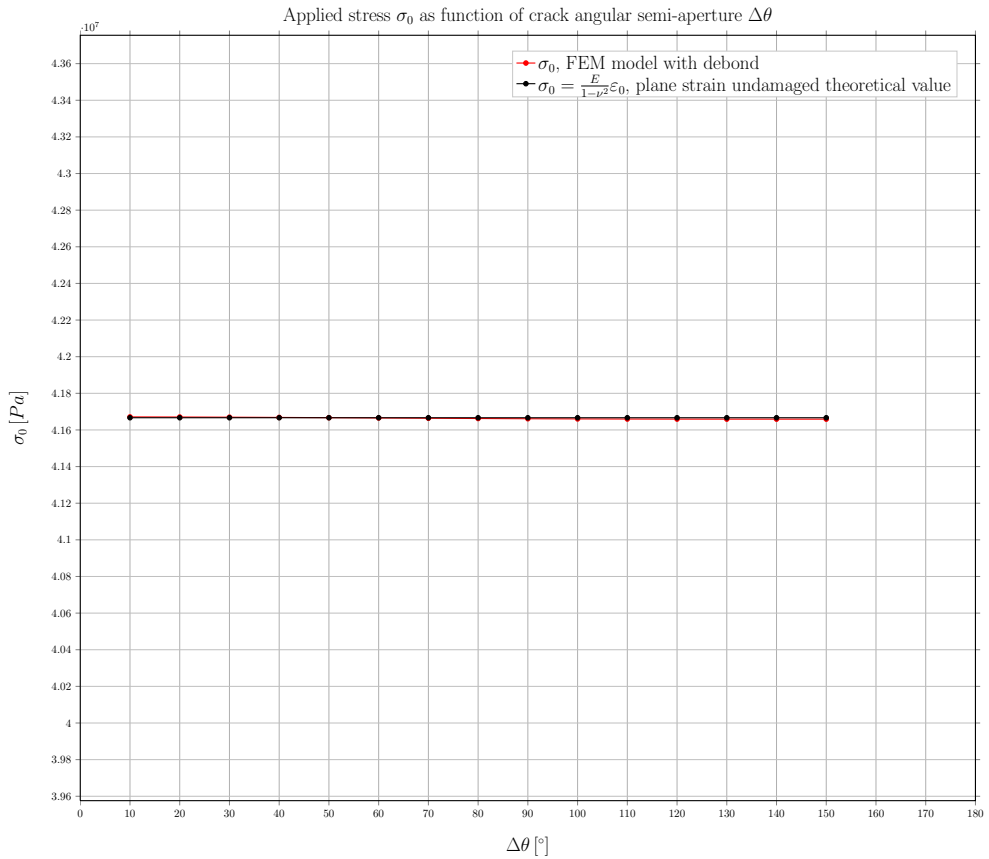

In red small strain FEM, in black analytical plain strain value.

G_0, $\delta = 0.5°$

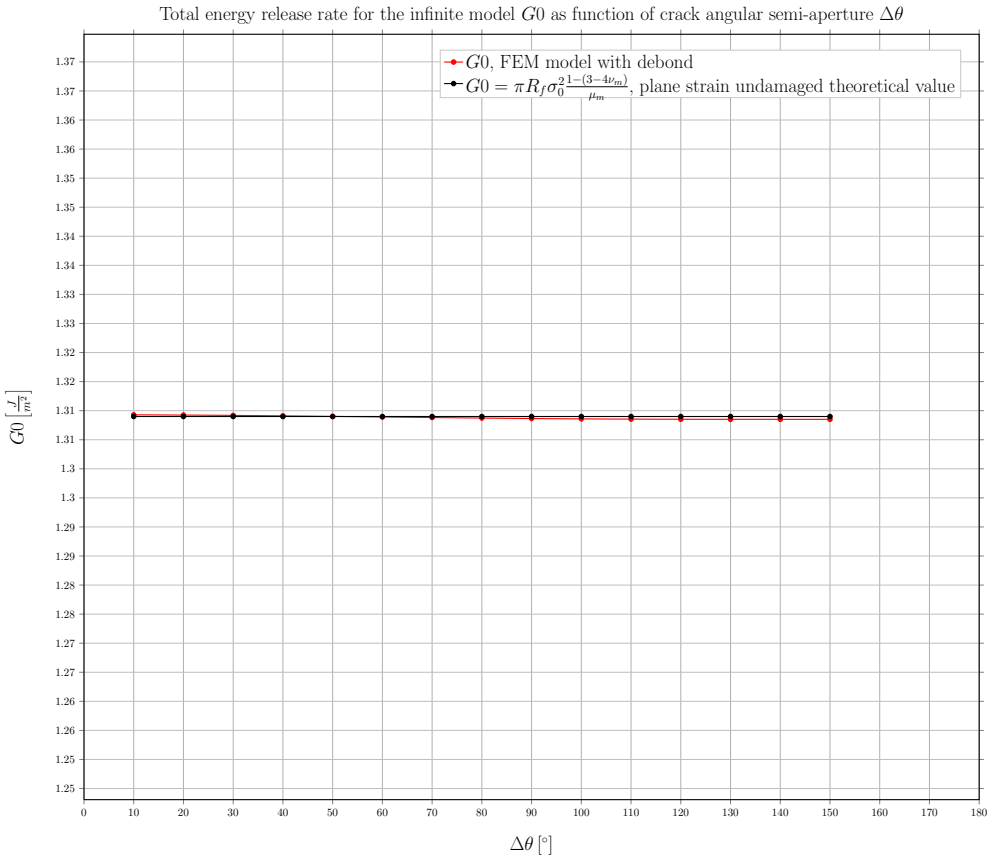

In red small strain FEM, in black analytical plain strain value.

J-Integral (Abaqus built-in routine), $\delta = 0.5°$

Normalized total energy release rate $\frac{G_{TOT}}{G_0}$ as function of crack angular semi-aperture $\Delta\theta$, calculated with Abaqus built-in J-Integral post-processing routine (*CONTOUR INTEGRAL)

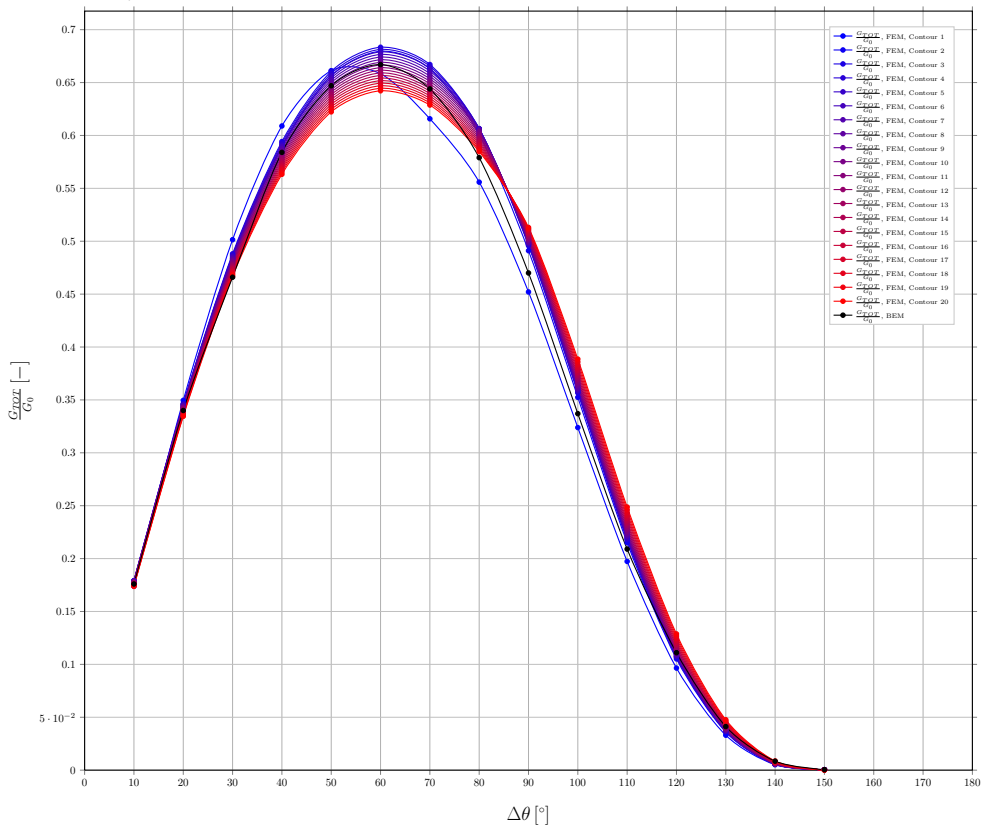

Fading from blue to red for contours further from the crack tip, FEM results; in black BEM results.

VCCT in forces (in-house Python routine), $\delta = 0.5°$

Normalized energy release rate $\frac{G_{(\cdot)}}{G_0}$ as function of crack angular semi-aperture $\Delta\theta$, calculated with in-house force-based VCCT post-processing routine

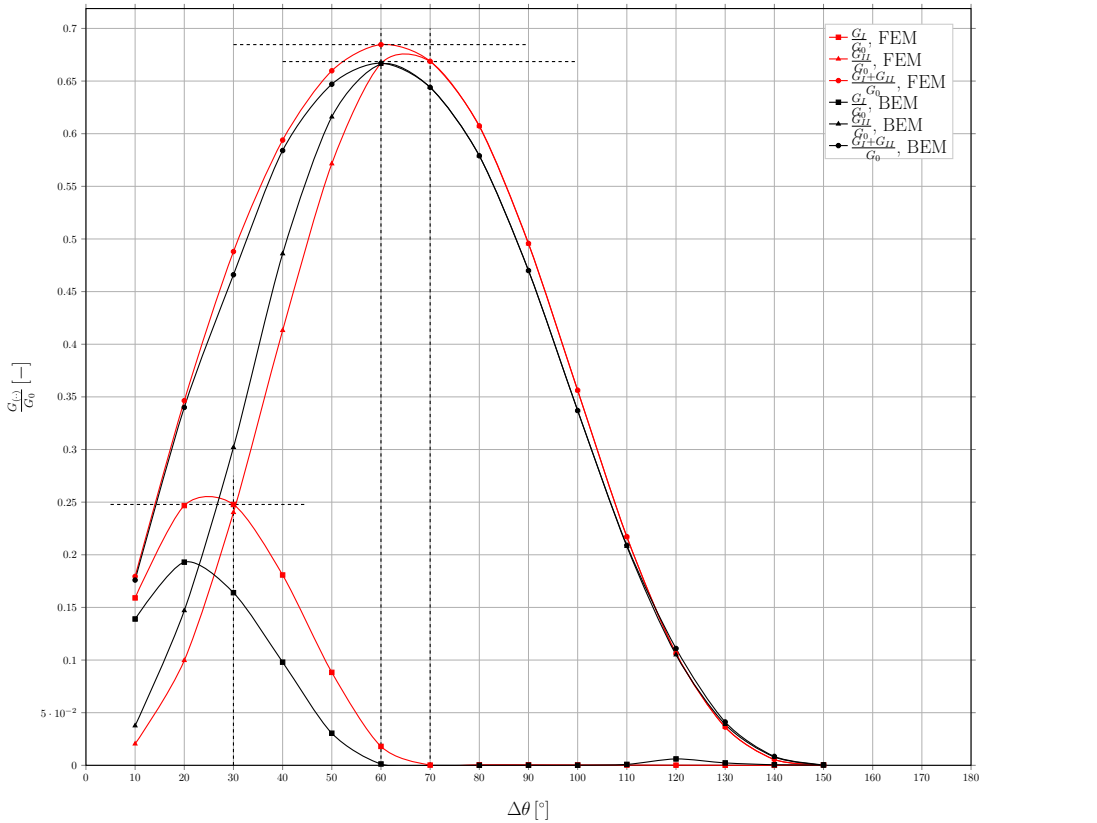

In green VCCT from FEM results, in black BEM results; positions of maxima highlighted by dashed lines.

J-Integral and VCCT in forces, $\delta = 0.5°$

Normalized energy release rate $\frac{G_{(\cdot)}}{G_0}$ as function of crack angular semi-aperture $\Delta\theta$, calculated with in-house force-based VCCT and Abaqus built-in J-Integral (*CONTOUR INTEGRAL) post-processing routines

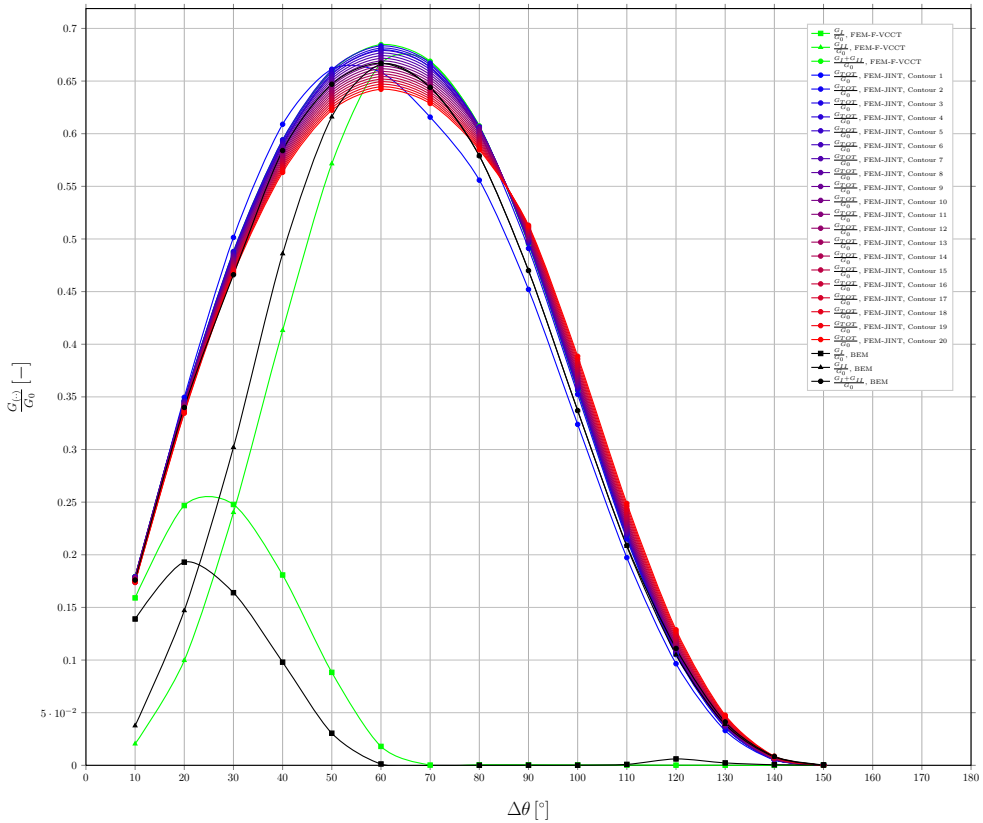

Fading from blue to red for contours further from the crack tip, J-Integral from FEM results; in green VCCT from FEM results; in black BEM results.

G_I from VCCI, stresses extracted on fiber surface, $\delta = 5.0°$

Normalized energy release rate $\frac{G_{(\cdot)}}{G_0}$ as function of crack angular semi-aperture $\Delta\theta$, calculated with in-house force-based and stress-based VCCT post-processing routines with stresses extracted on the fiber side of the interface

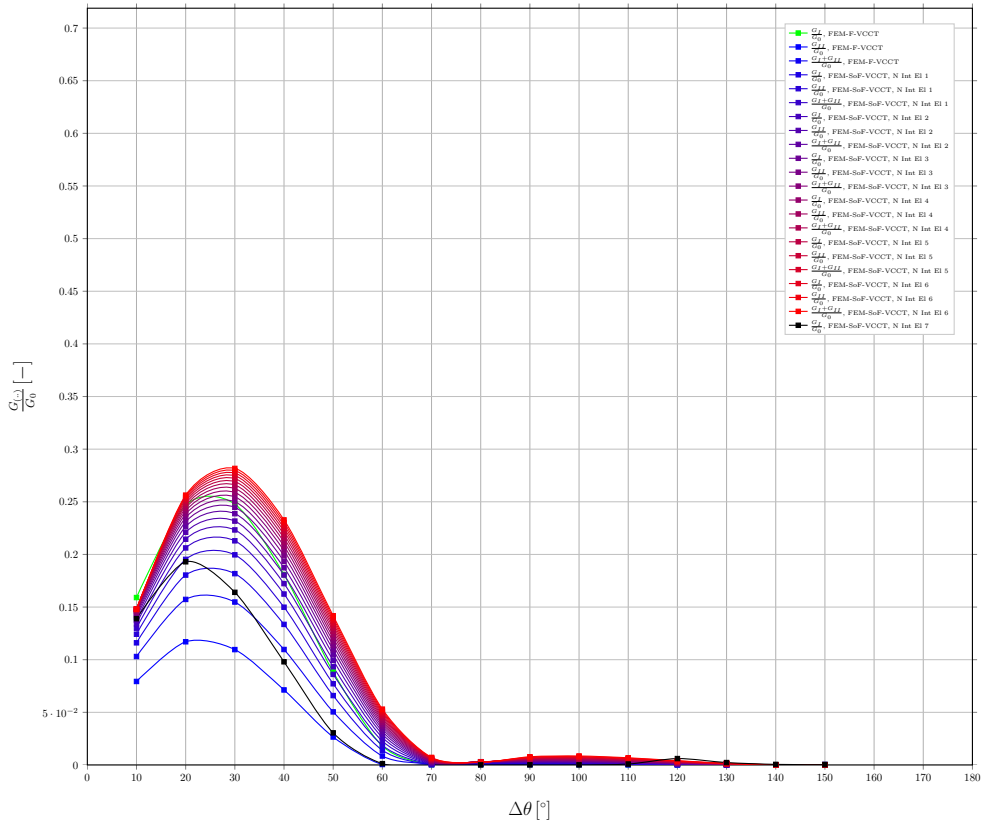

Fading from blue to red for increasing number of integration elements, Virtual Crack Closure Integral (VCCI) from FEM results; in green VCCT from FEM results; in black BEM results

$G_{//}$ from VCCI, stresses extracted on fiber surface, $\delta = 5.0°$

Normalized energy release rate $\frac{G_{(-)}}{G_0}$ as function of crack angular semi-aperture $\Delta\theta$, calculated with in-house force-based and stress-based VCCT post-processing routines with stresses extracted on the fiber side of the interface

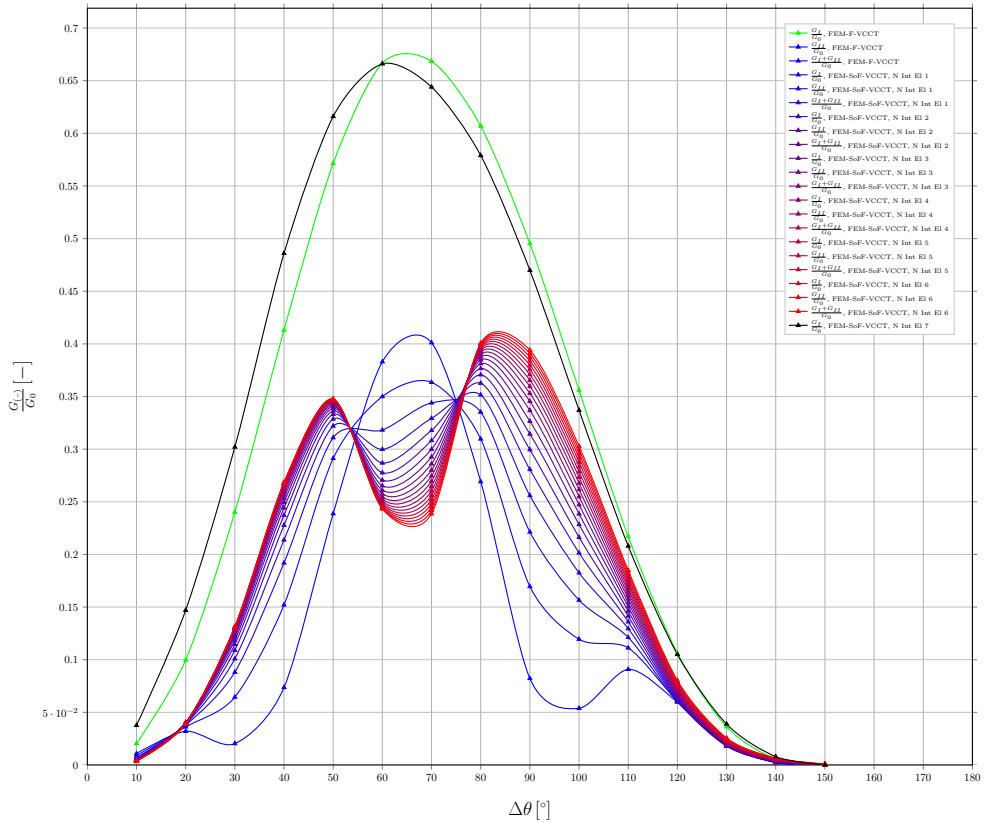

Fading from blue to red for increasing number of integration elements, Virtual Crack Closure Integral (VCCI) from FEM results; in green VCCT from FEM results; in black BEM results.

G_{TOT} from VCCI, stresses extracted on fiber surface, $\delta = 5.0°$

Normalized energy release rate $\frac{G_{(-)}}{G_0}$ as function of crack angular semi-aperture $\Delta\theta$, calculated with in-house force-based and stress-based VCCT post-processing routines with stresses extracted on the fiber side of the interface

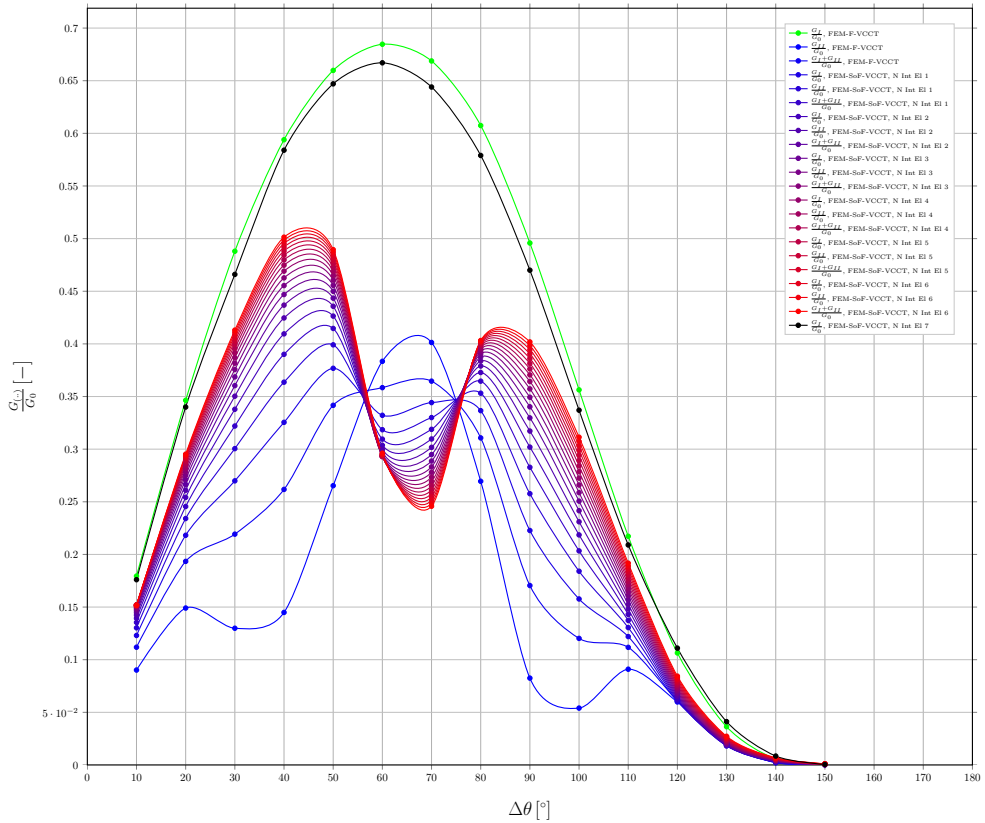

Fading from blue to red for increasing number of integration elements, Virtual Crack Closure Integral (VCCI) from FEM results; in green VCCT from FEM results; in black BEM results

Summary of $G_{(..)}$ from VCCI, stresses extracted on fiber surface,

$\delta = 5.0°$ Normalized energy release rate $\frac{G_{(..)}}{G_0}$ as function of crack angular semi-aperture $\Delta\theta$, calculated with in-house force-based and stress-based VCCT post-processing routines with stresses extracted on the fiber side of the interface

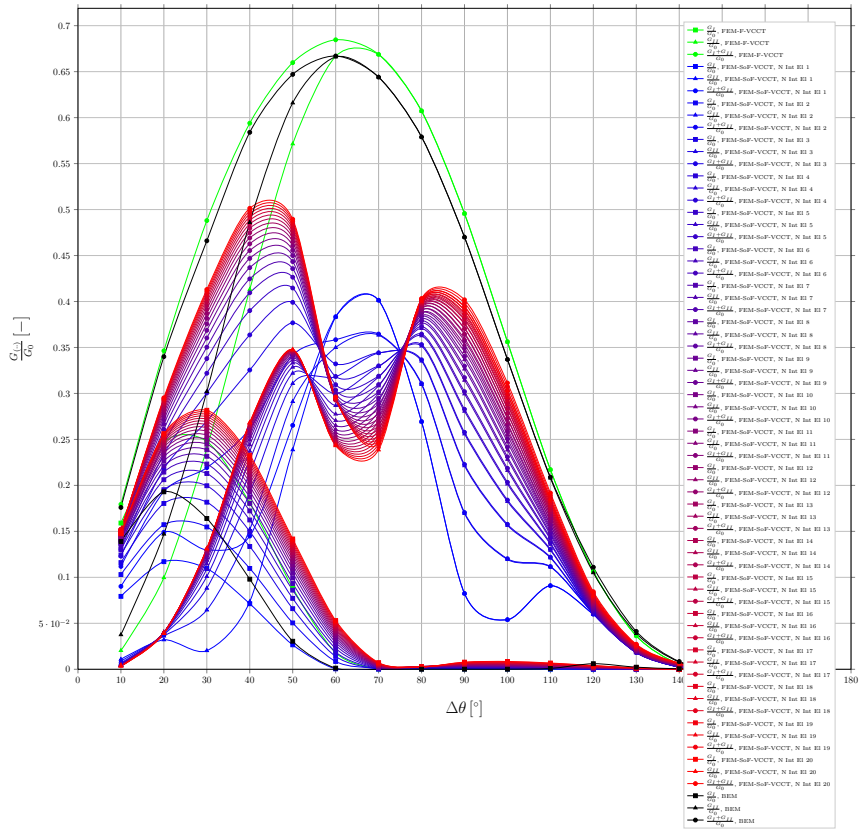

Fading from blue to red for increasing number of integration elements, Virtual Crack Closure Integral (VCCI) from FEM results; in green VCCT from FEM results; in black BEM results.

G_I from VCCI, stresses extracted on matrix surface, $\delta = 5.0°$

Normalized energy release rate $\frac{G_{(-)}}{G_0}$ as function of crack angular semi-aperture $\Delta\theta$, calculated with in-house force-based and stress-based VCCT post-processing routines with stresses extracted on the matrix side of the interface

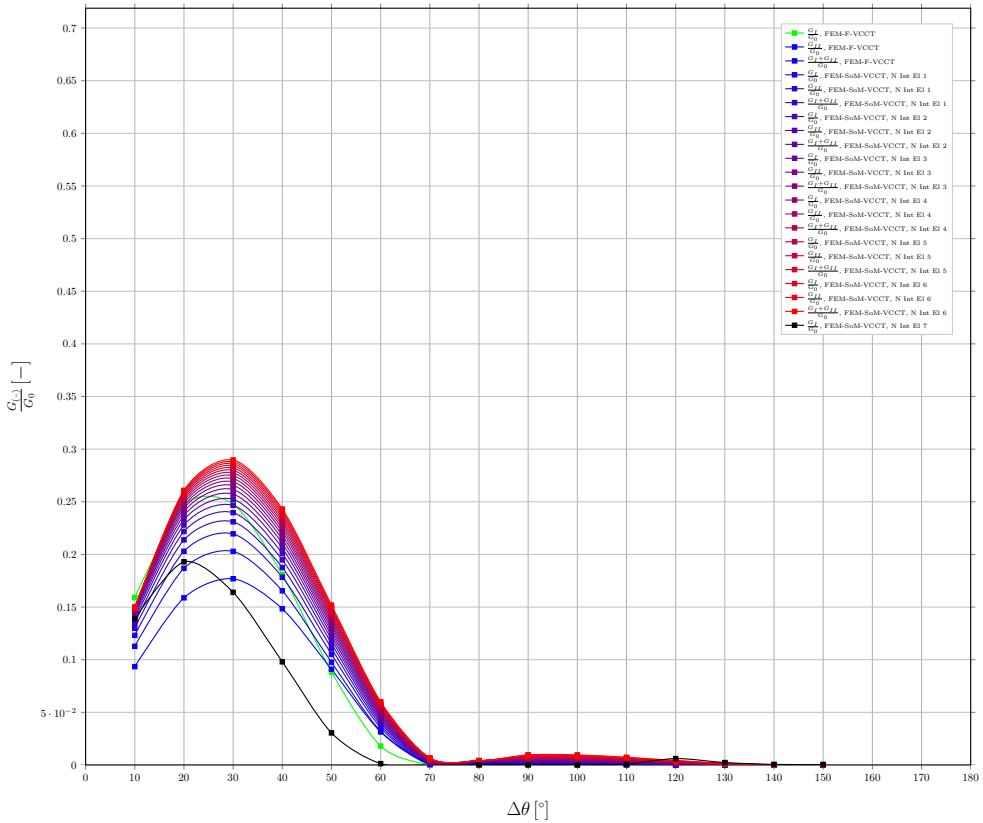

Fading from blue to red for increasing number of integration elements, Virtual Crack Closure Integral (VCCI) from FEM results; in green VCCT from FEM results; in black BEM results

G_{II} from VCCI, stresses extracted on matrix surface, $\delta = 5.0°$

Normalized energy release rate $\frac{G_{(\cdot)}}{G_0}$ as function of crack angular semi-aperture $\Delta\theta$, calculated with in-house force-based and stress-based VCCT post-processing routines with stresses extracted on the matrix side of the interface

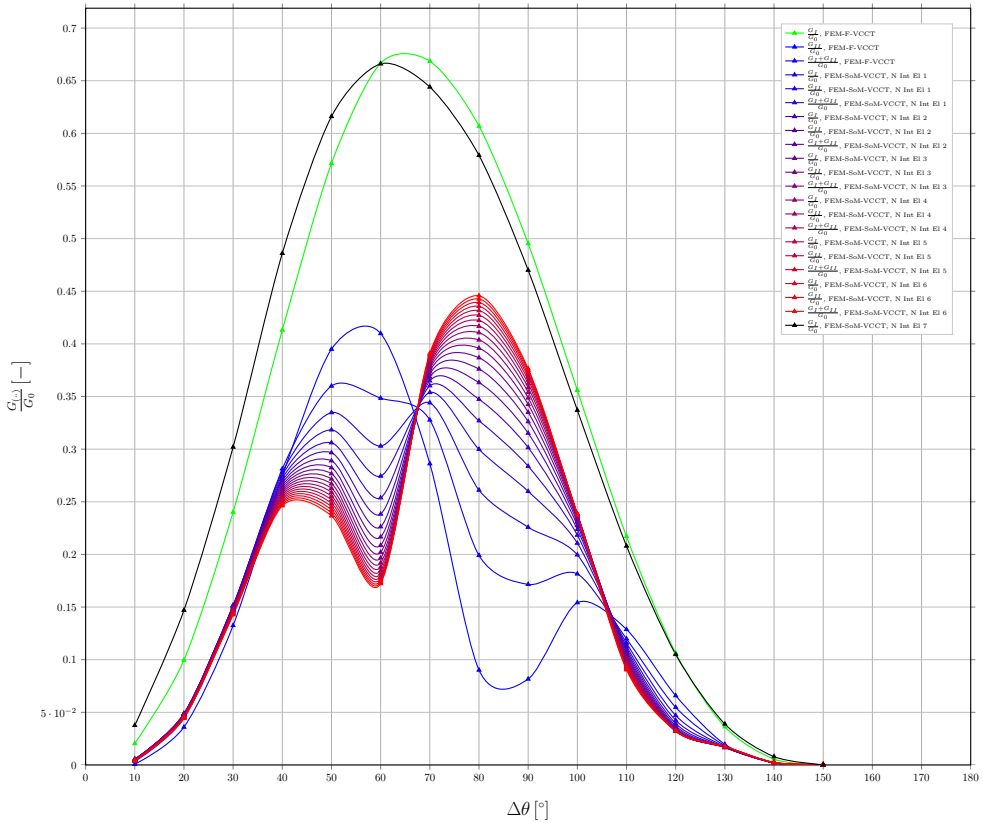

Fading from blue to red for increasing number of integration elements, Virtual Crack Closure Integral (VCCI) from FEM results; in green VCCT from FEM results; in black BEM results

G_{TOT} from VCCI, stresses extracted on matrix surface, $\delta = 5.0°$

Normalized energy release rate $\frac{G_{(-)}}{G_0}$ as function of crack angular semi-aperture $\Delta\theta$, calculated with in-house force-based and stress-based VCCT post-processing routines with stresses extracted on the matrix side of the interface

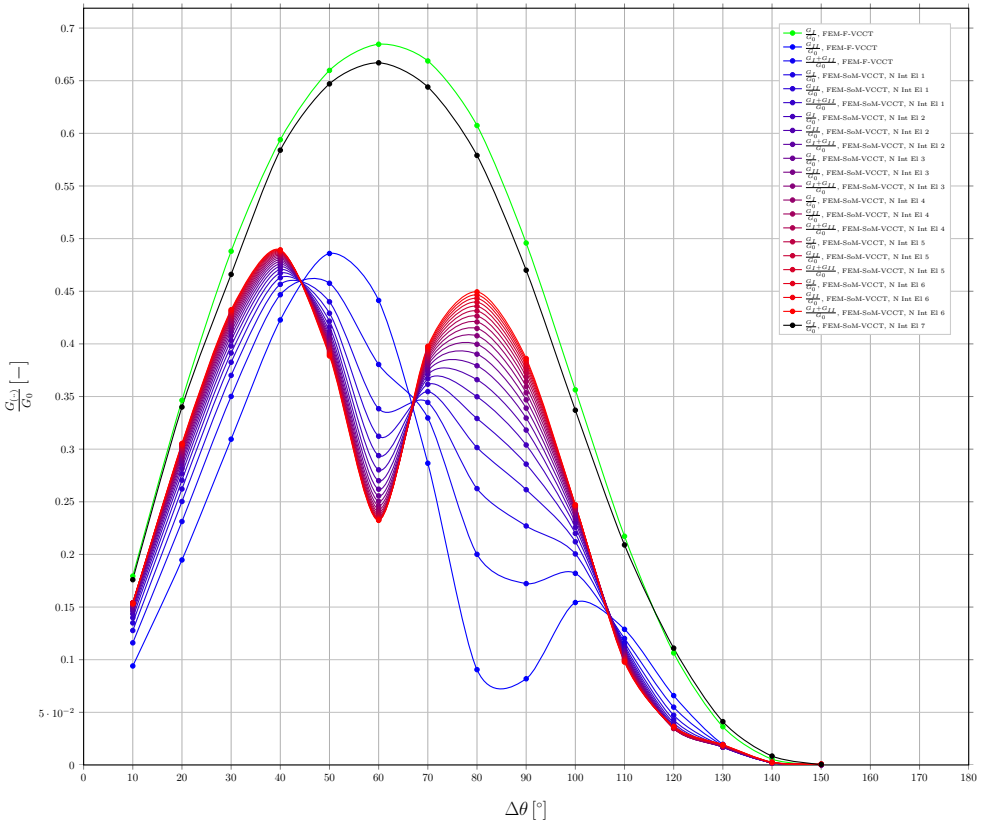

Fading from blue to red for increasing number of integration elements, Virtual Crack Closure Integral (VCCI) from FEM results; in green VCCT from FEM results; in black BEM results

Summary of $G_{(..)}$ from VCCI, stresses extracted on matrix surface,

$\delta = 5.0°$ Normalized energy release rate $\frac{G_{(..)}}{G_0}$ as function of crack angular semi-aperture $\Delta\theta$, calculated with in-house force-based and stress-based VCCT post-processing routines with stresses extracted on the matrix side of the interface

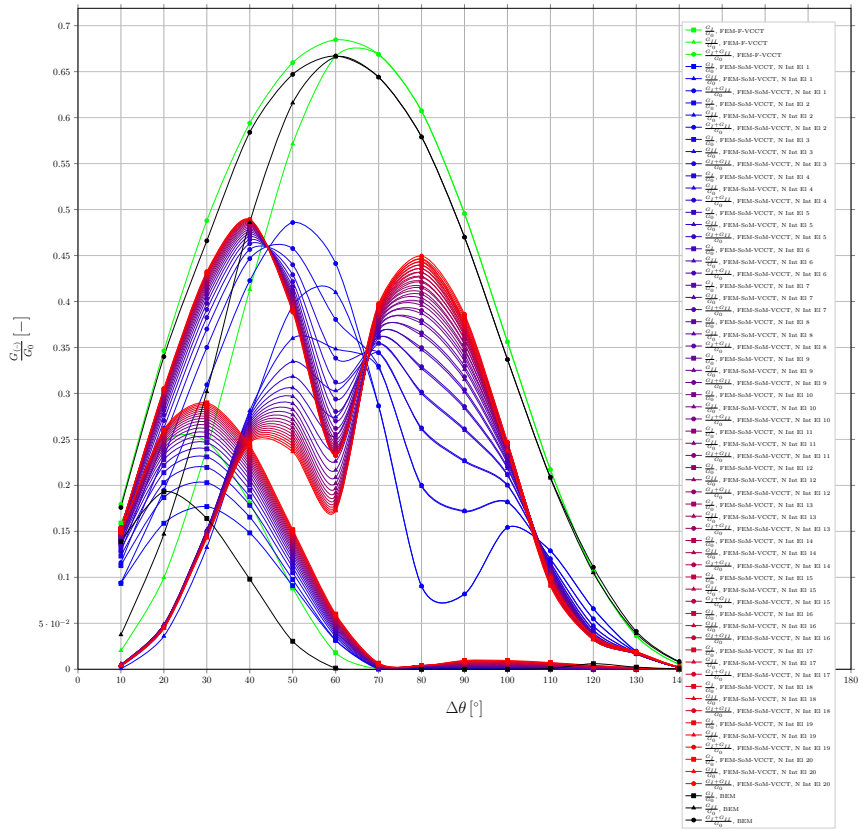

Fading from blue to red for increasing number of integration elements, Virtual Crack Closure Integral (VCCI) from FEM results; in green VCCT from FEM results; in black BEM results.

σ_0, $\delta = 0.4°$

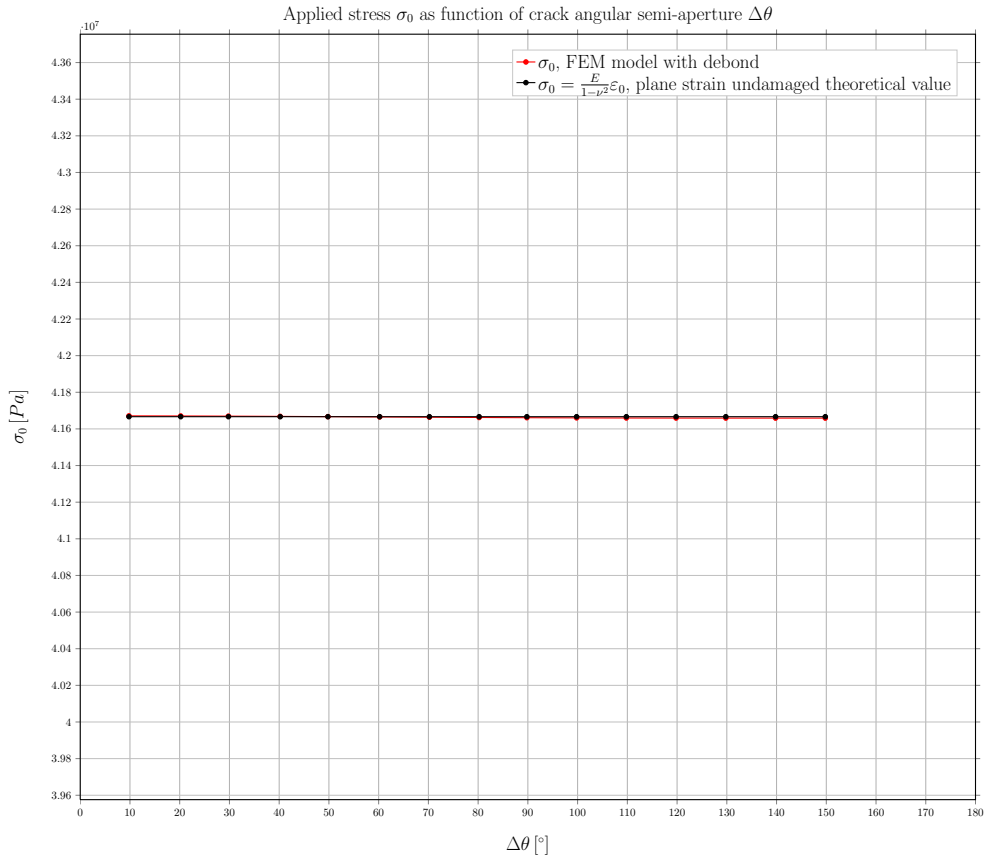

In red small strain FEM, in black analytical plain strain value.

G_0, $\delta = 0.4°$

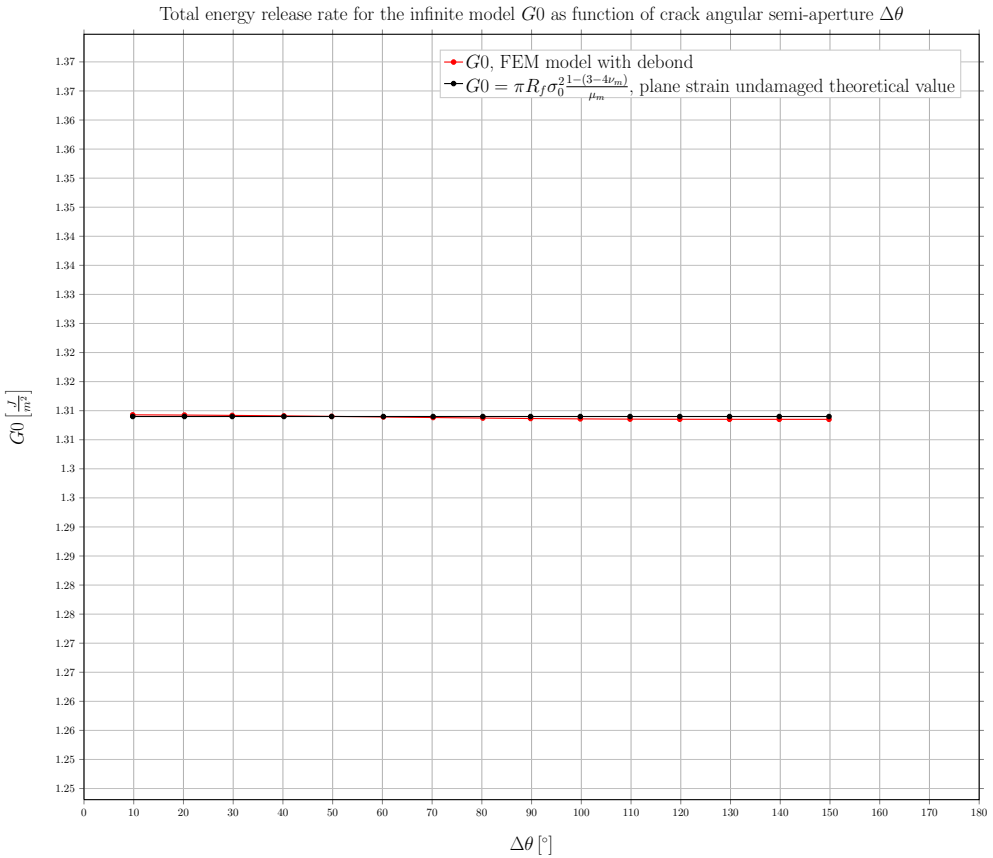

In red small strain FEM, in black analytical plain strain value.

J-Integral (Abaqus built-in routine), $\delta = 0.4°$

Normalized total energy release rate $\frac{G_{TOT}}{G_0}$ as function of crack angular semi-aperture $\Delta\theta$, calculated with Abaqus built-in J-Integral post-processing routine (*CONTOUR INTEGRAL)

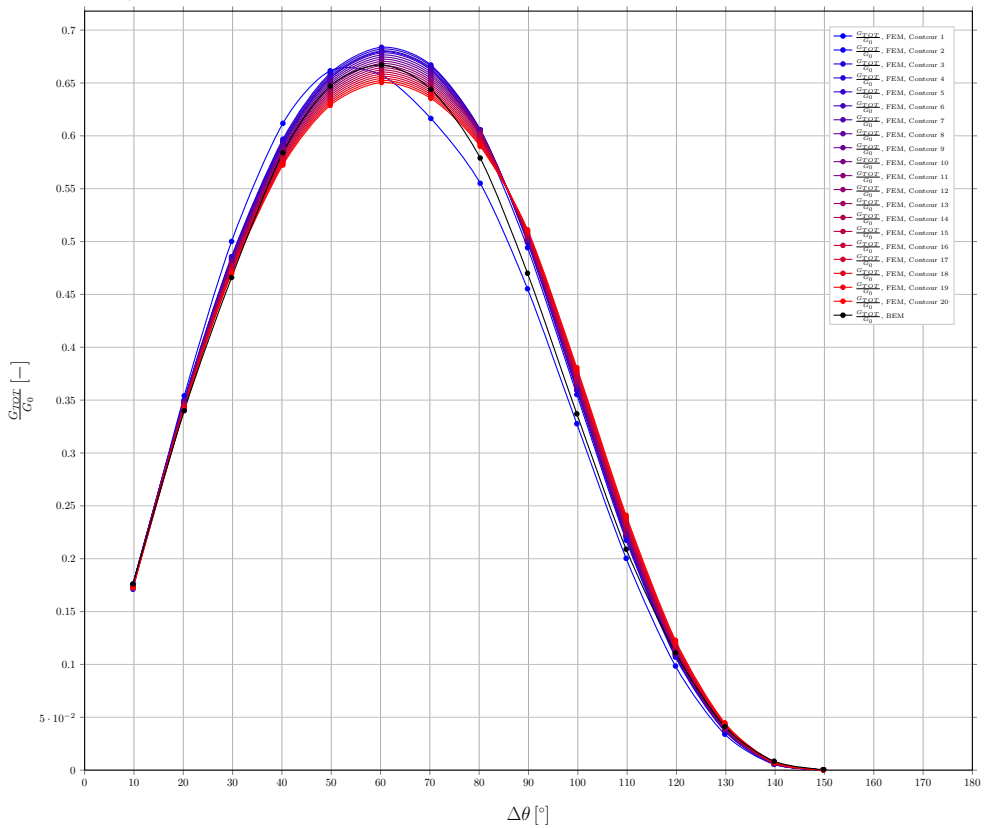

Fading from blue to red for contours further from the crack tip, FEM results; in black BEM results.

VCCT in forces (in-house Python routine), $\delta = 0.4°$

Normalized energy release rate $\frac{G_{(\cdot)}}{G_0}$ as function of crack angular semi-aperture $\Delta\theta$, calculated with in-house force-based VCCT post-processing routine

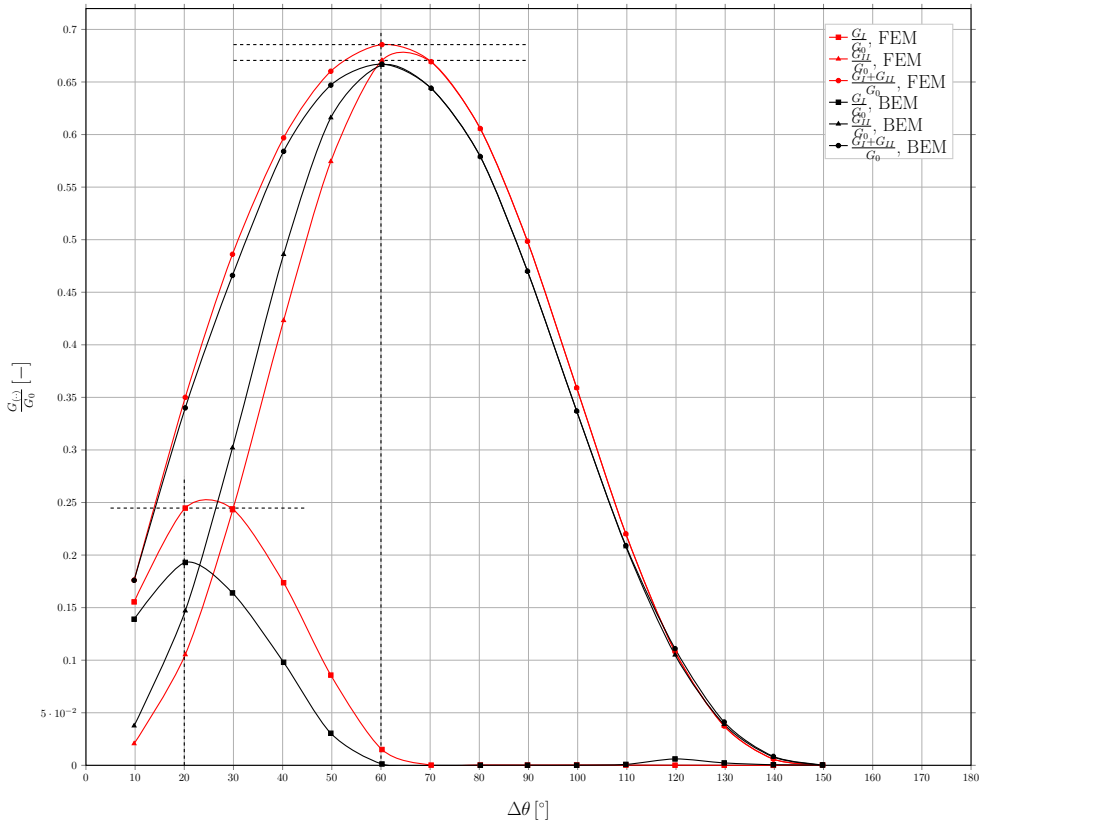

In green VCCT from FEM results, in black BEM results; positions of maxima highlighted by dashed lines.

VCCT, percentual error on BEM, $\delta = 0.4°$

$\Delta\theta$ [°]	$\frac{\frac{G_I}{G_0}\|_{FEM} - \frac{G_I}{G_0}\|_{BEM}}{\frac{G_I}{G_0}\|_{BEM}}$	$\frac{\frac{G_{II}}{G_0}\|_{FEM} - \frac{G_{II}}{G_0}\|_{BEM}}{\frac{G_{II}}{G_0}\|_{BEM}}$	$\frac{\frac{G_{TOT}}{G_0}\|_{FEM} - \frac{G_{TOT}}{G_0}\|_{BEM}}{\frac{G_{TOT}}{G_0}\|_{BEM}}$
10	11.84%	−45.09%	0.06%
20	26.79%	−28.36%	2.95%
30	48.73%	−19.81%	4.31%
40	77.24%	−12.93%	2.20%
50	181.34%	−6.75%	2.04%
60	1084.50%	0.68%	2.78%
70		3.99%	3.93%
80		4.79%	4.61%
90		5.62%	6.07%
100		6.18%	6.59%
110		3.83%	5.37%
120		1.31%	−2.40%
130		−4.97%	−9.28%
140		−30.42%	−29.99%
150		−61.36%	−14.84%

J-Integral and VCCT in forces, $\delta = 0.4°$

Normalized energy release rate $\frac{G_{(-)}}{G_0}$ as function of crack angular semi-aperture $\Delta\theta$, calculated with in-house force-based VCCT and Abaqus built-in J-Integral (*CONTOUR INTEGRAL) post-processing routines

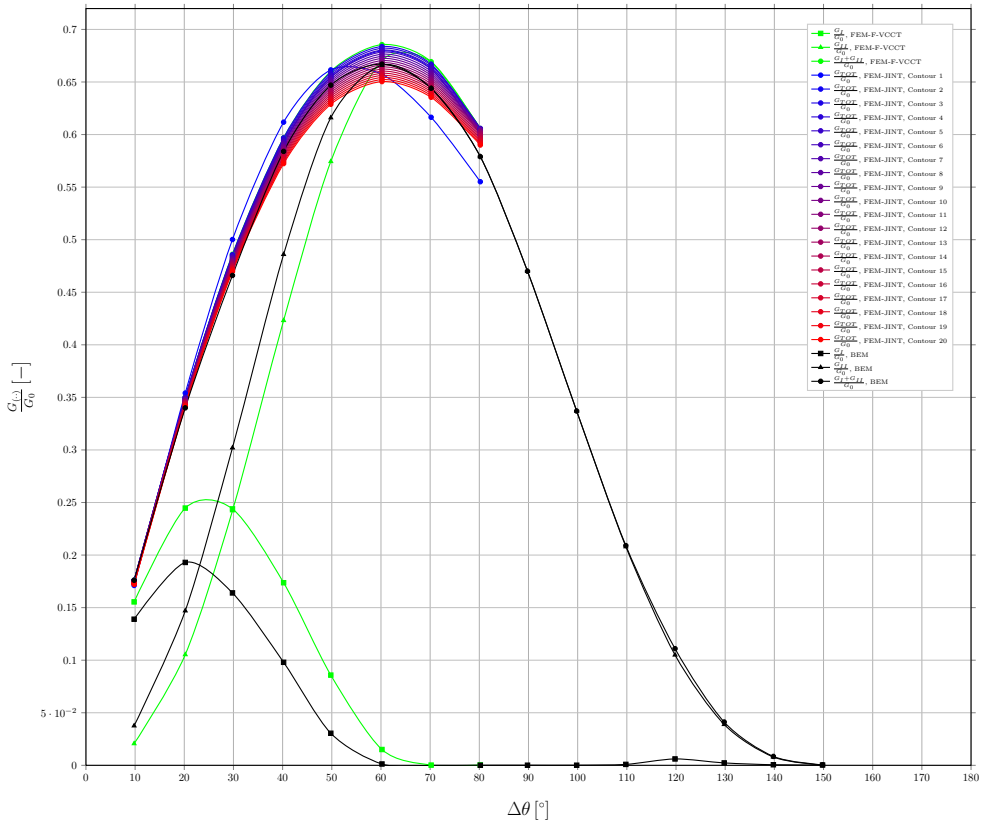

Fading from blue to red for contours further from the crack tip, J-Integral from FEM results; in green VCCT from FEM results; in black BEM results.

G_I from VCCI, stresses extracted on fiber surface, $\delta = 4.0°$

Normalized energy release rate $\frac{G_{(-)}}{G_0}$ as function of crack angular semi-aperture $\Delta\theta$, calculated with in-house force-based and stress-based VCCT post-processing routines with stresses extracted on the fiber side of the interface

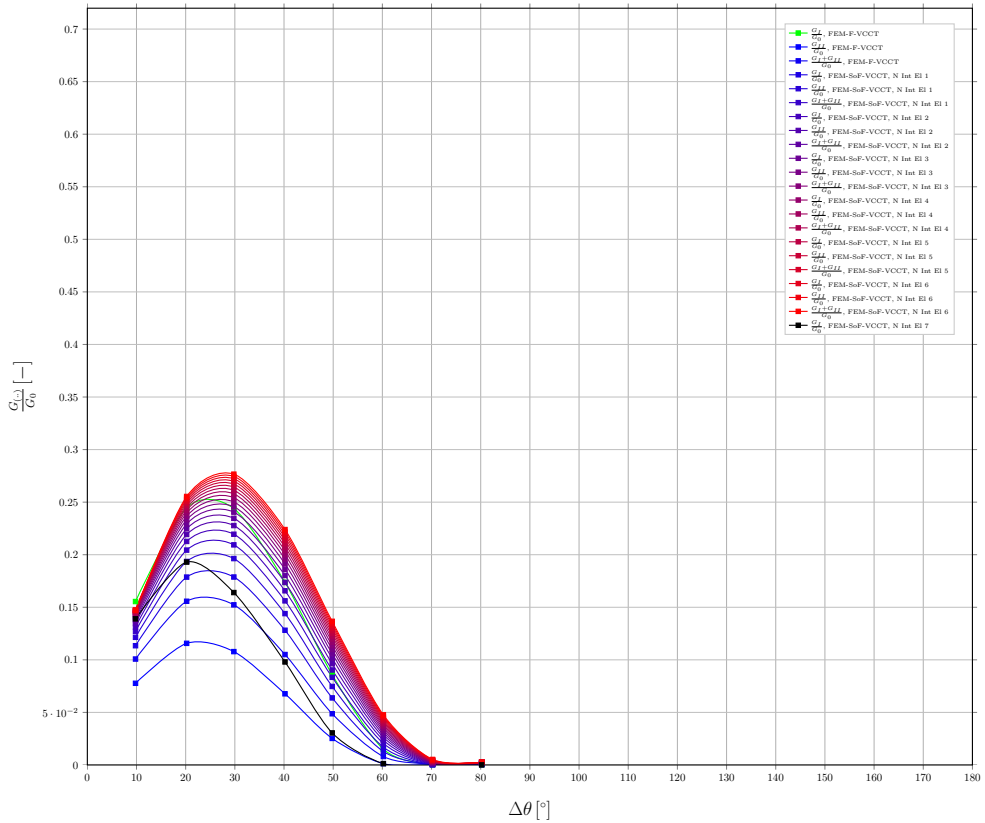

Fading from blue to red for increasing number of integration elements, Virtual Crack Closure Integral (VCCI) from FEM results; in green VCCT from FEM results; in black BEM results

$G_{//}$ from VCCI, stresses extracted on fiber surface, $\delta = 4.0°$

Normalized energy release rate $\frac{G_{(-)}}{G_0}$ as function of crack angular semi-aperture $\Delta\theta$, calculated with in-house force-based and stress-based VCCT post-processing routines with stresses extracted on the fiber side of the interface

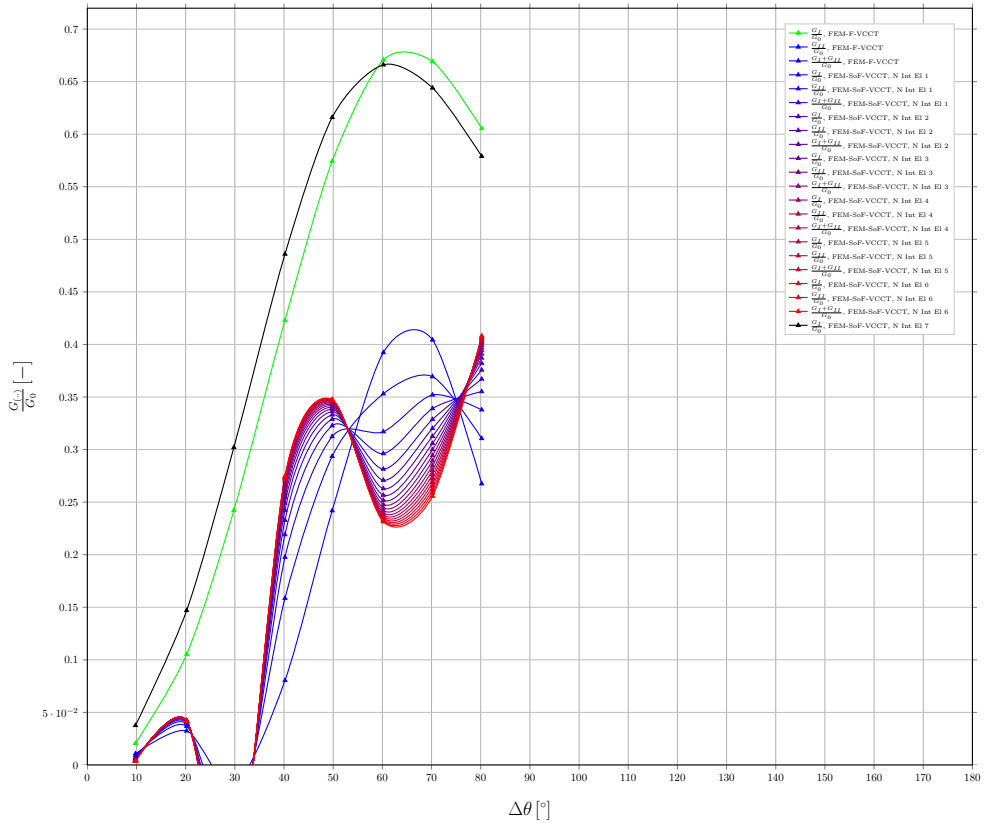

Fading from blue to red for increasing number of integration elements, Virtual Crack Closure Integral (VCCI) from FEM results; in green VCCT from FEM results; in black BEM results

G_{TOT} from VCCI, stresses extracted on fiber surface, $\delta = 4.0°$

Normalized energy release rate $\frac{G_{(-)}}{G_0}$ as function of crack angular semi-aperture $\Delta\theta$, calculated with in-house force-based and stress-based VCCT post-processing routines with stresses extracted on the fiber side of the interface

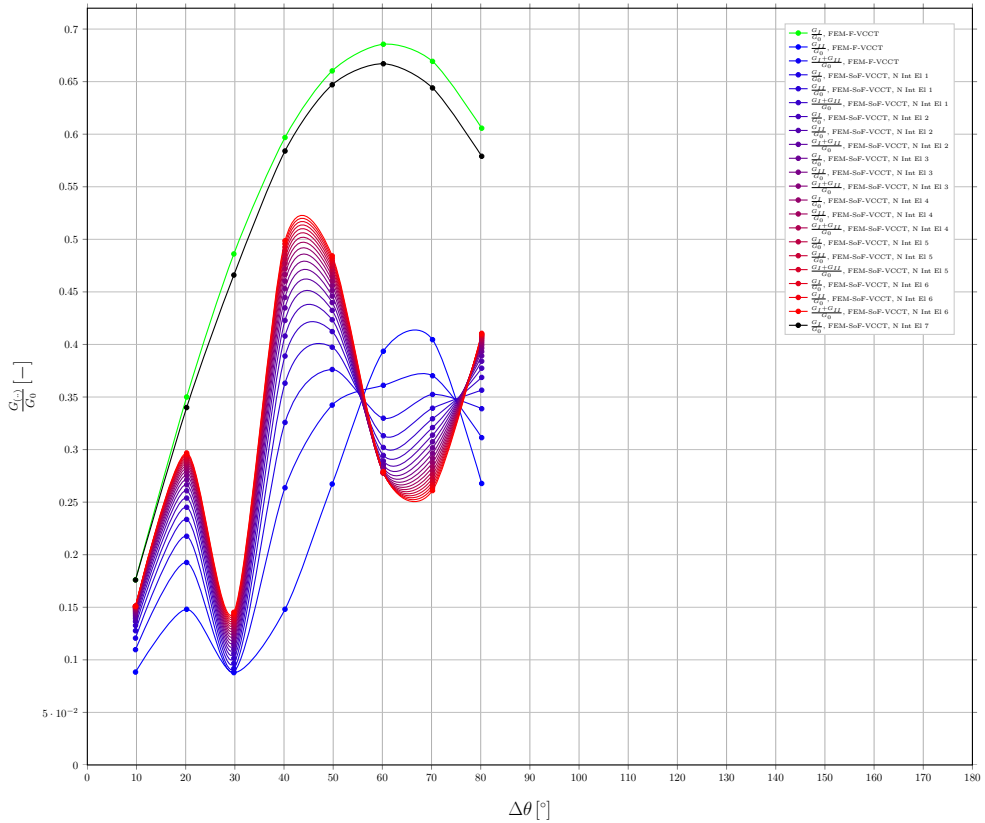

Fading from blue to red for increasing number of integration elements, Virtual Crack Closure Integral (VCCI) from FEM results; in green VCCT from FEM results; in black BEM results

Summary of $G_{(..)}$ from VCCI, stresses extracted on fiber surface,

$\delta = 4.0°$ Normalized energy release rate $\frac{G_{(..)}}{G_0}$ as function of crack angular semi-aperture $\Delta\theta$, calculated with in-house force-based and stress-based VCCT post-processing routines with stresses extracted on the fiber side of the interface

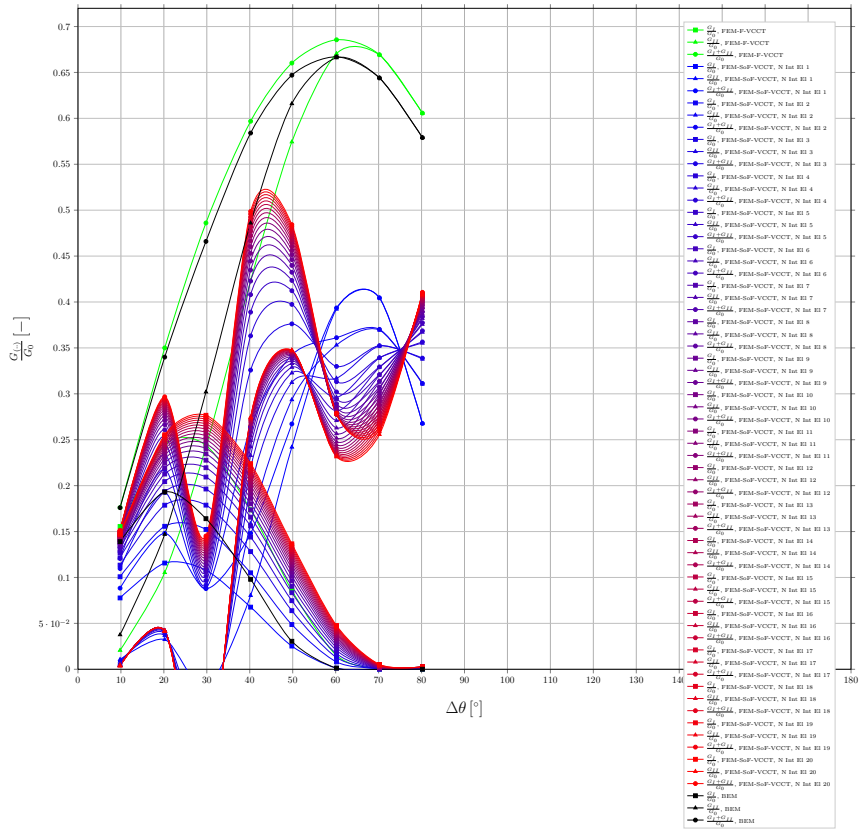

Fading from blue to red for increasing number of integration elements, Virtual Crack Closure Integral (VCCI) from FEM results; in green VCCT from FEM results; in black BEM results.

G_I from VCCI, stresses extracted on matrix surface, $\delta = 4.0°$

Normalized energy release rate $\frac{G_{(\cdot)}}{G_0}$ as function of crack angular semi-aperture $\Delta\theta$, calculated with in-house force-based and stress-based VCCT post-processing routines with stresses extracted on the matrix side of the interface

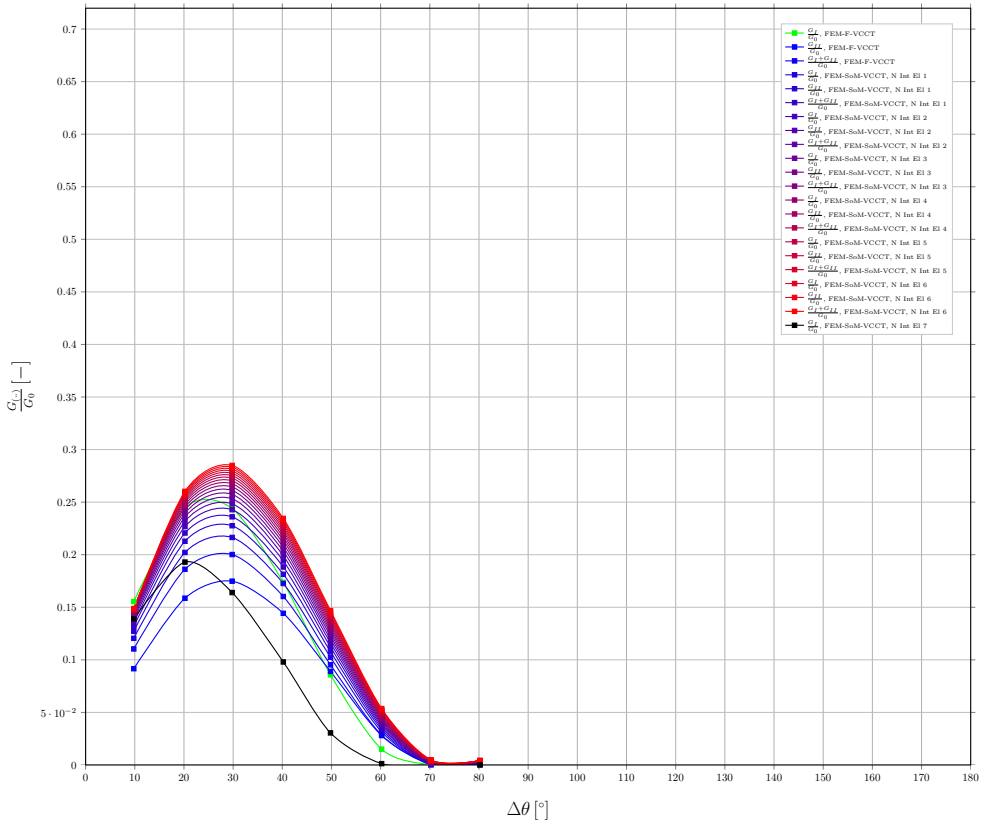

Fading from blue to red for increasing number of integration elements, Virtual Crack Closure Integral (VCCI) from FEM results; in green VCCT from FEM results; in black BEM results

G_{II} from VCCI, stresses extracted on matrix surface, $\delta = 4.0°$

Normalized energy release rate $\frac{G_{(\cdot)}}{G_0}$ as function of crack angular semi-aperture $\Delta\theta$, calculated with in-house force-based and stress-based VCCT post-processing routines with stresses extracted on the matrix side of the interface

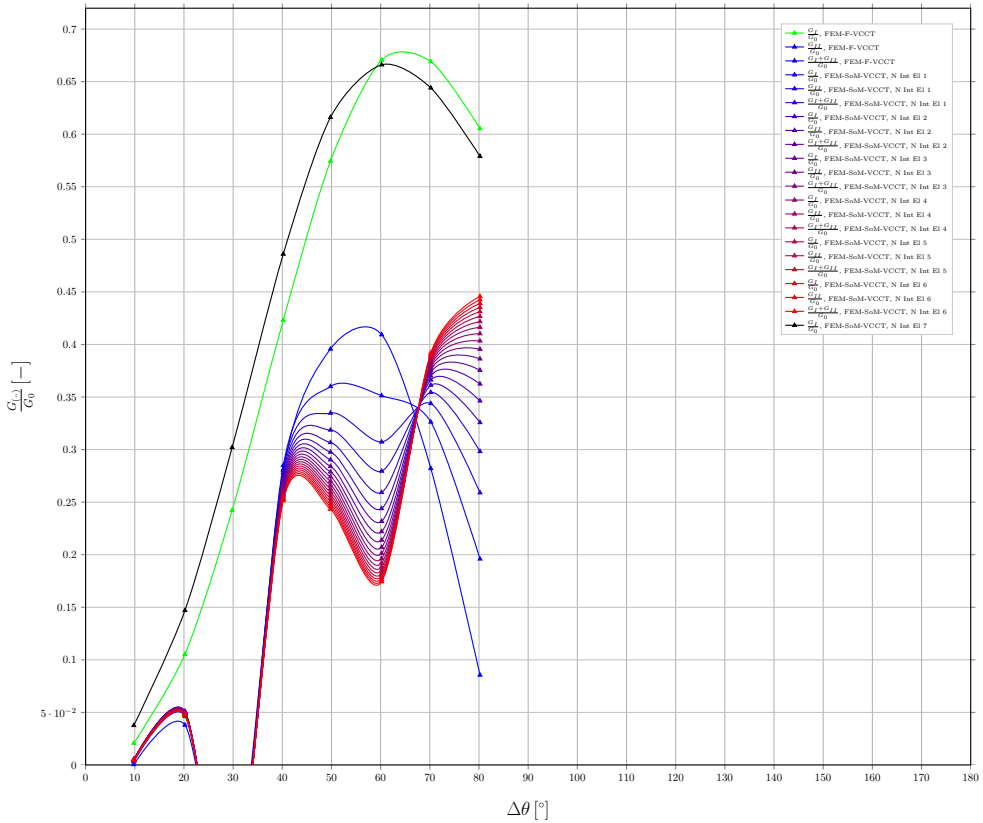

Fading from blue to red for increasing number of integration elements, Virtual Crack Closure Integral (VCCI) from FEM results; in green VCCT from FEM results; in black BEM results.

G_{TOT} from VCCI, stresses extracted on matrix surface, $\delta = 4.0°$

Normalized energy release rate $\frac{G_{(-)}}{G_0}$ as function of crack angular semi-aperture $\Delta\theta$, calculated with in-house force-based and stress-based VCCT post-processing routines with stresses extracted on the matrix side of the interface

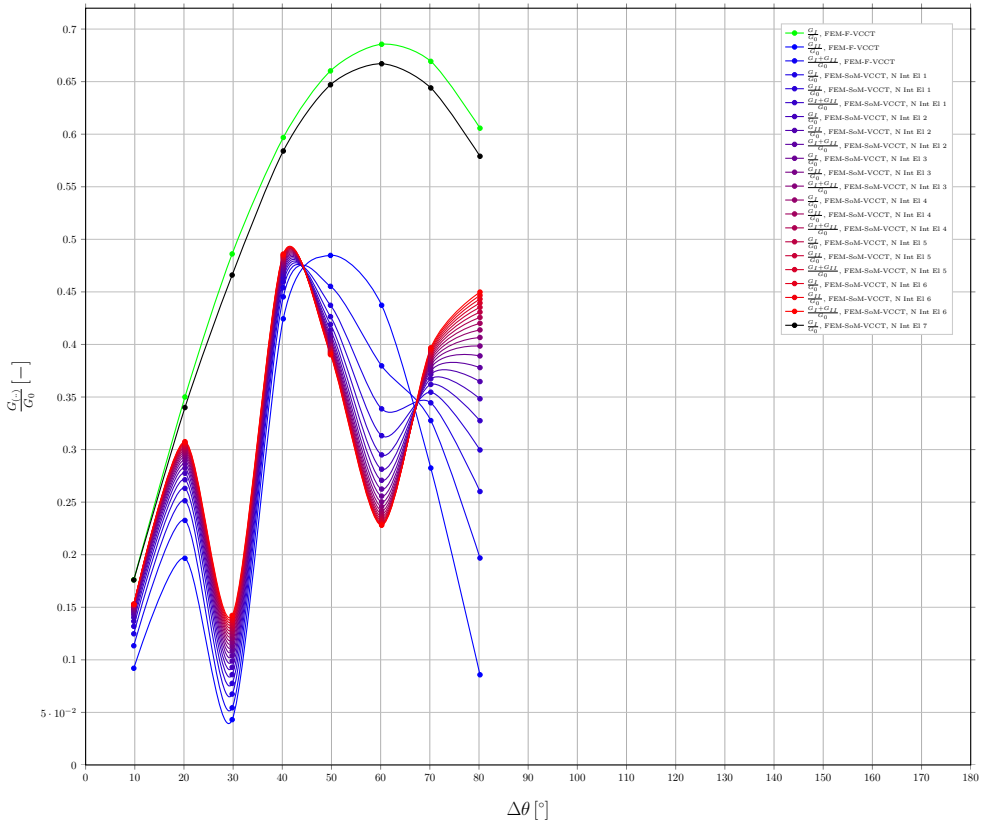

Fading from blue to red for increasing number of integration elements, Virtual Crack Closure Integral (VCCI) from FEM results; in green VCCT from FEM results; in black BEM results.

Summary of $G_{(..)}$ from VCCI, stresses extracted on matrix surface,

$\delta = 4.0°$ Normalized energy release rate $\frac{G_{(..)}}{G_0}$ as function of crack angular semi-aperture $\Delta\theta$, calculated with in-house force-based and stress-based VCCT post-processing routines with stresses extracted on the matrix side of the interface

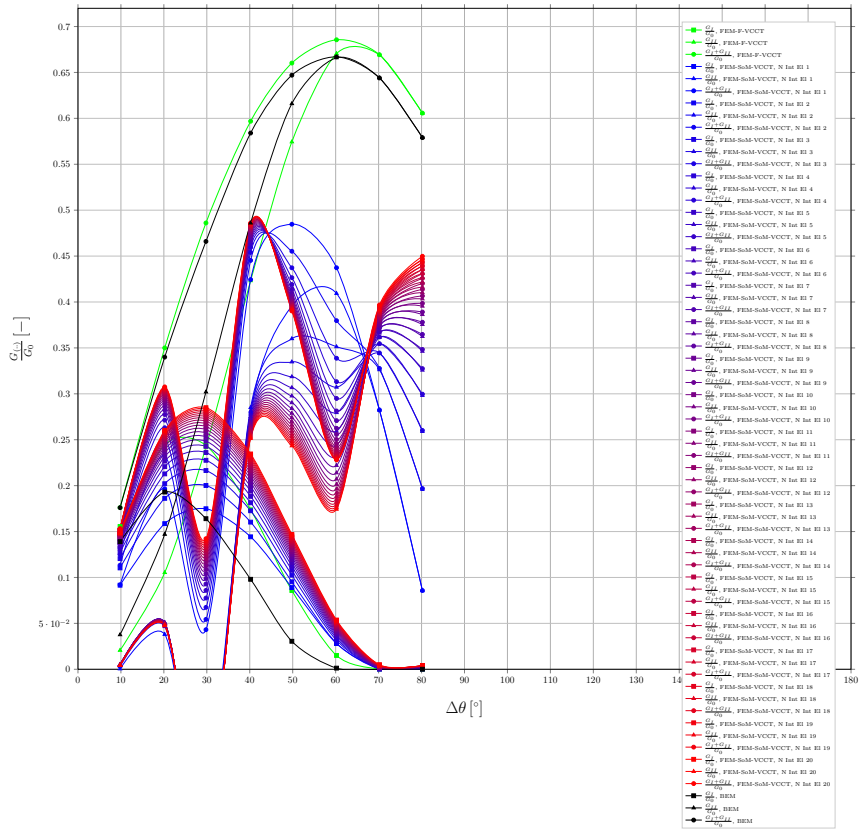

Fading from blue to red for increasing number of integration elements, Virtual Crack Closure Integral (VCCI) from FEM results; in green VCCT from FEM results; in black BEM results.

σ_0, $\delta = 0.3°$

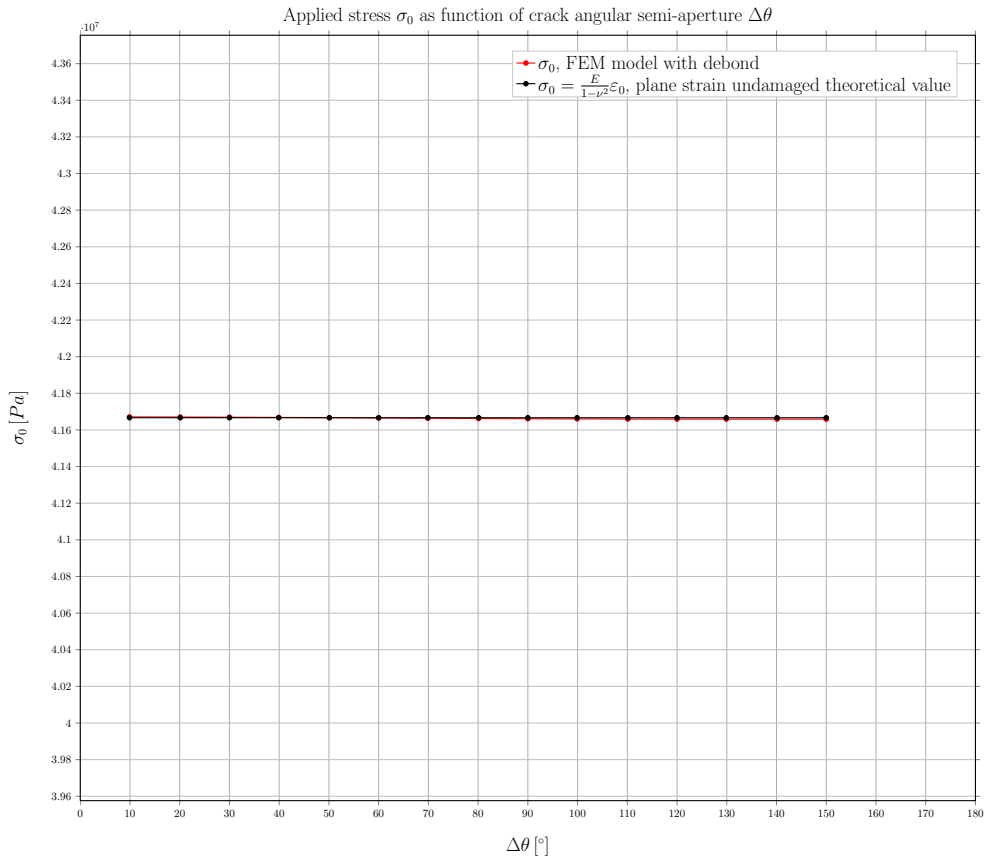

In red small strain FEM, in black analytical plain strain value.

G_0, $\delta = 0.3°$

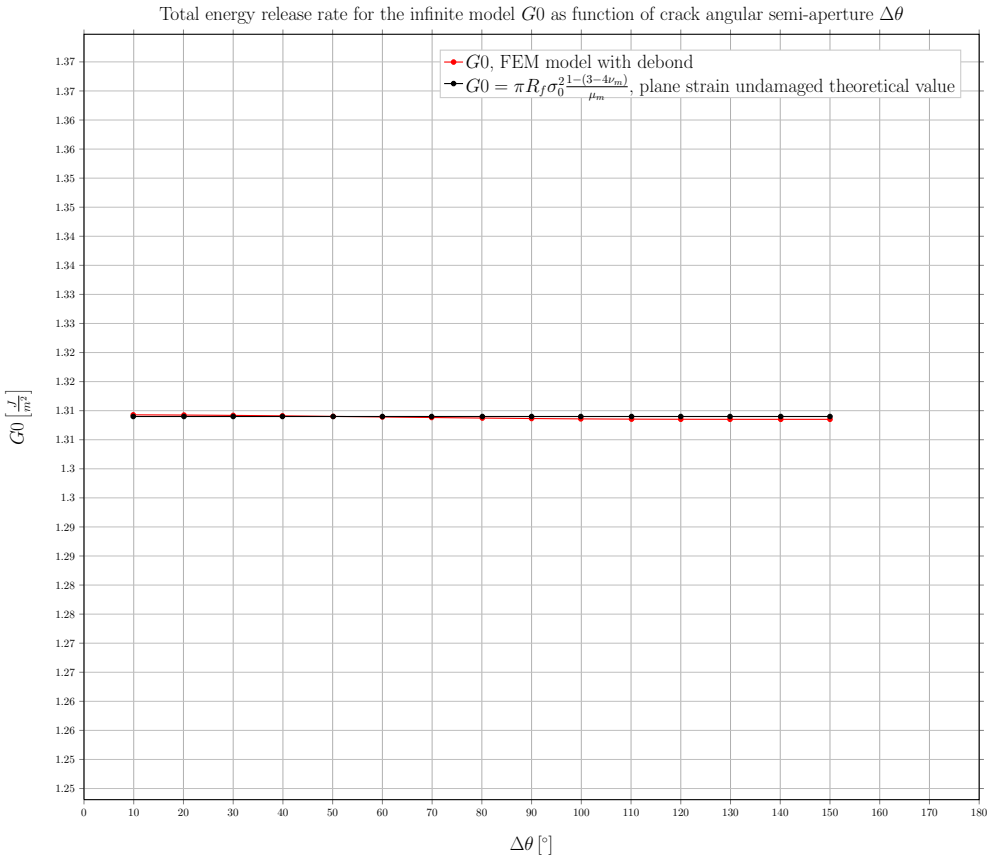

In red small strain FEM, in black analytical plain strain value.

J-Integral (Abaqus built-in routine), $\delta = 0.3°$

Normalized total energy release rate $\frac{G_{TOT}}{G_0}$ as function of crack angular semi-aperture $\Delta\theta$, calculated with Abaqus built-in J-Integral post-processing routine (*CONTOUR INTEGRAL)

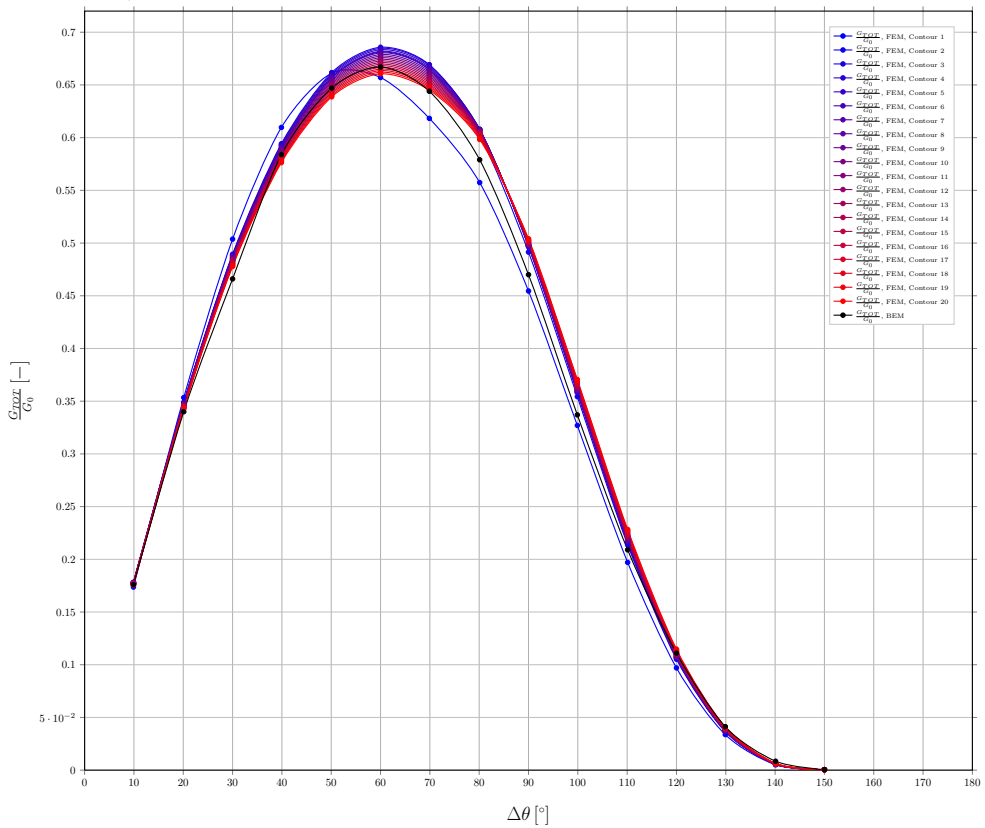

Fading from blue to red for contours further from the crack tip, FEM results; in black BEM results.

VCCT in forces (in-house Python routine), $\delta = 0.3°$

Normalized energy release rate $\frac{G_{(\cdot)}}{G_0}$ as function of crack angular semi-aperture $\Delta\theta$, calculated with in-house force-based VCCT post-processing routine

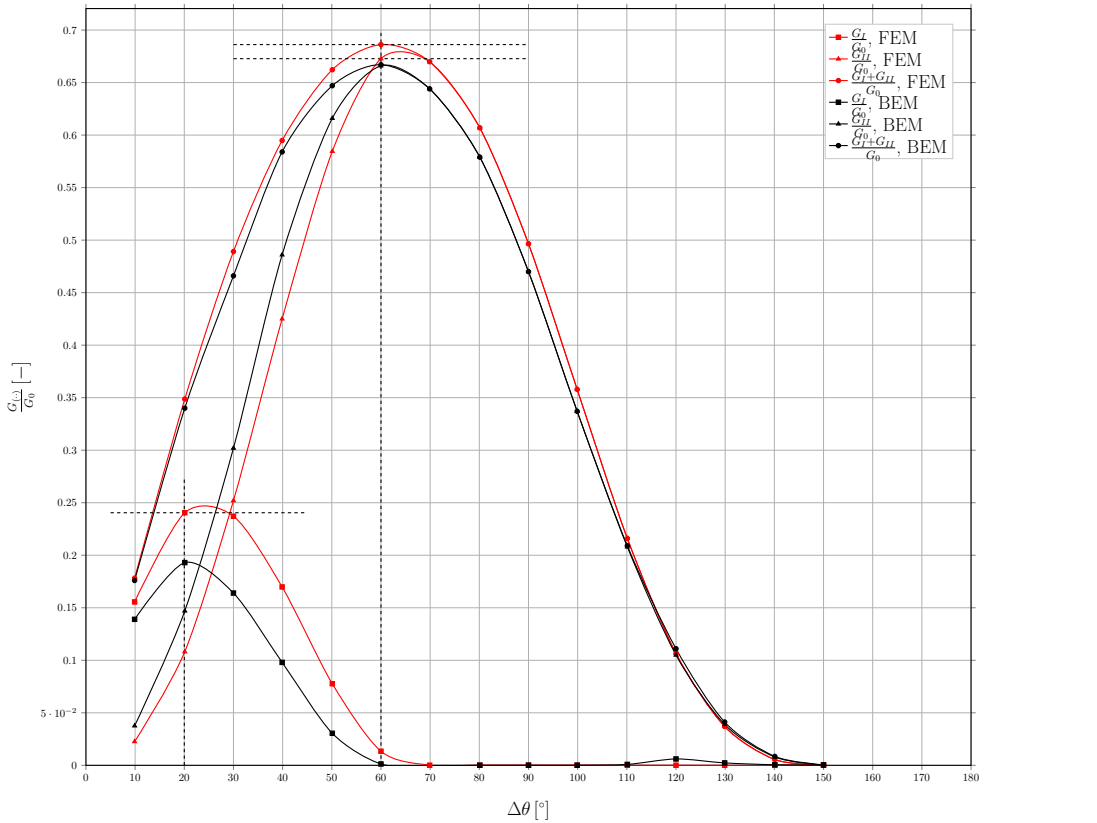

In green VCCT from FEM results, in black BEM results; positions of maxima highlighted by dashed lines.

VCCT, percentual error on BEM, $\delta = 0.3°$

$\Delta\theta$ [°]	$\frac{\frac{G_I}{G_0}\|_{FEM} - \frac{G_I}{G_0}\|_{BEM}}{\frac{G_I}{G_0}\|_{BEM}}$	$\frac{\frac{G_{II}}{G_0}\|_{FEM} - \frac{G_{II}}{G_0}\|_{BEM}}{\frac{G_{II}}{G_0}\|_{BEM}}$	$\frac{\frac{G_{TOT}}{G_0}\|_{FEM} - \frac{G_{TOT}}{G_0}\|_{BEM}}{\frac{G_{TOT}}{G_0}\|_{BEM}}$
10	11.91%	−39.86%	1.23%
20	24.60%	−26.37%	2.56%
30	44.60%	−16.55%	4.97%
40	73.27%	−12.54%	1.86%
50	154.60%	−5.10%	2.35%
60	955.70%	1.01%	2.87%
70		3.99%	4.01%
80		4.79%	4.83%
90		5.62%	5.66%
100		6.18%	6.22%
110		3.83%	3.38%
120		1.31%	−4.08%
130		−4.97%	−10.17%
140		−30.42%	−34.90%
150		−61.36%	−0.52%

J-Integral and VCCT in forces, $\delta = 0.3°$

Normalized energy release rate $\frac{G_{(\cdot)}}{G_0}$ as function of crack angular semi-aperture $\Delta\theta$, calculated with in-house force-based VCCT and Abaqus built-in J-Integral (*CONTOUR INTEGRAL) post-processing routines

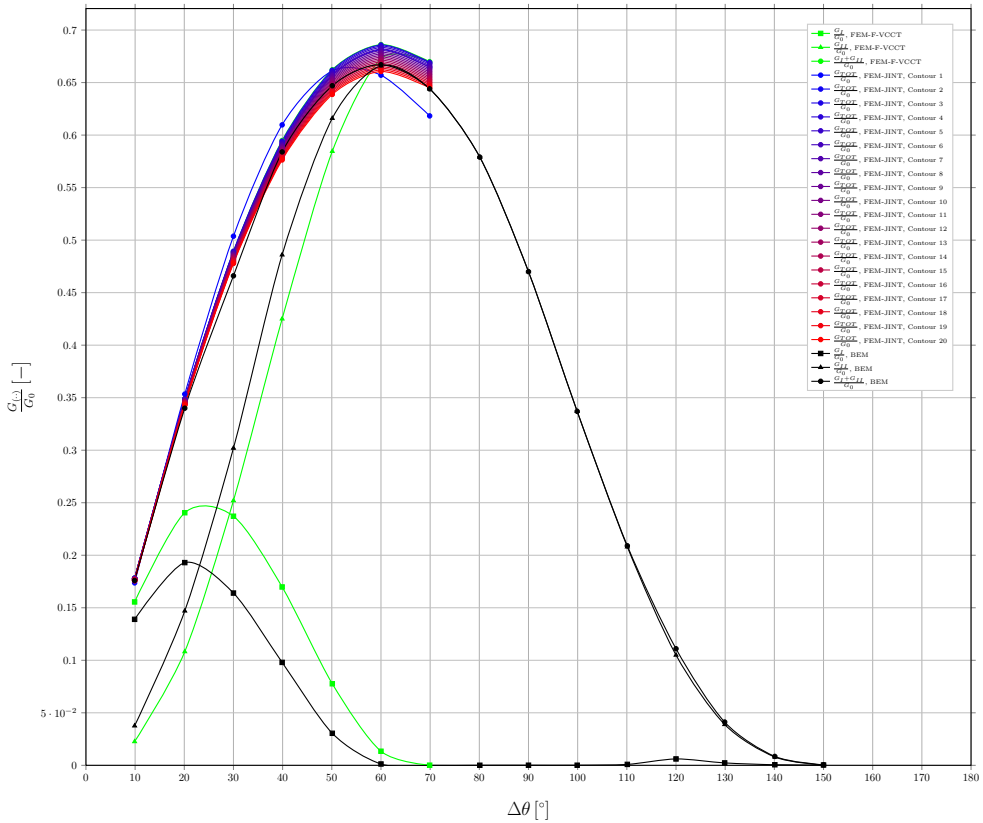

Fading from blue to red for contours further from the crack tip, J-Integral from FEM results; in green VCCT from FEM results; in black BEM results.

G_I from VCCI, stresses extracted on fiber surface, $\delta = 3.0°$

Normalized energy release rate $\frac{G_{(-)}}{G_0}$ as function of crack angular semi-aperture $\Delta\theta$, calculated with in-house force-based and stress-based VCCT post-processing routines with stresses extracted on the fiber side of the interface

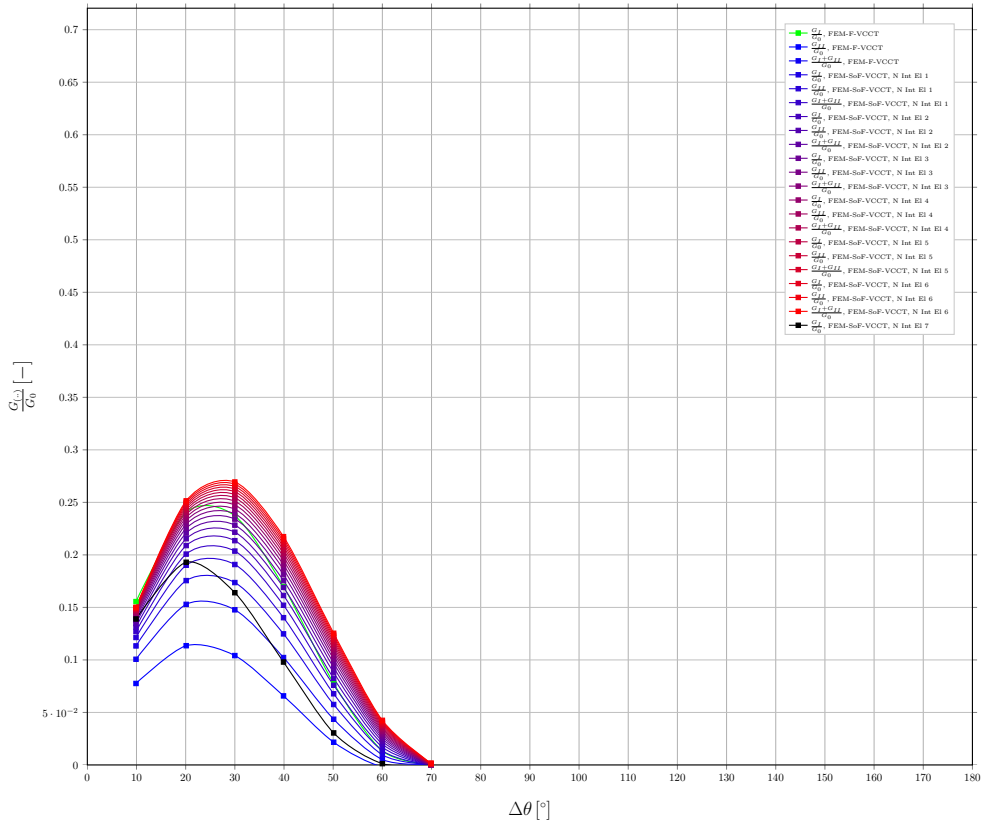

Fading from blue to red for increasing number of integration elements, Virtual Crack Closure Integral (VCCI) from FEM results; in green VCCT from FEM results; in black BEM results

$G_{//}$ from VCCI, stresses extracted on fiber surface, $\delta = 3.0°$

Normalized energy release rate $\frac{G_{(-)}}{G_0}$ as function of crack angular semi-aperture $\Delta\theta$, calculated with in-house force-based and stress-based VCCT post-processing routines with stresses extracted on the fiber side of the interface

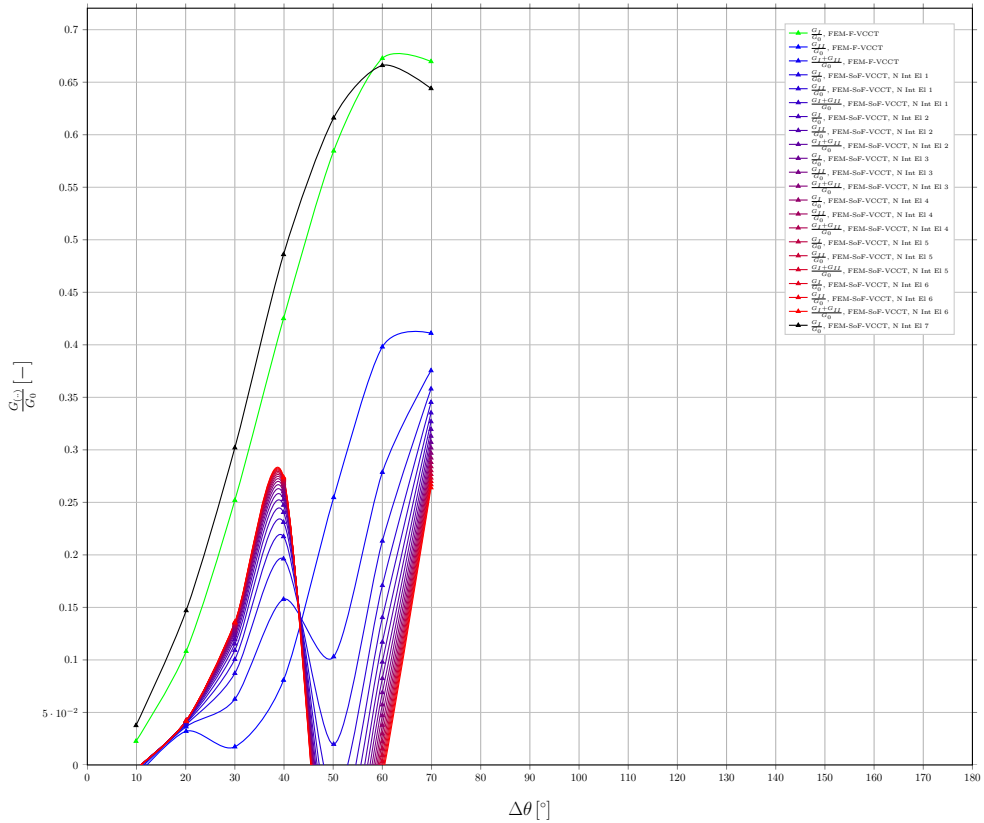

Fading from blue to red for increasing number of integration elements, Virtual Crack Closure Integral (VCCI) from FEM results; in green VCCT from FEM results; in black BEM results

G_{TOT} from VCCI, stresses extracted on fiber surface, $\delta = 3.0°$

Normalized energy release rate $\frac{G_{(-)}}{G_0}$ as function of crack angular semi-aperture $\Delta\theta$, calculated with in-house force-based and stress-based VCCT post-processing routines with stresses extracted on the fiber side of the interface

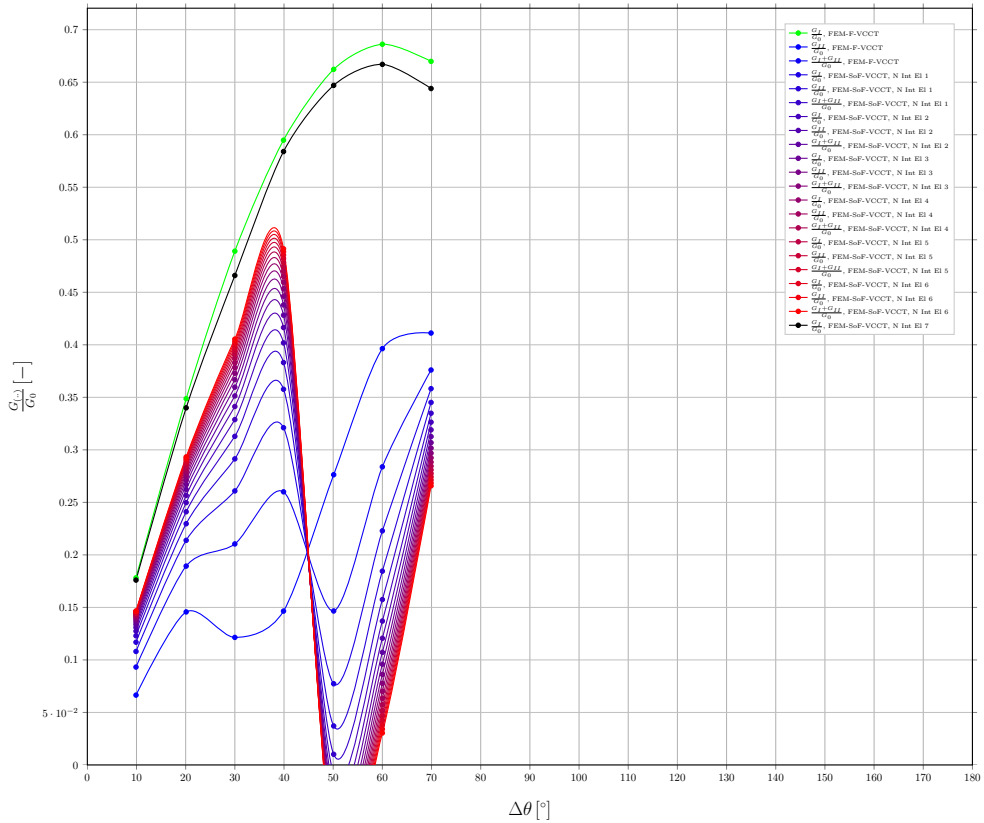

Fading from blue to red for increasing number of integration elements, Virtual Crack Closure Integral (VCCI) from FEM results; in green VCCT from FEM results; in black BEM results

Summary of $G_{(..)}$ from VCCI, stresses extracted on fiber surface,

$\delta = 3.0°$ Normalized energy release rate $\frac{G_{(..)}}{G_0}$ as function of crack angular semi-aperture $\Delta\theta$, calculated with in-house force-based and stress-based VCCT post-processing routines with stresses extracted on the fiber side of the interface

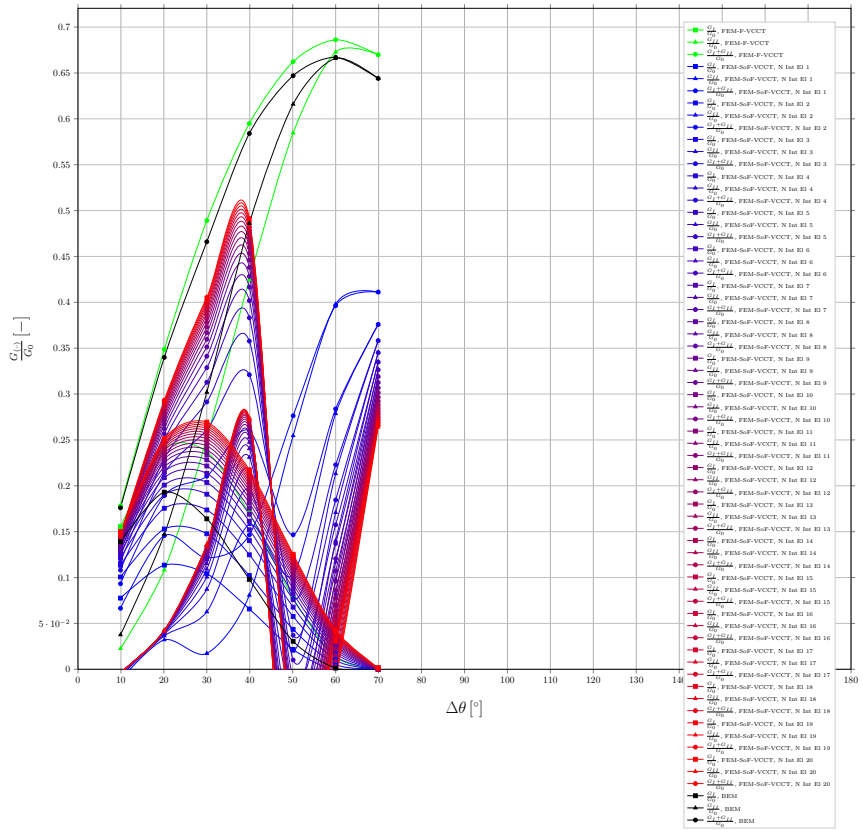

Fading from blue to red for increasing number of integration elements, Virtual Crack Closure Integral (VCCI) from FEM results; in green VCCT from FEM results; in black BEM results.

G_I from VCCI, stresses extracted on matrix surface, $\delta = 3.0°$

Normalized energy release rate $\frac{G_{(\cdot)}}{G_0}$ as function of crack angular semi-aperture $\Delta\theta$, calculated with in-house force-based and stress-based VCCT post-processing routines with stresses extracted on the matrix side of the interface

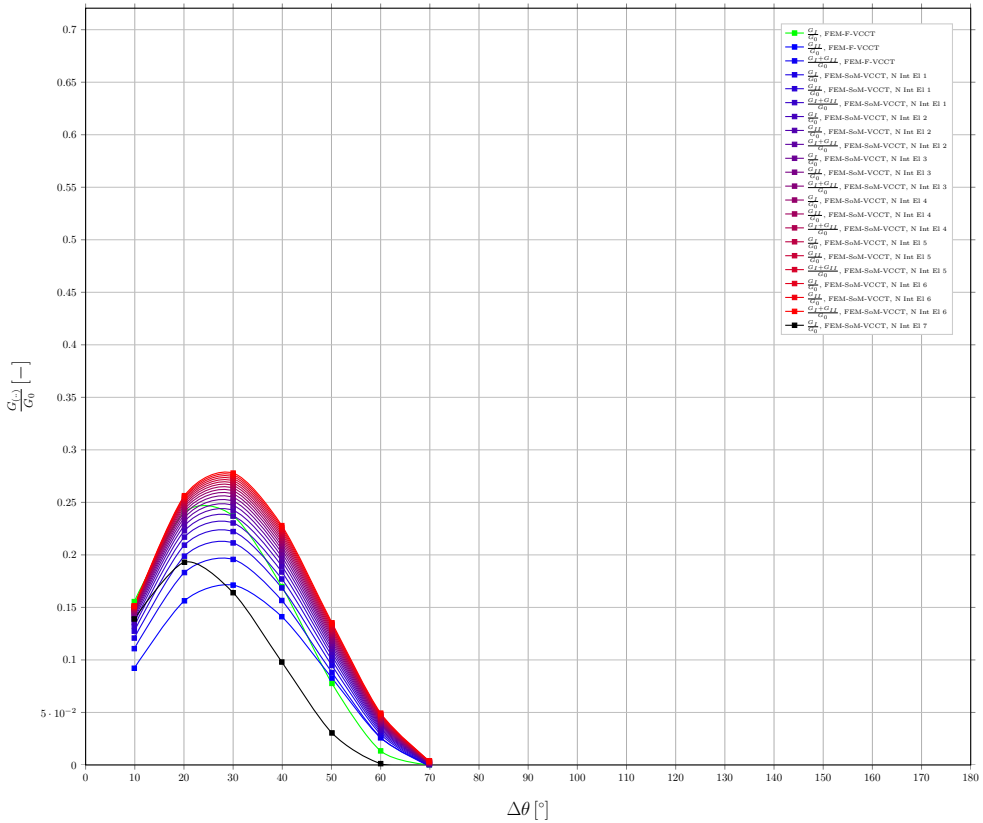

Fading from blue to red for increasing number of integration elements, Virtual Crack Closure Integral (VCCI) from FEM results; in green VCCT from FEM results; in black BEM results

G_{II} from VCCI, stresses extracted on matrix surface, $\delta = 3.0°$

Normalized energy release rate $\frac{G_{(-)}}{G_0}$ as function of crack angular semi-aperture $\Delta\theta$, calculated with in-house force-based and stress-based VCCT post-processing routines with stresses extracted on the matrix side of the interface

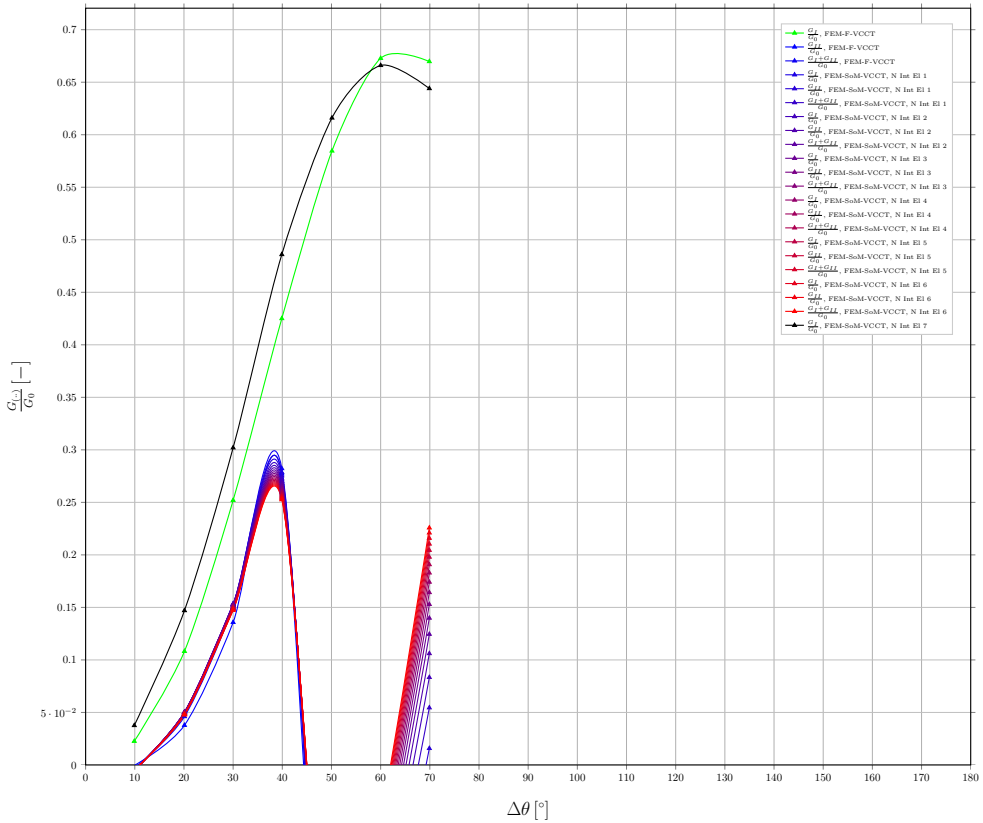

Fading from blue to red for increasing number of integration elements, Virtual Crack Closure Integral (VCCI) from FEM results; in green VCCT from FEM results; in black BEM results

G_{TOT} from VCCI, stresses extracted on matrix surface, $\delta = 3.0°$

Normalized energy release rate $\frac{G_{(-)}}{G_0}$ as function of crack angular semi-aperture $\Delta\theta$, calculated with in-house force-based and stress-based VCCT post-processing routines with stresses extracted on the matrix side of the interface

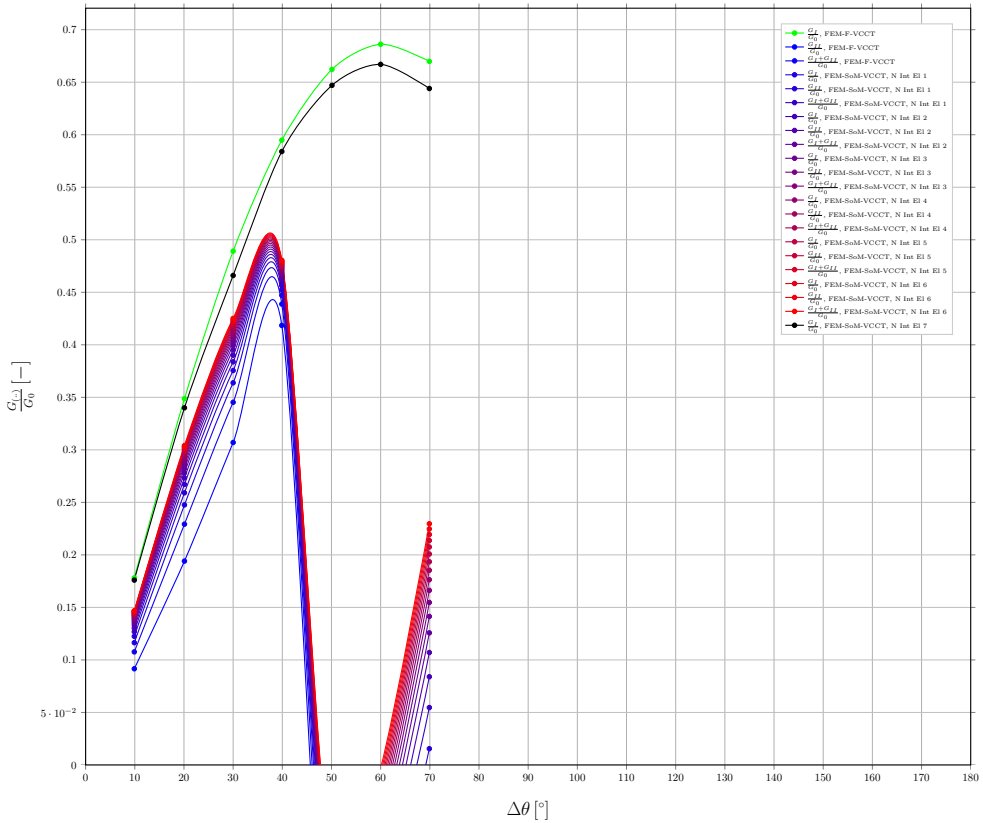

Fading from blue to red for increasing number of integration elements, Virtual Crack Closure Integral (VCCI) from FEM results; in green VCCT from FEM results; in black BEM results.

Summary of $G_{(..)}$ from VCCI, stresses extracted on matrix surface, $\delta = 3.0°$

Normalized energy release rate $\frac{G_{(..)}}{G_0}$ as function of crack angular semi-aperture $\Delta\theta$, calculated with in-house force-based and stress-based VCCT post-processing routines with stresses extracted on the matrix side of the interface

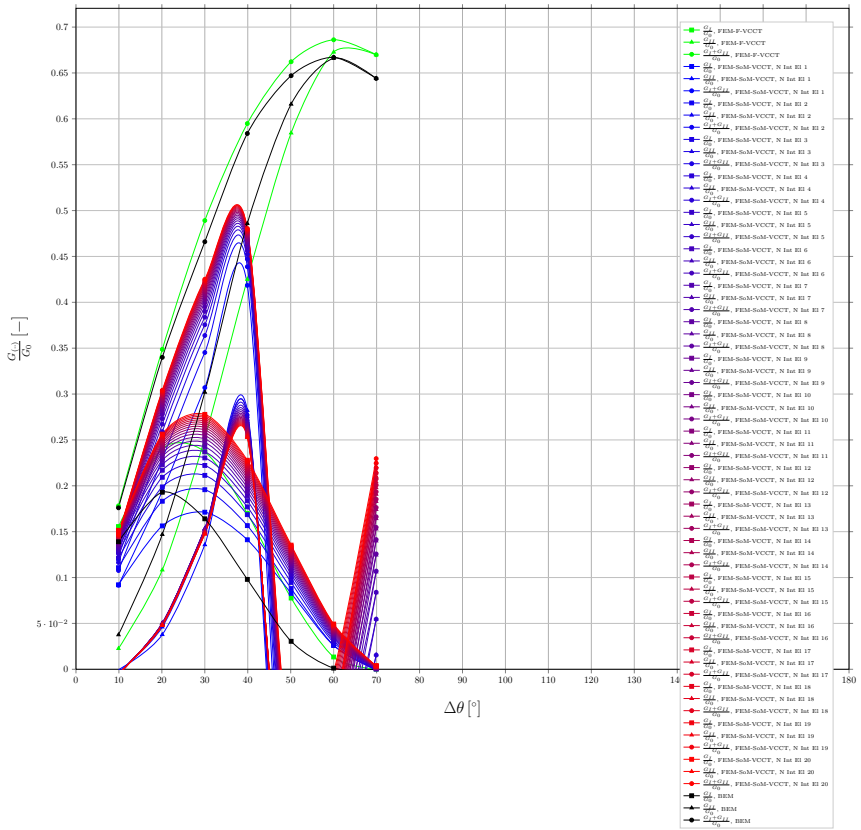

Fading from blue to red for increasing number of integration elements, Virtual Crack Closure Integral (VCCI) from FEM results; in green VCCT from FEM results; in black BEM results.

σ_0, $\delta = 0.2°$

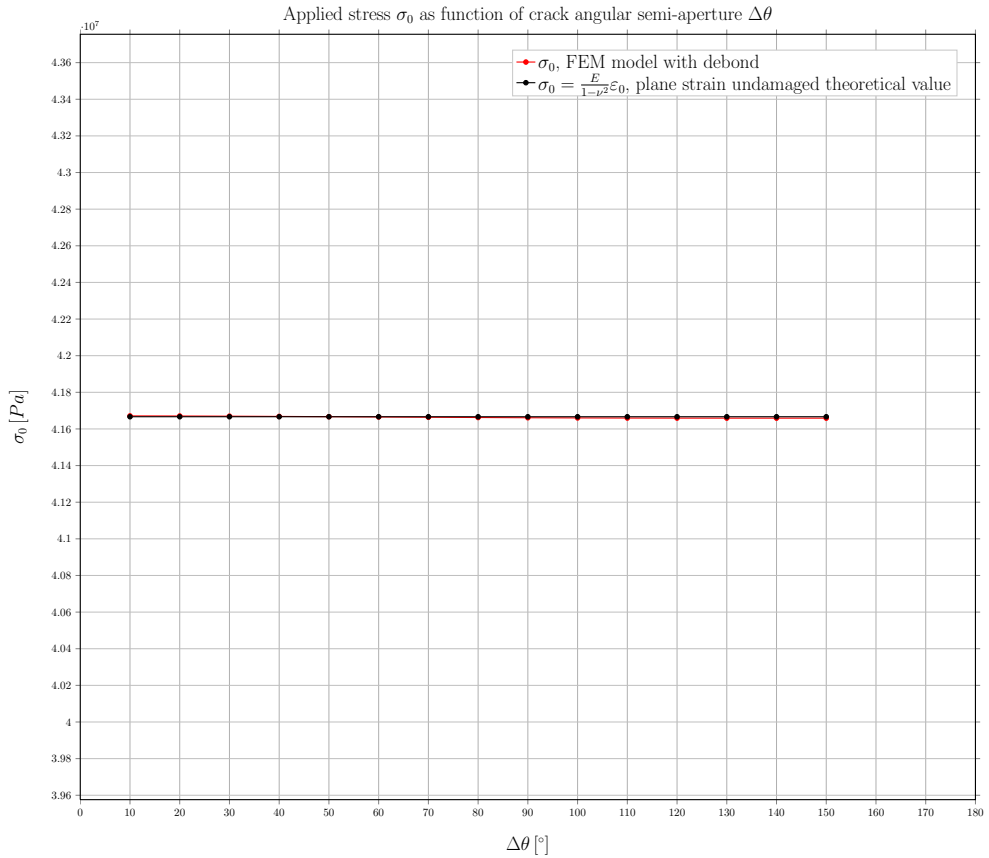

In red small strain FEM, in black analytical plain strain value.

G_0, $\delta = 0.2°$

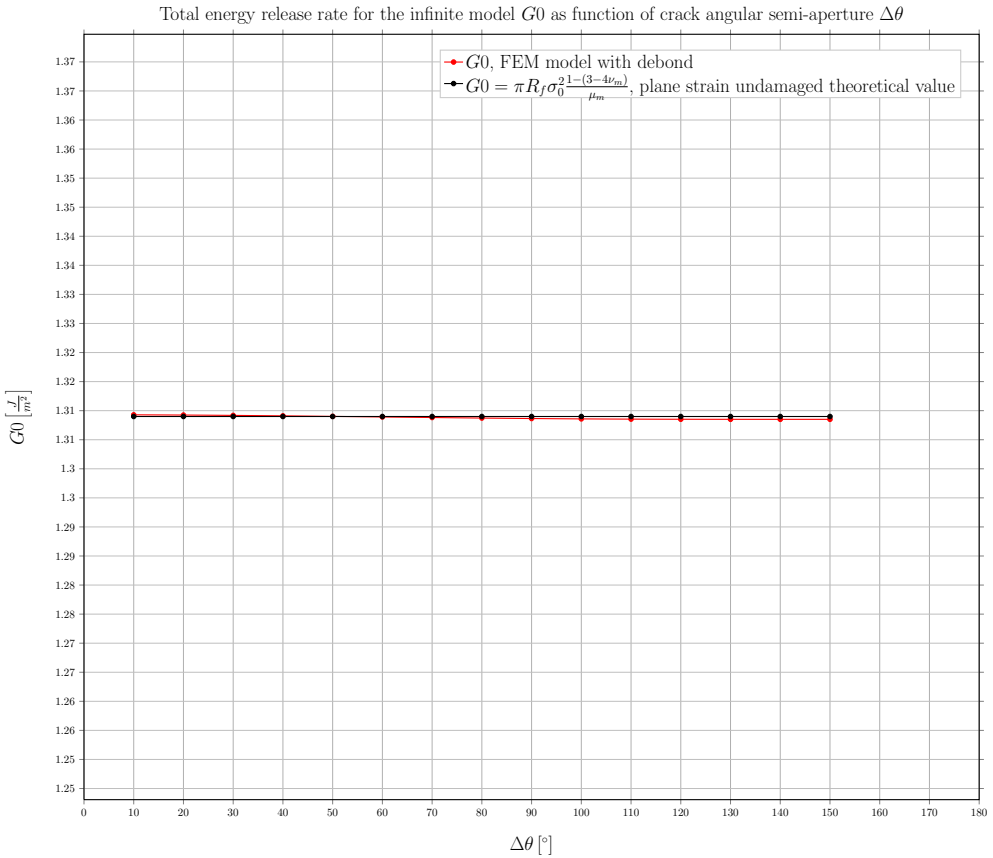

In red small strain FEM, in black analytical plain strain value.

VCCT in forces (in-house Python routine), $\delta = 0.2°$

Normalized energy release rate $\frac{G_{(\cdot)}}{G_0}$ as function of crack angular semi-aperture $\Delta\theta$, calculated with in-house force-based VCCT post-processing routine

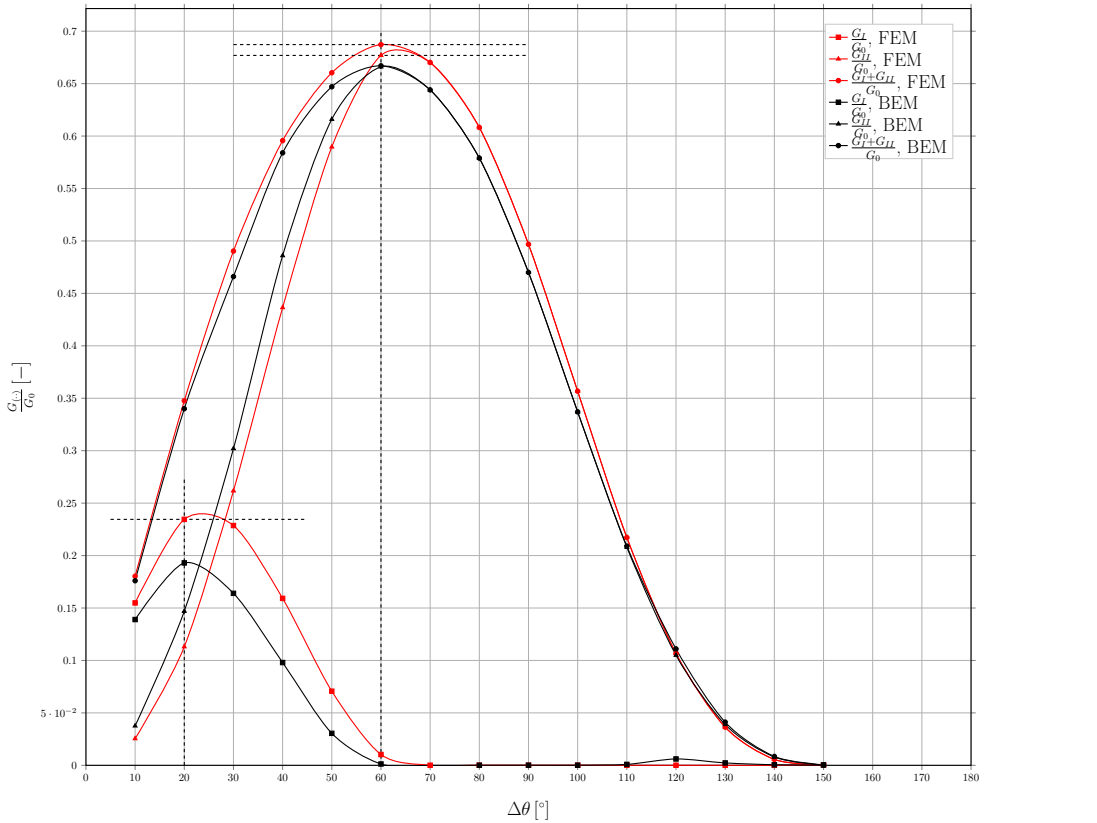

In green VCCT from FEM results, in black BEM results; positions of maxima highlighted by dashed lines.

VCCT, percentual error on BEM, $\delta = 0.2°$

$\Delta\theta$ [°]	$\frac{\frac{G_I}{G_0}\|_{FEM} - \frac{G_I}{G_0}\|_{BEM}}{\frac{G_I}{G_0}\|_{BEM}}$	$\frac{\frac{G_{II}}{G_0}\|_{FEM} - \frac{G_{II}}{G_0}\|_{BEM}}{\frac{G_{II}}{G_0}\|_{BEM}}$	$\frac{\frac{G_{TOT}}{G_0}\|_{FEM} - \frac{G_{TOT}}{G_0}\|_{BEM}}{\frac{G_{TOT}}{G_0}\|_{BEM}}$
10	11.41%	−32.33%	2.44%
20	21.51%	−23.07%	2.24%
30	39.40%	−13.34%	5.22%
40	62.43%	−10.19%	1.99%
50	131.80%	−4.28%	2.06%
60	712.56%	1.64%	3.03%
70		4.05%	4.06%
80		5.02%	5.05%
90		5.69%	5.71%
100		5.83%	5.86%
110		4.45%	3.97%
120		1.55%	−3.88%
130		−6.42%	−11.60%
140		−28.46%	−33.11%
150		−67.88%	−0.52%

G_I, VCCT in forces

Normalized energy release rate $\frac{G_I}{G_0}$ as function of crack angular semi-aperture $\Delta\theta$, $VF_f = 7.9 \cdot 10^{-5}$, $\frac{L}{R_f} \sim 100$ calculated with in-house force-based VCCT post-processing routine

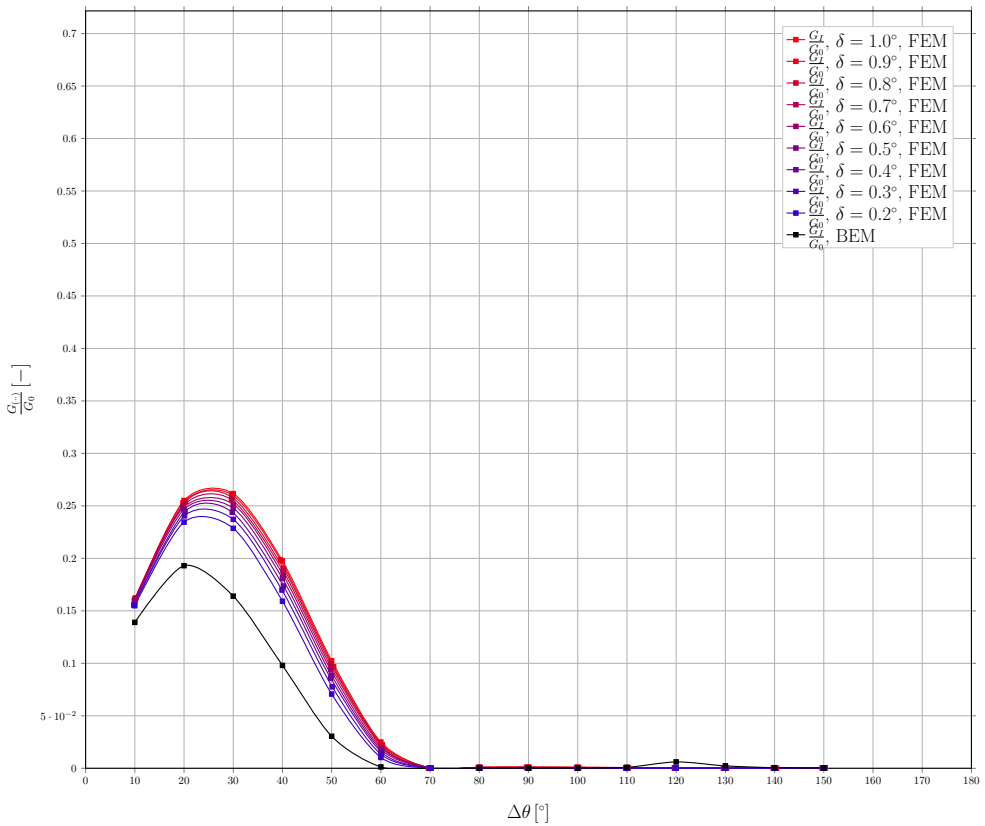

Fading from red to blue for decreasing size of elements at the interface, VCCT from FEM results; in black BEM results.

G_I Error with respect to BEM, VCCT in forces

Error of of normalized energy release rate with respect to BEM results $\Delta\frac{G_I}{G_0} = \frac{G_I}{G_0}|_{FEM} - \frac{G_I}{G_0}|_{BEM}$ as function of crack angular semi-aperture $\Delta\theta$, $VF_f = 7.9 \cdot 10^{-5}$, $\frac{L}{R_f} \sim 100$ calculated with in-house force-based VCCT post-processing routine

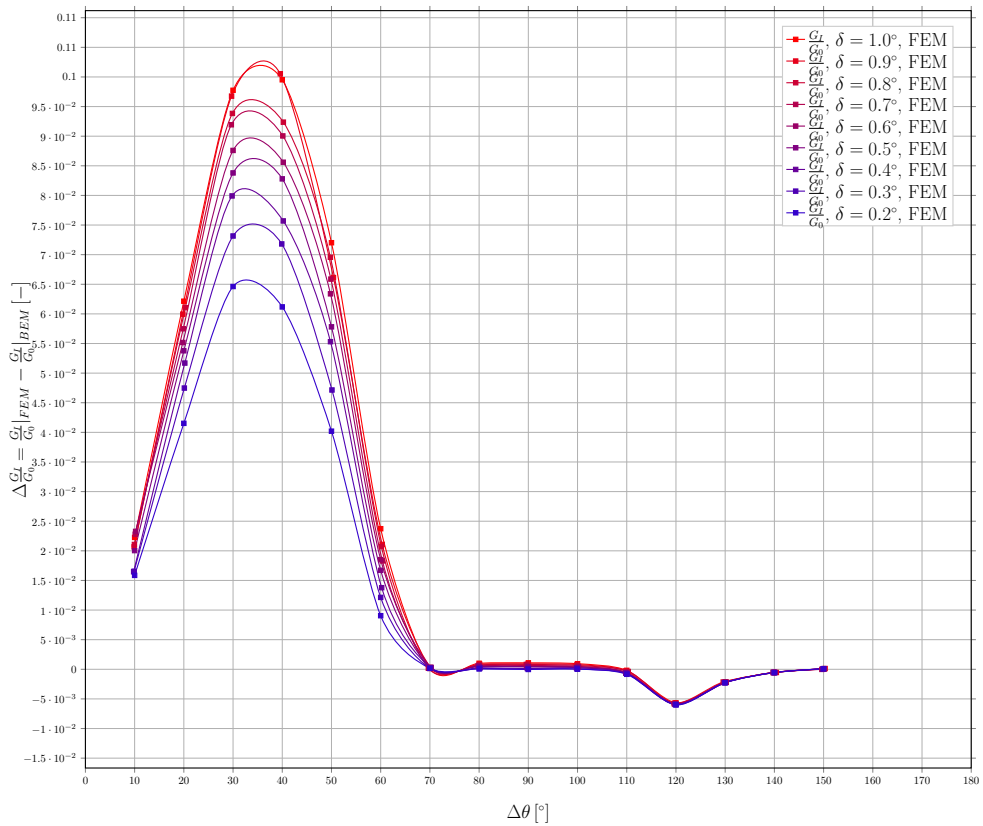

Fading from red to blue for decreasing size of elements at the interface, VCCT from FEM results.

$G_{//}$, VCCT in forces

Normalized energy release rate $\frac{G_{II}}{G_0}$ as function of crack angular semi-aperture $\Delta\theta$, $VF_f = 7.9 \cdot 10^{-5}$, $\frac{L}{R_f} \sim 100$ calculated with in-house force-based VCCT post-processing routine

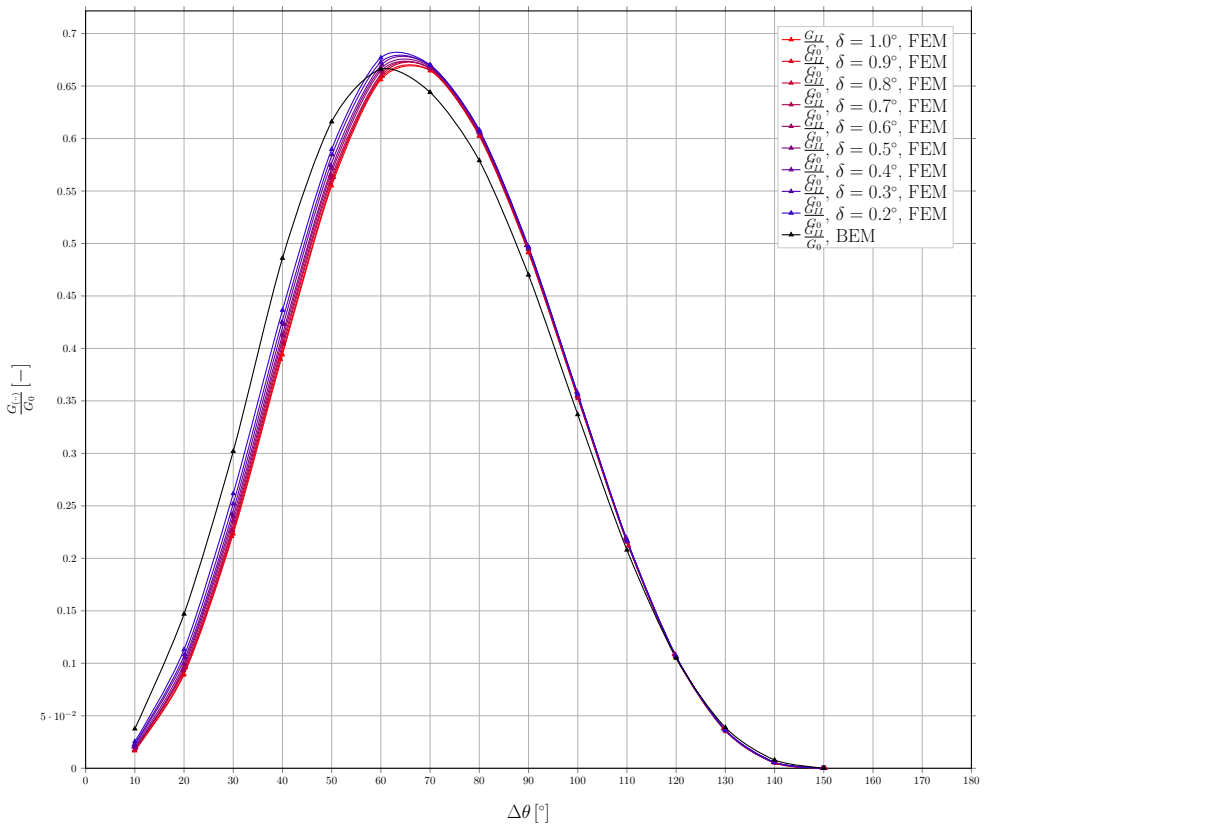

Fading from red to blue for decreasing size of elements at the interface, VCCT from FEM results; in black BEM results.

G_{II} Error with respect to BEM, VCCT in forces

Error of of normalized energy release rate with respect to BEM results $\Delta\frac{G_I}{G_0} = \frac{G_I}{G_0}|_{FEM} - \frac{G_I}{G_0}|_{BEM}$ as function of crack angular semi-aperture $\Delta\theta$, $VF_f = 7.9 \cdot 10^{-5}$, $\frac{L}{R_f} \sim 100$ calculated with in-house force-based VCCT post-processing routine

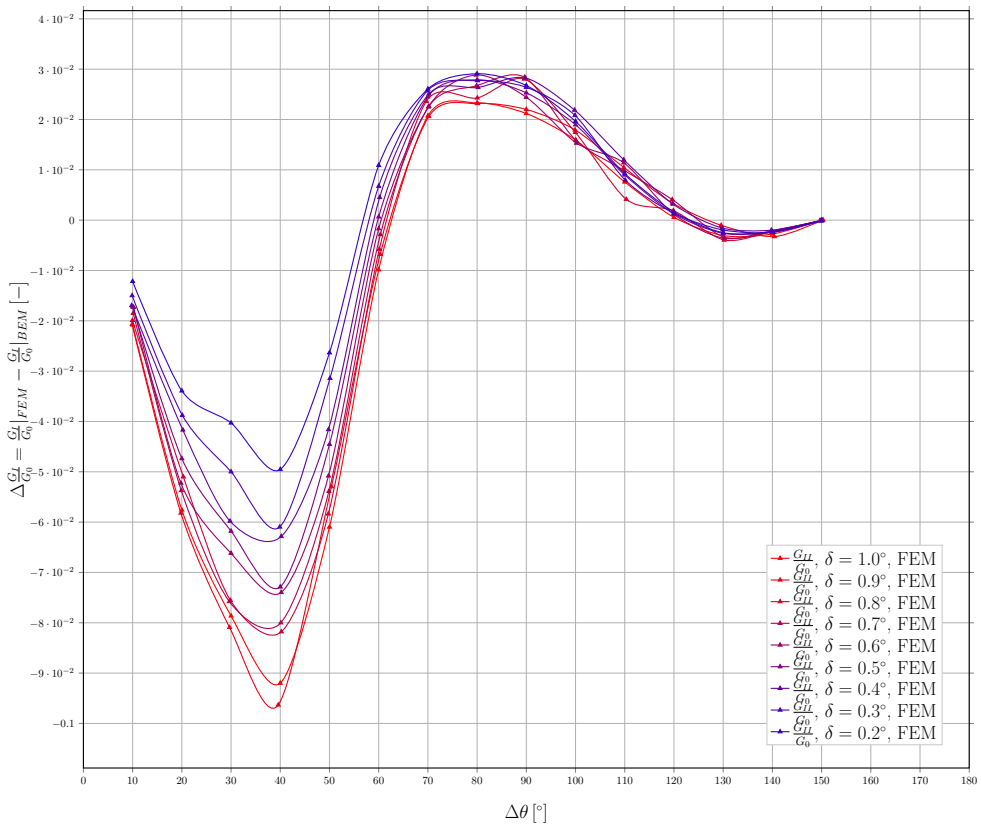

Fading from red to blue for decreasing size of elements at the interface, VCCT from FEM results.

G_{TOT}, VCCT in forces

Normalized energy release rate $\frac{G_I+G_{II}}{G_0}$ as function of crack angular semi-aperture $\Delta\theta$, $VF_f = 7.9 \cdot 10^{-5}$, $\frac{L}{R_f} \sim 100$ calculated with in-house force-based VCCT post-processing routine

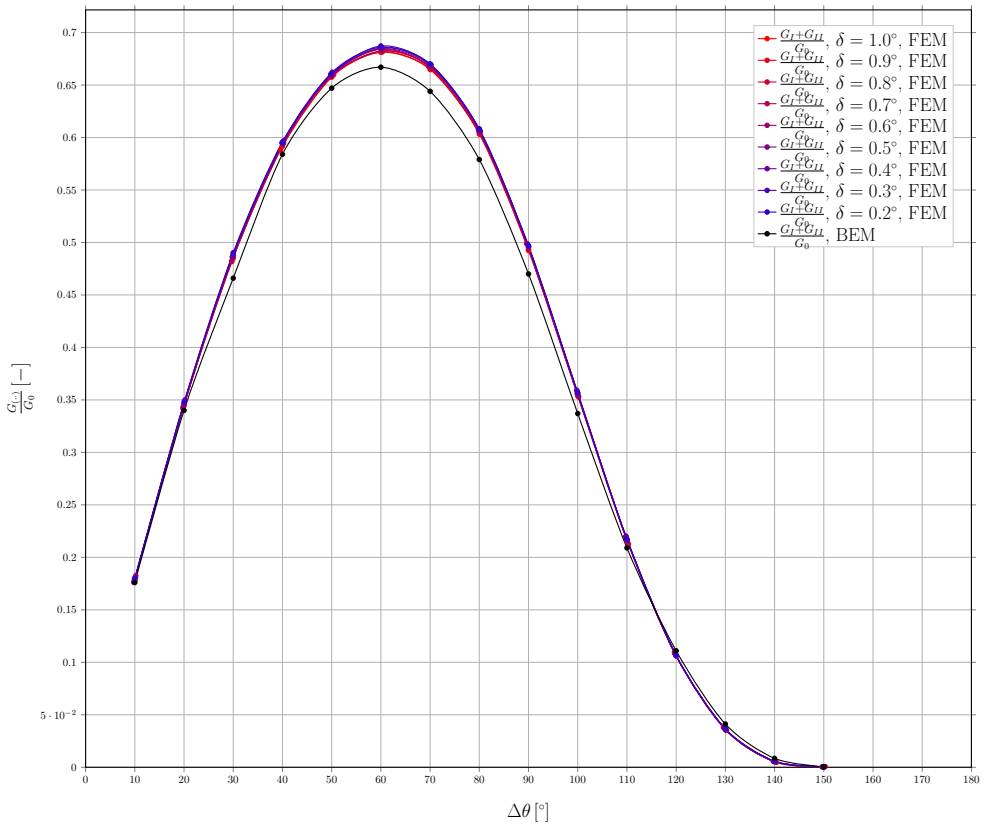

Fading from red to blue for decreasing size of elements at the interface, VCCT from FEM results; in black BEM results.

G_{TOT} Error with respect to BEM, VCCT in forces

Error of of normalized energy release rate with respect to BEM results $\Delta\frac{G_I+G_{II}}{G_0} = \frac{G_I+G_{II}}{G_0}|_{FEM} - \frac{G_I+G_{II}}{G_0}|_{BEM}$ as function of crack angular semi-aperture $\Delta\theta$, $VF_f = 7.9 \cdot 10^{-5}$, $\frac{L}{R_f} \sim 100$ calculated with in-house force-based VCCT post-processing

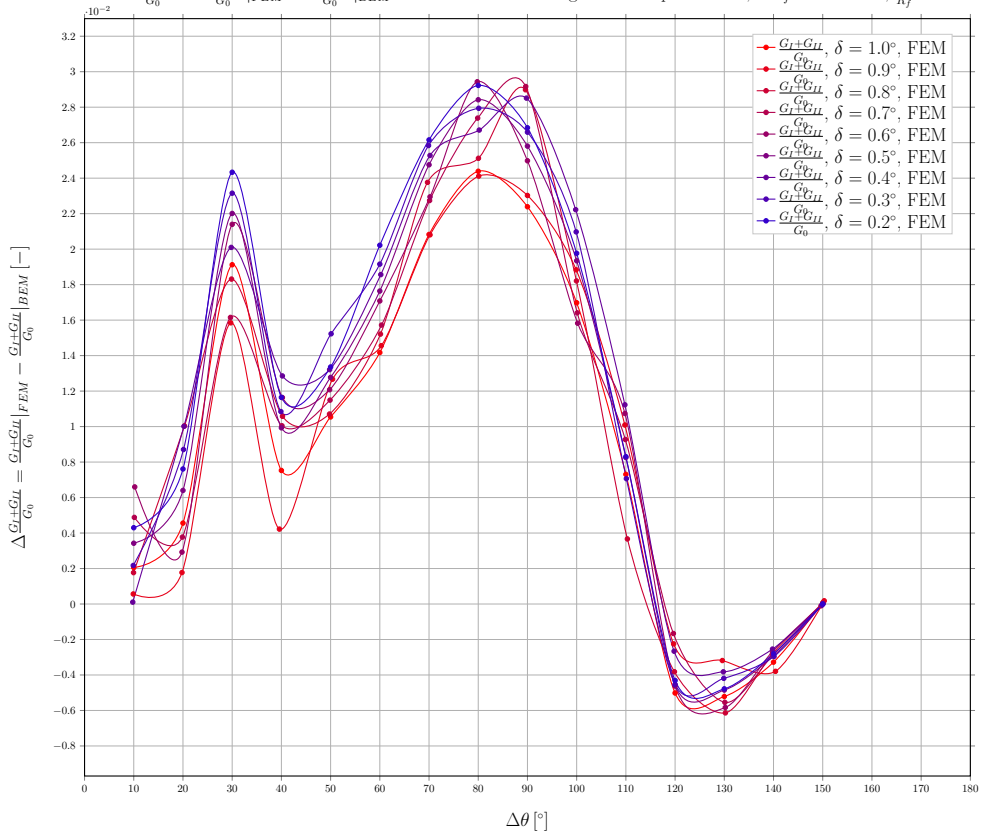

Fading from red to blue for decreasing size of elements at the interface, VCCT from FEM results.

SUMMARY & CONCLUSION

Summary

- ✓ Implemented Virtual Crack Closure Integral (VCCI) method for the calculation of G_I and G_{II}
- ✓ Analysis of free infinite RVE ($\frac{L}{R_f} \sim 100$) for several mesh refinements $\delta \in [1.0°, 0.2°]$
- ✓ G_I,G_{II} and G_{TOT} calculated using Abaqus built-in J-Integral routine, in-house implemented VCCT and VCCI routines

Conclusion

- ✓ Good agreement of J-Integral results with G_{TOT} from BEM
- ✓ J-Integral convergence improves refining the mesh
- ✓ For $\delta = 0.4°, 0.3°, 0.2°$ maxima are at the right angle (20° for G_I, 60° for G_{II} and G_{TOT}) with in-house VCCT
- ✓ G_{TOT} relative errors of VCCT over BEM are small ($\sim$ 5% or less) for every $\Delta\theta$
- ✓ G_{II} relative errors of VCCT over BEM are small ($\sim$ 5% or less) for $\Delta\theta > 40°$
- ✓ Results tend to converge to BEM values as the mesh is refined

Conclusion

- G_I relative errors of VCCT over BEM are high ($> 10\%$)
- G_{II} relative errors of VCCT over BEM are high ($> 10\%$) for $\Delta\theta \leq 40°$
- G_I of VCCI has correct functional form but values are overestimated (except for very small integration lengths)
- G_{II} (and consequently G_{TOT}) of VCCI provides strange results

Next steps

➔ New analysis with $\delta = 0.05°$ to see if a better agreement of G_l values is attained


Doc
MASE
UNIVERSITÉ
DE LORRAINE
EEIGM
LULEÅ
UNIVERSITY
OF TECHNOLOGY
Education and Culture
Erasmus Mundus